Adrenal Gq Signaling: Implications for Maintenance of Zonation and Steroidogenesis

by

Matthew J. Taylor

A dissertation submitted in partial fulfillment
of the requirements for the degree of
Doctor of Philosophy
(Molecular and Integrative Physiology)
in The University of Michigan
2019

Doctoral Committee:

Professor William E. Rainey, Chair
Professor Gary D. Hammer
Professor Jairam K. Menon
Professor Yatrik M. Shah

Matthew J. Taylor

motay@umich.edu

ORCID: 0000-0003-4385-0681

DEDICATION

To my parents, Joe and Beth
For their unconditional love and support from the beginning

To Liz
For meeting me halfway through with her steadfast
love, patience and guidance until the end.

ACKNOWLEDGEMENTS

There are so many people to thank that have helped me through the long process of reaching this point. First, I would like to thank Dr. Yatrik Shah, because my spark for scientific research started in his lab. I was his first employee, and planned on only staying for 2 years to build my resume for an application to medical school. I had very little lab experience coming in, but Yatrik took a chance on me and spent a lot of his first 6 months as faculty teaching me several lab techniques. His enthusiasm for research was infectious, and led me to view research as an exciting career option rather than a stepping stone to medical school. This experience ultimately changed the trajectory of my career, and I decided to apply to graduate school after 4 productive years in his lab.

Next, I would like to thank Dr. Bill Rainey, my graduate mentor. I have had an outstanding experience in his lab over the last 5 years, and I cannot adequately express how much his mentorship has meant to my development – both as a scientist and a person. Professionally, he provides the perfect balance in a mentor. He lets his trainees develop ideas and work independently, while still remaining involved in the project. Outside of work, Dr. Rainey has become what I consider a close friend and cares deeply about personal development in graduate school. Since I had never travelled abroad prior to graduate school, he made it a priority to send me to several international (and national) conferences to present my science during my graduate career. All of this

meant so much to me, and I won't forget his exceptional mentorship. I also need to thank my dissertation committee – Drs. Shah and Rainey, as well as Dr. Gary Hammer and Dr. Jairam Menon. Our committee meetings were productive and helped me define a direction for the research. Thanks to the Molecular and Integrative Physiology Department, which after 4 years in the Shah Lab and 5.5 years in the Rainey Lab, truly feels like a family and home to me. Dr. Bishr Omary was a fantastic Chair for MIP (and was always more than willing to write recommendation letters for me), and Dr. Santiago Schnell has been excellent as the new Chair – both of whom highly value graduate education. Thanks to the three Graduate Chairs during my time as a student – Dr. Scott Pletcher, Dr. Sue Moenter, and Dr. Dan Michele – their guidance to students in the graduate program was instrumental in my success. Thanks to Michele Boggs, the PhD program administrator, who helps MIP PhD students with so many things – it is greatly appreciated.

I also must thank members of the Rainey Lab and the entire UM Adrenal Research Team. Specifically, Matthew Ullenbruch, Emily Frucci, Dr. Juilee Rege, Dr. Kazu Nanba, Dr. Tobias Else, Dr. Namita Hattangady, Dr. Adina Turcu, Dr. Yewei Xing Dr. Antonio Lerario, and Dr. Katie Basham all played huge parts in helping this project along the way. Thanks to everyone in these groups for providing an intellectually stimulating environment and for all your help in troubleshooting my experiments and interpreting my data. Science is a team effort and none of this would have been possible alone.

To my friends from MIP, specifically Andrew Schwartz, Danny Triner, and Dr. Jon Gumucio, and my PIBS friends, especially Jim Ropa, Dr. Dave Bushart, Corey

Cunningham, Dr. Travis Kochan, and Dr. Keita Uchida – thanks for always being there to celebrate our milestones and sympathize with eachother over our scientific rough patches, all the while wondering when we would ever finish graduate school. Thanks to ESPA (Engaging Scientists in Policy and Advocacy), a graduate student organization that I joined in my final year. Thanks specifically the founders Sara Wong, Charles Lu, and Seth Wiley. This experience gave me an extracurricular outlet to engage in science advocacy. I hope I was able to help the organization as much as it helped me branch out as a science advocate and communicator.

I have so many friends in my life to thank that it's difficult to single out everyone, and doing so would take more pages than anyone wants to read, so I'll do this in groups. To my Ann Arbor friends, our group got really close over the years and Liz and I will definitely miss all the fun times, from tailgates to boat outings to dinners together. It always gave me needed breaks from my work. We will be back often. To my college/high school friends/other friends, I'm thankful that we've remained so close despite living in different areas of the country. Our daily text conversations, usually about something like sports rather than anything actually important, always gave me a lot of laughs and something to take my mind off science. I would be remiss to not specifically thank Art Reyes, Dr. Kevin Bingle, and Dr. Kevin Poole, who have each had my back for many years. Even though we don't see each other ofter, I always look forward to our times hanging out together.

Properly thanking my parents, Joe and Beth, for everything they have done for me in my life would require a page length longer than this dissertation itself, so I will try to be concise. You provide the perfect balance of guidance when I need it, while also

letting me make my own decisions. Going back to graduate school at age 27 is certainly not the norm, but because you were there to support me along the way, it made it possible for me. Thank you for always being there to listen and give advice along the way.

Finally, I cannot thank Liz enough for being there for me over the last 3 years. You heard a lot of excitement over successful experiments and a lot of complaining of failed experiments throughout that time. My explanations of what I do on a day-to-day basis probably didn't make much sense sometimes, but you were always there with encouragement, crucial advice when you could provide it, or just the patience to listen to me vent over the standard frustrations of graduate school. As ridiculous as it may seem, along with Liz, I also must thank Finn (our dog). Getting a puppy in the last year of graduate school wasn't the easiest thing, but coming home to the two of them instantly puts me in a good mood everyday. I couldn't be more excited for our next chapter in Chicago.

TABLE OF CONTENTS

LIST OF FIGURES

LIST OF TABLES

ABSTRACT

The human adrenal cortex can be divided into three zones that secrete distinct steroid hormones. The zona glomerulosa (ZG) produces aldosterone, a mineralocorticoid that is important for sodium/potassium homeostasis and blood pressure regulation. The zona fasciculata (ZF) produces cortisol, a glucocorticoid that participates in glucose homeostasis, and the zona reticularis serves as a secondary site for sex steroid production. The adrenal cortex undergoes cell renewal through centripetal displacement from the outer ZG to the inner adrenomedullary border where cells undergo apoptosis. Cells transition to the steroidogenic phenotype of each zone during the displacement process through gaining and losing zone-specific steroidogenic enzymes. There remain many unanswered questions regarding the cellular and molecular processes that regulate adrenocortical zonation. Understanding the mechanisms leading to cortical zonation and factors that cause dysregulation of steroid production could provide insight into adrenal physiology and disease.

Primary aldosteronism (PA) is a common cause of hypertension that results from excess aldosterone production and inappropriate adrenal expression of aldosterone synthase (CYP11B2). Despite its high prevalence, there are few appropriate animal models for PA. Physiologic adrenal aldosterone production is regulated by the renin angiotensin-aldosterone system (RAAS) which is activated in states of low renal tubule sodium levels or intravascular volume, leading to increased renal sodium retention.

Angiotensin II induces ZG aldosterone production via Gq-coupled receptors that trigger calcium signaling and transcription of CYP11B2. Recently, a series of DREADD (designer receptors exclusively activated by designer drugs) were developed to provide a chemogenetic method to modulate G-protein pathways. Included are transgenic receptors that stimulate Gq signaling only upon the binding of a synthetic ligand (clozapine N-oxide, CNO). This dissertation project tested the overall hypothesis that transgenic mice with targeted ZG/ZF GqDREADD expression would provide an inducible/reversible model for primary aldosteronism and a model to define the role of Gq signaling in functional adrenal zonation.

In this study, we demonstrated that $AS^{Cre/+}$::hM3Dq mice respond to CNO treatment with an increase in aldosterone production and upregulation of Cyp11b2 expression in both the ZG and ZF. This increase in aldosterone caused renal negative feedback with suppression of renin in a manner similar to that seen in patients with PA. When mice were given CNO in conjunction to a high sodium diet, Cyp11b2 mRNA/protein and aldosterone were highly elevated, confirming that the induction of Cyp11b2 was autonomous and not RAAS dependent. Mice treated with CNO plus high sodium diet also developed hypertension in response to elevated aldosterone concentration. Analysis of adrenals from CNO treated mice demonstrated that ZF cells take-on some, but not all properties of ZG cells. The transcriptional, histological, hormonal and hypertensive phenotypes were all reversible upon CNO washout. In summary, this dissertation project resulted in the development of an inducible and reversible mouse model of adrenal-derived hyperaldosteronism and hypertension. The project also provides evidence that Gq signaling contributes to functional zonation and

cellular ability to produce aldosterone. Future work will be needed to address the molecular mechanism by which Gq signaling activates Cyp11b2 expression and aldosterone production in ZF cells. This mouse model will also facilitate testing and discovery of therapeutic targets to block inappropriate aldosterone production and action in patients with PA.

CHAPTER 1

Introduction

1.1 Background

The adrenal gland is a multifaceted organ that controls electrolyte balance, the stress response, and in humans, acts as a secondary site for sex steroid precursor production. The adrenal cortex is comprised of cells that produce the steroid hormones responsible for these tasks, and makes up 90% of the tissue. The remaining 10% of the gland located in its center is the adrenal medulla, which produces catecholamines, a class of hormones that mediate the sympathetic nervous system response to stress. The cortex is derived from mesoderm, whereas the medulla is derived from neuroectoderm. While there are known interactions between the cortex and medulla, they largely function separate from one another.

The adrenal glands are located above the kidneys in humans, and were not documented by the earliest anatomists, but were first anatomically described by Bartolomeo Eustachius as a suprarenal organ in 1563 (1, 2). The differentiation between cortex and medulla was not recognized until 1805 by Georges Curvier (1), with adrenocortical zonation characterized by Julius Arnold in 1866 (3, 4). The physiological functions of the adrenals went unrecognized until the middle of the 19th century, when physiologists such as Thomas Addison and Charles-Edouard Brown-Sequard began to

describe adrenal function and disease (1, 5). Through adrenalectomy experiments, Brown-Sequard was the first to show that adrenal glands secreted hormones that were necessary for life (6). Nearly 100 years later, Hans Selye provided the first description of the hypothalamic-pituitary-adrenal axis, and named two of the main adrenal steroid classes ‘glucocorticoids’ and ‘mineralocorticoids,’ arguing for the first time that both were essential for life (7). Subsequent studies from the mid to late 1900s identified the adrenal steroid products and the enzymes that were responsible for the steps required for steroidogenesis. With this came the identification of several adrenal diseases of hormone excess and deficiency. The mechanisms that control adrenal homeostasis and the factors that contribute to the etiology of adrenal diseases remain active areas of research.

Aldosterone is the primary mineralocorticoid produced in humans, and its function is to facilitate sodium retention, effectively maintaining intravascular volume and pressure. Autonomous excessive secretion of aldosterone that results in hypertension was first described by Jerome Conn in 1954 (8) and is now commonly referred to as primary aldosteronism (PA) or Conn Syndrome. Significant progress has been made with regard to the diagnoses and treatment options for this disease. However, treatment and diagnoses can be improved through further understanding of how the adrenal cortex maintains its zonation of steroidogenic enzymes and the mechanisms that cause zonal dysregulation, as seen in PA.

1.2 Adrenal Zonation

The three steroid-producing functions of the human adrenal cortex are separated into distinct zones: the outermost zona glomerulosa (ZG) controls mineralocorticoid secretion, the middle zona fasciculata (ZF) produces glucocorticoids, and innermost zona reticularis (ZR) is a secondary site for sex steroid precursor production (Figure 1.1A). The medulla resides below the ZR, and the adrenal capsule is a connective tissue comprised of mesenchymal cells that surround the cortex. Upon histological examination, it is apparent that the three zones are morphologically different. The ZG is distinguished by closely packed cells, described as 'rosette'-like structures (3). These cells are responsible for the secretion of aldosterone, the main mineralocorticoid. Aldosterone's primary actions are to control renal sodium retention and potassium excretion. The ZG is molecularly characterized by its exclusive expression of aldosterone synthase (CYP11B2) (9). Aldosterone is tightly controlled by the renin-angiotensin-aldosterone system (RAAS). The restriction of CYP11B2 to the ZG is due to the exclusive ZG expression of the angiotensin II (AngII) receptor type 1 (AT_1R) (10), which initiates aldosterone production through its binding of AngII. The mechanism of action of AT_1R, a G-protein coupled receptor, will be covered in further detail in the coming sections.

The ZF is the largest zone in the normal adrenal gland, with lipid-rich cells that are organized in cord-like fascicles in between the ZG and ZR. The ZF is the glucocorticoid-producing zone that impacts physiologic metabolism via a circadian cycle but is also known to be highly responsive to stress and infection. The main glucocorticoid in humans is cortisol, and its production relies on the hypothalamic-

pituitary-adrenal (HPA) axis. Corticotropin-releasing hormone (CRH) is released from the periventricular nucleus of the hypothalamus in response to stress. CRH signals to corticotroph cells of the anterior pituitary gland, which respond through the synthesis and release of adrenocorticotropic hormone (ACTH). ACTH binds to its receptor (melanocortin receptor type 2, MC2R) in the adrenal cortex, which acts through Gs signaling to upregulate cyclic adenosine monophosphate (cAMP) through activation of adenylate cyclase (11). This pathway increases steroidogenesis through increased expression of the enzymes required for cortisol synthesis and LDL receptors for uptake of cholesterol, the precursor to all steroids (11, 12). 11β-hydroxylase (CYP11B1) is the final enzyme in cortisol synthesis, and is expressed exclusively in the ZF (9). Its transcription is also upregulated by ACTH (13, 14). Glucocorticoids, primarily cortisol in humans, are synthesized and secreted into circulation. Cortisol acts on target tissues to regulate metabolism and immunity, among several diverse functions.

Finally, humans and higher level primates have an innermost ZR comprised of eosinophilic cells arranged in a net-like ‘reticular’ pattern. The ZR does not appear in humans until around age 6-8, during a period called adrenarche (15, 16). Adrenarche precedes puberty and is the postnatal emergence of the adrenal’s production of precursor sex steroids coinciding with the differentiation of the ZR. In children, the increase in ZR synthesized steroids initiate development of pubic and axillary hair growth (17). The ZR continues to produce these sex steroid precursors until later in life when the production declines. The production of these steroids is partly increased through ACTH, as the MC2R receptor is also present in the ZR, but it is thought that other unknown factors also regulate adrenal androgen production (18). ACTH is also

necessary for ZR development at adrenarche (19-21). Androgen biosynthesis is zonally regulated through the ZR specific expression of cytochrome B5 (CYB5), which enhances the 17, 20 lyase activity of CYP17A1. Additionally, the sulfotransferase enzyme SULT2A1 is exclusive to the ZR, allowing for sulfated products.

Stem/Progenitor Cells and Centripetal Displacement

Early research involving adrenal enucleation (removal of the adrenal cortex and medulla, leaving only the adrenal capsule and subcapsular cells) in rats illustrated that stem/progenitor cells exist in the capsule and adrenocortical periphery, and can repopulate the entire adrenal cortex (22). Further research has confirmed that the primary site for adrenocortical cellular proliferation is the ZG and the outer ZF, where there are presumed stem/progenitor cells (23-26). Like many epithelial tissues, the adrenocortical homeostasis is maintained through self-renewal (24, 27). Several studies have demonstrated that this renewal is centripetal in nature, with cells underlying the capsule moving inward toward the medulla during their life-cycle (25, 28-34). In contrast, cells undergo apoptosis in the ZR near the medullary border (35, 36). The length of time for the entire adrenal cortex to regenerate has been studied in mice, with data showing anywhere from ~20-120 days, which suggests that this process may be variable between cells, age, sex and other factors (25, 28, 33, 36). One particular recent study used a *Rosa26-mTomato/mGFP* reporter mouse crossed to a mouse with a knock-in allele of Cre recombinase in the *Cyp11b2* locus (*AS*-Cre), allowing for irreversible GFP marking and lineage tracing of Cyp11b2-positive cells (28). Over time, this revealed that Cyp11b2-positive cells repopulate the entire adrenal cortex, even after losing Cyp11b2 expression and gaining Cyp11b1 expression. This suggests that the

majority of ZF cells were once aldosterone-producing ZG cells. It also argues that the majority of progenitor cells give rise to mainly ZG cells, rather than the other differentiated steroidogenic cell types.

In addition to the subcapsular cells, cells of the capsule have been demonstrated to have stem-like properties. These cells are mesenchymal, and do not express steroidogenic factor-1 (Sf1), the master regulator transcription factor of steroidogenesis. One capsular cell population is sonic hedgehog (Shh) responsive and is marked by the Shh target gene *Gli1* (37, 38). The Gli1-postive cells play a role in the establishment of the early definitive cortex during development and have the capacity to convert to a Sf1-positive steroidogenic cell phenotype (37). Another described capsular cell pool expresses the Wilms tumor protein homolog 1 (WT1). These cells were demonstrated to have the capacity to differentiate into a steroidogenic phenotype, as well as into a Gli1 expressing capsular cell, and WT1 expression can regulate *Gli1* transcription. While these cell populations have stem-like properties, the capsular contribution to the normal cortical homeostasis seems to be uncommon.

Pathways Controlling Zonation and Cell-Renewal

Paracrine signals play a dynamic role in the control of adrenal cell renewal and zonation. Wnt/β-catenin signaling has been characterized as vital for the maintenance of a ZG state and the cortex as a whole. The disruption of this pathway through knockdown of β-catenin in Sf1-positive cells causes adrenal developmental defects, as well as adrenal atrophy in later adult life, while full adrenal knockout of β-catenin results in adrenal aplasia (39). Furthermore, constitutive activation of this pathway leads to a

disorganization of the ZG/ZF boundary, dysregulated steroidogenesis, and increased aldosterone synthesis (40-42). Mutations in this pathway can also cause adrenal diseases such as adrenocortical carcinoma, and aldosterone-producing adenomas (43-45). Further evidence for the importance of the Wnt pathway lies in the newly found role of capsular R-spondin 3 (Rspo3) to signal to ZG cells to maintain Wnt pathway activation. Disruption of *Rspo3* leads to loss of the ZG and cell replenishment (46). Together, these studies outline a vital role for the Wnt pathway in adrenal cell renewal and maintenance of undifferentiated progenitor cells.

Another well-characterized pathway involved in adrenal cell renewal is Shh signaling. Shh-positive cells are localized to the ZG in the subcapsular region. In addition to the previously mentioned capsular cells, lineage tracing has been performed in Shh-positive subcapsular cells (37). The study demonstrated that the shortly after birth, the entire cortex is derived from these cells. It is likely that these Shh-positive cells also interact with the previously mentioned Gli1-postive cells of the capsule, as Gli1 is a Shh target (47). Additionally, disruption of *Shh* in mice results in adrenal hypoplasia and decreased cell proliferation (48, 49). Most recently, it has also been shown that Shh-positive progenitors in the ZG are necessary for the regeneration of the adrenal gland following atrophy, and that a cross-talk between Shh-signaling and Wnt/β-catenin signaling exists (38). In summary, it is clear that both the Shh and Wnt pathways are critical to the adrenocortical progenitor cells and the cell renewal of the cortex.

Endocrine factors are also a key regulator in the maintenance of adrenal zones, as it has been demonstrated that both AngII and ACTH increase proliferation (50). With respect to AngII, this has been exhibited through low sodium or high potassium

treatment in rats, which both activate the RAAS and cause an expansion of the ZG (51-56). Conversely, when animals are fed a high sodium diet, the ZG regresses (56, 57). These changes in proliferation have been attributed to AT_1R, as demonstrated through experiments involving its blockade (51, 57). Similarly, ACTH administration in rats produces hyperplasia of the ZF (58, 59), and conversely, dexamethasone (a synthetic corticosteroid that exerts negative feedback regulation on the HPA axis) causes the ZF to drastically regress (60). One study used BrdU pulse-chasing to illustrate that ACTH can stimulate proliferation in a population of possibly quiescent progenitor cells in the outer cortex (25).

The action of ACTH through its receptor, effectively activating cAMP/PKA signaling, is a main driver of ZF zonation and identity (61, 62). Mutation of a regulatory subunit of PKA (*Prkar1a*) that causes constitutive PKA activation results in glucocorticoid excess and a Cushing's syndrome-like phenotype (63, 64). This mutation also has clinical significance, as it is a reported cause of ACTH-independent Cushing's syndrome (glucocorticoid excess) (65). Furthermore, transgenic expression of this mutation in mice demonstrated that PKA inactivates Wnt signaling, enhancing the ZG to ZF lineage conversion and increasing the rate of centripetal migration (66). Through these studies, the effects of the ZF-specific ACTH-mediated PKA signaling pathway on adrenal zonation have been well-characterized. However, future work is needed to further understand the contribution of the ZG-specific AngII-mediated Gq signaling pathway in maintaining adrenal zonation.

Mouse vs. Human Zonation

Mice are a common model for human adrenal function and disease, including within this dissertation project. Because of this, it is worth noting that mice have several adrenal differences compared to humans. The most striking difference is that mice lack a functional ZR, and therefore do not make adrenal androgens (27). Moreover, after birth, mice have an 'X-zone' located in between the ZF and medulla (67, 68) (Figure 1.1B). The X-zone is thought to be remnants of the fetal adrenal gland, and it disappears after puberty in males and pregnancy in females (67, 69, 70). This zone has high expression of the enzyme 20α-hydroxysteroid dehydrogenase, which has been suggested to play a role in catabolism of progesterone and 11-deoxycorticosterone, precursor steroids in adrenal steroidogenesis (27, 71). However, the role of the X-zone is largely undetermined at this point. The presence of this zone is similar to the human 'fetal zone,' however unlike mice, this human zone regresses rapidly after birth through apoptosis (72-74). Other species differences related to steroidogenesis will be covered in the following section.

1.3 Adrenal Steroidogenesis

The adrenal cortex is the site of corticosteroid hormone synthesis, and produces three main classes of steroids: mineralocorticoids, glucocorticoids and androgens and androgen precursors. All adrenal steroids are derived from de novo synthesis with cholesterol as the precursor. While some enzymatic steps overlap between zones, the exclusive expression of certain enzymes in each zone dictates the products that are synthesized (Figure 1.2A).

Cholesterol Mobilization and Early Regulatory Steps

Adrenal cells have stores of cholesteryl esters in cytoplasmic lipid droplets, most of which is derived from dietary cholesterol. Dietary cholesterol circulates in the plasma as low density lipoprotein (LDL), and upon adrenal cell uptake, cholesterol is esterified for storage through a mechanism mediated by acyl-coenzyme A:cholesterol acyltransferase 1 (75, 76). *De novo* synthesis of cholesterol is also possible in adrenal cells, albeit not a major source compared to the LDL pathway. This synthesis occurs through the conversion of acetate to cholesterol by the enzyme 3-hydroxy-3methylglutaryl co-enzyme A reductase, which is suppressed when cellular LDL-derived cholesterol concentrations are high.

Adrenal cellular cholesterol mobilization is critical to initiate steroid hormone production and is controlled by steroid acute regulatory protein (StAR). StAR is a transport protein responsible for the movement of cholesterol from the outer mitochondrial membrane to the inner mitochondrial membrane (77). Upon transport, cytochrome P450 side-chain cleavage, encoded by *CYP11A1*, catalyzes the 3 reactions, converting cholesterol to pregnenolone (21, 26). The cholesterol mobilization and side-chain cleavage are the early rate-limiting steps in steroidogenesis. The enzymatic steps that follow are facilitated by a series of cytochrome P450s and hydroxysteroid dehydrogenases that differ depending on the zone.

Late Steps of Steroidogenesis

In the ZG, the first enzymatic step following side-chain cleavage is the irreversible conversion of pregnenolone to progesterone by 3β-hydroxysteroid dehydrogenase type 2 (HSD3B2, Hsd3b1 in mice). This is followed by theprogesterone to 11-deoxycorticosterone conversion by 21-hydroxylase (CYP21A2, Cyp21a1 in mice). At this point, ZG cells are specifically primed to make aldosterone with their expression of CYP11B2, which carries out three reactions to the final product of aldosterone. 11β-hydroxylation takes 11-deoxycorticosterone to corticosterone, and 18-hydroxylation converts this to 18-hydroxycorticosterone, which is also a bioactive mineralocorticoid. Finally, 18-methyl oxidation produces aldosterone (78).

ZF specific cortisol synthesis is a direct result of the higher expression of 17α-hydroxylase (CYP17A1) in the ZF compared to the ZG. Pregnenolone or progesterone can undergo the 17α–hydroxylation step catalyzed by this enzyme. As in the ZG, the next steps are mediated by HSD3B2 (before or after the 17α–hydroxylation) and CYP21A2, which produces 11-deoxycortisol. The ZF also has specific expression of the final enzyme CYP11B1, a cytochrome P450 with high sequence homology to CYP11B2 (13). CYP11B1 catalyzes the final step to produce cortisol.

The ZR produces small amounts of active androgens but large amounts of 19 carbon (C_{19}) steroids that have minimal androgenic activity, but are precursors to bioactive androgens. ZR cells also utilize CYP17A1, which in this case carries out two reactions that convert pregnenolone to the androgen precursor dehydroepiandrosterone (DHEA). 17α-hydroxylation is the first step catalyzed by CYP17A1, as in ZF cells. Then, specifically in the ZR, the same enzyme carries out a 17, 20-lyase conversion. As

previously mentioned, the activity of this second step is increased through the ZR specific expression of CYB5 (79). The relatively low ZR HSD3B2 expression also helps facilitate DHEA synthesis. Finally, sulfated steroids are synthesized in the ZR through the activity of SULT2A1.

Mouse vs. Human Steroidogenesis

In addition to zonation, mice have differing features of steroidogenesis compared to humans (Figure 1.2B). First, although humans use LDL as their main source of cholesterol, mice rely on high density lipoproteins (HDL) for most of their cholesterol. This uptake of cholesteryl esters from HDL occurs through scavenger receptor B1, a process that seems to be less utilized in human adrenal cells (80). Another important difference is the lack of CYP17A1 in the mouse adrenal gland. Without this 17α-hydroxylation step, the ZF cannot produce cortisol, leaving corticosterone as the dominant glucocorticoid in mice (Figure 1.2) (27, 81). Additionally, the absence of CYP17A1 is also a reason that the mouse adrenal gland does not make sex steroid precursors (Figure 1.2) (27, 81).

1.4 Adrenal Aldosterone Production

Adrenal aldosterone production is a tightly regulated process occurring only in adrenal ZG cells that has multiple mechanisms of stimulation. Aldosterone production is regulated both acutely and chronically, with rate-limiting steps at both stages. The main agonists to aldosterone production are AngII, elevated serum potassium (K^+), and to some extent, ACTH. AngII is the primary stimulator of aldosterone synthesis, and is

controlled by the RAAS feedback loop. The juxtaglomerular (JG) cells of the kidney increase transcription of *REN* (*Ren1* in mice), the gene that encodes renin, in response to decreased renal perfusion (82). Renin secretion from JG cells is also stimulated by the macula densa cells of the renal distal convoluted tubule in response to low sodium concentration. Renin is responsible for the hydrolysis of the liver secreted protein angiotensinogen to angiotensin I, which is then converted to AngII in the vasculature of many tissues by angiotensin-converting enzyme (83). In addition to its action on ZG cells, AngII is a potent vasoconstrictor, acting on its receptor (AT_1R) in vascular smooth muscle cells (84). The other mechanism through which AngII exerts its effect on blood pressure is stimulation of aldosterone secretion. AT_1R is highly expressed in the adrenal gland, specifically in ZG cells, and it activates downstream pathways that result in the production of aldosterone. Aldosterone's action to increase sodium retention in renal distal convoluted tubules and collecting ducts initiates a negative feedback signal to inhibit renin production, thus completing the feedback loop.

Acute Regulation of Aldosterone Production

AngII mediates the mobilization of cholesterol in ZG cells, which is the early rate-limiting step of aldosterone production (85). This starts by the activation of cholesteryl ester hydrolase through ERK signaling (86). The second step of this process is the mobilization within the mitochondria by StAR, which has been detailed above. StAR is regulated in both a transcriptional and post-translational manner following AngII binding (87). This response occurs within minutes of the AngII stimulus (88).

The ligand bound AT1R can trigger several signaling pathways. Since it is a Gq coupled receptor, it activates the Gq family of proteins, leading to phosphoinositide-specific phospholipase C (PLC) stimulation (89-93). PLC hydrolyzes phosphatidylinositol 4,5-bisphosphate (PIP_2) into inositol 1,4,5-trisphosphate (IP_3) and diacylglycerol (DAG). The role of IP3 is to increase cytosolic calcium through initiating its efflux into the cytoplasm from the smooth endoplasmic reticulum (94, 95) (Figure 1.3). AngII also activates L- and T-type calcium channels to increase extracellular calcium influx (96). The induction of cytoplasmic calcium concentration through these mechanisms is essential for aldosterone synthesis. Calcium activates calcium/calmodulin-dependent kinases (CaMKs), a step that is critical to aldosterone production (97, 98). Meanwhile, DAG activates protein kinase C (PKC), an enzyme that has conflicting reports as to its role of either enhancing (91, 99) or suppressing (94, 100) aldosterone secretion. In addition, it has been demonstrated that DAG activation of PKC can increase the expression and phosphorylation of StAR, corroborating its participation in aldosterone secretion (101, 102). Phospholipase D activation is another pathway acutely regulated by AngII, which is an additional route to elevate DAG levels (103-105).

K^+ and ACTH can also activate the early stages of aldosterone production. The main reported K^+ effect is glomerulosa cell membrane depolarization that opens L- and T-type calcium channels (106, 107). ACTH binding to the Gs coupled MC2R activates cAMP/PKA signaling, as described above. The phosphorylation of StAR by PKA activates the early rate-limiting step of aldosterone production. PKA can also open L-

type calcium channels through phosphorylation, which increase calcium concentrations and aldosterone secretion (108, 109).

Chronic Regulation of Aldosterone Production

The “chronic” regulatory step for aldosterone production is the AngII-increased expression of CYP11B2 in ZG cells, through activation of *CYP11B2* transcription and expansion of the ZG through hypertrophy and hyperplasia. The chronic response is delayed, depending on an increase in intracellular calcium, and taking several hours to days before an effect is observed (110). Several in vivo studies, most often with a stimulus such as a low sodium diet, have demonstrated the specificity of AngII regulation of CYP11B2 with no effect on CYP11B1 (111-113). This illustrates that AngII does not participate in glucocorticoid synthesis, and is solely a mineralocorticoid agonist. The AngII-mediated increase in *CYP11B2* expression is at the transcriptional level, and several studies have defined the transcription factors that participate in this response. Following the increase in cytosolic calcium, CaMKs increase expression or phosphorylation of regulatory transcription factors that include Nurr1, cAMP response element binding protein (CREB), and activating transcription factor family members (ATFs). These factors then bind to the promoter region of *CYP11B2*, upregulating its transcription within the nucleus (110, 114, 115) (Figure 1.3). On the contrary, high expression of the transcriptional regulator SF1 has been shown to repress AngII-stimulated CYP11B2 expression (116, 117).

Potassium can also stimulate CYP11B2 in a similar manner to that of AngII (118, 119) and a high potassium diet expands the ZG in vivo (120). ACTH can activate

CYP11B2 expression in vitro, but sustained ACTH treatment of ZG cells convert them to a glucocorticoid-producing phenotype (121). It appears that initially, ACTH can activate CYP11B2, but over time this effect is diminished (111, 122). One possibility for why ACTH might not effectively activate ZG aldosterone production is that the activated AT_1R can also couple to Gi proteins, which directly inhibits ACTH's ability to increase cAMP signaling. Thus, mechanisms are in place to prevent ZG glucocorticoid production (123).

1.5 Primary Aldosteronism

In 1954, the University of Michigan clinician scientist Dr. Jerome Conn encountered a 34-year old female patient that presented with a history of hypertension, described muscle spasms, and weakness (8). Conn suspected that the metabolic alkalosis and hypokalemia observed in this patient might be due to high aldosterone levels. This was confirmed by a urinary test, and when potassium supplementation did not chronically correct the symptoms, the adrenal glands were examined. When a benign adrenal tumor was found and removed, the symptoms were cured, and Conn reported the first case of PA (also termed Conn Syndrome) (8, 124).

PA can be defined as the inappropriate (renin independent) secretion of aldosterone that results in hypertension. Due to the other role of aldosterone in mediating potassium secretion, PA can also cause hypokalemia. In some cases, such as with Conn's patient, PA can cause metabolic alkalosis through concomitant loss of hydrogen ions with the retention of sodium. In the time that has followed since Conn's initial description, many advances in PA research have been made. Antibodies against

CYP11B2 that do not cross-react with CYP11B1 have been developed, making detection of the localization of adrenal aldosterone producing cells possible (125, 126). New sequencing technologies have allowed for the identification of somatic and germline mutations that cause autonomous aldosterone production. In the last 20 years, research has demonstrated that PA is more common than previously thought, affecting anywhere from 5-10% of the hypertensive population (127-130), and 20% of those with resistant hypertension (131-133). The sustained hypertension and high levels of aldosterone in PA make those affected susceptible to severe cardiovascular complications, including cardiac fibrosis and stroke (134-141). With the prevalence and risks in mind, research to improve diagnostics and treatments of PA is imperative.

Subtypes of Primary Aldosteronism

PA has 2 main subtypes: idiopathic hyperaldosteronism (IHA), which is often bilateral adrenal disease (also referred to as bilateral adrenal hyperplasia, BAH), and aldosterone-producing adenoma (APA), which is commonly unilateral. These two subtypes combine to represent approximately 95% of cases (~65% IHA and ~30% APA) (127). IHA refers to hyperplasia of the CYP11B2-expressing ZG with micro- and/or macronodules (142). APAs are benign tumors in the adrenal cortex with a high expression of CYP11B2 and often cause a more severe phenotype than seen in IHA patients (142). Unilateral hyperplasia, adrenocortical carcinoma, and ectopic secretion of aldosterone represent rare causes of sporadic PA.

There are also inherited forms of PA that comprise a much smaller population. Familial hyperaldosteronism (FH) type I is an interesting subtype caused by a chimeric

fusion between CYP11B1 and CYP11B2 (143). The chimeric enzyme is driven by ACTH, and can be suppressed through glucocorticoid treatment (144). FH type II refers to inherited incidents of APA or IHA and there is currently no known genetic cause. Recently, a mutation in the *CLCN2* chloride channel was described in a subset of cases with FH type II (145). FH type III and IV refer to germline mutations in *KCNJ5* and *CACNA1H*, respectively. All subtypes with each subtype's prevalence (146, 147) are outlined in Table 1.2.

Recent discoveries have also uncovered non-neoplastic regions of CYP11B2 expressing cells, termed aldosterone producing cell clusters (APCC) (126). These are found in otherwise normal adrenal glands or adjacent to APA (148-151), and their prevalence increases with age (152). A buildup of adrenal APCC may increase renin-independent aldosterone production that may progress to PA, but further research is needed on this topic.

Genetic Mutations Causing Primary Aldosteronism

Several somatic and germline mutations have been linked to cases of PA, especially those that are driven by APA. The most common APA mutations are in *KCNJ5* (153-155), a gene that encodes an inward rectifying potassium channel. These mutations cause membrane depolarization due to a lack of ion selectivity, which leads to increased opening of calcium channels, and calcium influx into adrenal cells. *CACNA1D* encodes a voltage dependent L-type calcium channel and APA have mutations that increase intracellular calcium by lowering the threshold for channel opening (156-159). Recently, *CACNA1D* mutations were found in APCC (150, 160).

CACNA1H encodes a different voltage-gated calcium channel that is expressed in ZG cells, and its mutations has been reported in a form of early-onset familial PA. These mutations cause inappropriate aldosterone production through increased calcium cellular influx through the mutated channel (161). *ATP1A1* is a subunit of an Na^+/K^+ ATPase. APA mutations in *ATP1A1* lead to membrane depolarization and H^+ influx, acidification of the cell, and activation of aldosterone production (162). Finally, *ATP2B3* encodes a calcium ATPase responsible for pumping calcium out of the cytoplasm. APA have mutations in *ATP2B2* that increase intracellular calcium through decreased function (162). There are several cases that do not contain these common mutations, suggesting that there are additional mutations to be discovered.

Diagnosis and Treatment of Primary Aldosteronism

It is under a physician's discretion as to whether to screen for PA in patients that present with hypertension. While some PA patients present with hypokalemia, the majority (72%) are normokalemic, thus serum potassium cannot be used to eliminate the need for PA screening (146). The current Endocrine Society guidelines recommend testing hypertensive patients that exhibit any of the following additional risks: sustained blood pressure over 150/100, resistant hypertension (uncontrolled blood pressure on 3 or more drugs, or controlled blood pressure on 4 or more drugs), hypokalemia, adrenal incidentaloma, sleep apnea, family history of early onset hypertension, and first degree relatives with PA (146). However, PA remains severely underdiagnosed due to the difficulty of clinical workup and the false notion that PA is a rare disease (163, 164).

In short, PA testing usually begins with biochemical determination of an initial aldosterone and renin ratio to help determine if autonomous aldosterone production is present. If positive, this is followed by a CT scan to determine if there are any nodules. If there is a nodule detected, lateralization studies are still recommended due to the fact that CT scans are not reliable for defining the affected adrenal in PA (165-167). The recommended next step to determine if PA is unilateral or bilateral is adrenal vein sampling (AVS). This is an invasive, difficult to perform and costly procedure that can distinguish unilateral from bilateral disease. Aldosterone is measured from the adrenal vein on both sides, and compared to peripheral blood. Cortisol is used as a positive control to ensure that the catheter is correctly placed (with higher levels in the AV than peripherally) (146). High aldosterone levels on both sides indicate bilateral disease and high aldosterone on one side suggests unilateral disease. From here, treatment options can be decided: typically, mineralocorticoid receptor antagonists (MRAs) for bilateral disease and adrenal resection for unilateral disease. The invasive procedures for this diagnostic workup highlight a need for PA biomarkers. Treatment improvements through current research are needed to lessen the use of adrenal vein sampling and to improve physician access to a more simple method to diagnose the subtypes of this disease (168).

1.6 Animal Models of Primary Aldosteronism

Since the discovery of PA, there have been a considerable amount of in vivo findings regarding disruptions in normal adrenal function that result in a phenotype of hyperaldosteronism (Table 1.2) (169). One of the first transgenic targets was leak-type

potassium channels, namely Task1 and Task3. *Task1* (*Kcnk3*) deletion results in hyperaldosteronism in female mice due to ectopic expression of Cyp11b2 in the ZF, leading to elevated blood pressure (170). Interestingly, male mice appear normal and when females are administered testosterone the phenotype is abolished. The double deletion of *Task1* and *Task3* (*Kcnk9*) leads to a marked increase in aldosterone without zonation defects (171). High sodium diet is not able to suppress this aberrant aldosterone production. Mice with only a *Task3* deletion do not have as robust of a response, but still have elevated aldosterone production, despite high sodium diet administration with suppressed renin (172, 173). These mice also exibit increased blood pressure. Additional studies have looked at the phenotype of mice with deletions of large Ca^{2+}-activated potassium channels. *Kcnmb1* deletion causes increased aldosterone production that is enhanced by a high potassium diet (174). *Kcnma1* knockout leads to a similar phenotype, albeit a minor hypertension response (175). These mice also have increased vascular tone, which could also be responsible for their hypertension.

Constitutive activation of the Wnt pathway also appears to upregulate aldosterone production. Deletion of *Apc*, a member of the β-catenin destruction complex, causes an increase in aldosterone and corticosterone synthesis in these mice (176). When β-catenin is constitutively activated, as in the ΔCat mice, the adrenal gland undergoes hyperplasia, disruption of the ZG/ZF zonal boundaries and increased aldosterone levels are observed in female mice (42). The increased aldosterone is likely due to the expansion of the ZG cell population and consequently an increase in

Cyp11b2-postive cells. This is clinically relevant, as β-catenin activating mutations are drivers of adrenal disease, as previously mentioned.

Several other mouse models disrupting various protein pathways have demonstrated phenotypes of autonomous aldosterone production as well. Mice with decreased expression of *Tgfb1*, which encodes TGFβ1, exhibited an increase in aldosterone and corticosterone with a negative correlation to the amount of *Tgfb1* they expressed (10% to 300% of normal *Tgfb1* expression) (177). These mice also had hypertension which was rescued through treatment with sprinonolactone. Mice with an irregular circadian clock through whole body inactivation of *Cry1/Cry2* have increased aldosterone production, which appears to result from the high levels of hydroxysteroid dehydrogenase b6 (Hsd3b6) rather than increased Cyp11b2 expression (178). One group used a non-transgenic method of a mouse mutagenesis screening by treating mice with N-ethyl-N-nitrosourea (Enu) to introduce random point mutations. This resulted in some mouse lines that had increased aldosterone production, which was linked to the genes *Sspo*, *Dguok*, *Hoxaas2*, and *Clstn3* (179).

There have also been studies aiming to increase aldosterone production through transgenic implantation of *Cyp11b2* itself. Using a transgenic approach, mice were made with a a more stable 3' untranslated region for *Cyp11b2* resulting in increased Cyp11b2 expression and aldosterone production, even in the presence of high sodium (180). In addition, another group described transgenic expression of human *CYP11B2* under the control of the human *CYP11B1* promoter. These mice did exhibit elevated aldosterone and blood pressure as a result of expression of the human transgene (181).

Recently, a group found that deletion of the ubiquitin ligase *Siah1a* resulted in a smaller X-zone, larger medulla, and Cyp11b2 zonal localization defects (182). There was also increased aldosterone production in these mice. These mice had additional defects of higher levels of catecholamines and upregulated adrenal cAMP signaling. They also found a possible link to human disease, where patients with PA had variants of *SIAH1.*

These current in vivo PA models have improved our understanding of the many factors that influence both physiologic and inappropriate aldosterone production. However, there are still several unknown factors contributing to aldosterone production that can be discovered in vivo. Furthermore, the current models of PA could be improved to better recapitulate the disease. This dissertation project describes a new PA model of activated Gq signaling that is both inducible and reversible; characteristics that are not present in the current transgenic models.

1.7 Summary

In recent years, the adrenal research field has seen major scientific breakthroughs, but there remain many questions regarding adrenal zonation, steroidogenesis, and causes of adrenal disease. New technologies such as liquid chromatography tandem mass spectrometry (LC-MS/MS) allow the detection of many steroids in one sample, giving the possibility to find biomarkers of adrenal disease for improved diagnostics. Furthermore, cutting edge sequencing tools have progressed our understanding of the genetic factors that underlie adrenal disease, providing targets for precision therapies to treat adrenal disease. Finally, improved mouse transgenic

technologies continue to provide models that improve our understanding of the mechanisms regulating zonation of the adrenal cortex.

The roles of several pathways have been described in maintaining adrenal zonal boundaries and determining adrenal cell fate. Moreover, many pathways have been implicated in adrenal aldosterone production through in vitro experiments. Within the adrenal cortex, Gq signaling is a ZG specific pathway that is activated through AngII and increases the transcription of *CYP11B2* through intracellular calcium signaling. However, the function that Gq signaling might serve in the regulation of adrenocortical homeostasis has not been probed. Moreover, the level of plasticity of adrenal cells to transition to an alternate steroidogenic phenotype with the stimulus of Gq signaling is also unclear. The following dissertation project focuses on the role of Gq signaling in adrenal aldosterone production and regulation of adrenal functional zonation. Using a mouse model of adrenocortical-specific inducible Gq signaling, we determine that Gq signaling in the ZF can stimulate Cyp11b2 expression and aldosterone synthesis. This mouse model will help define the mechanisms controlling adrenocortical cell plasticity and serve as a tool for researchers interested in studying aldosterone excess and new treatment strategies.

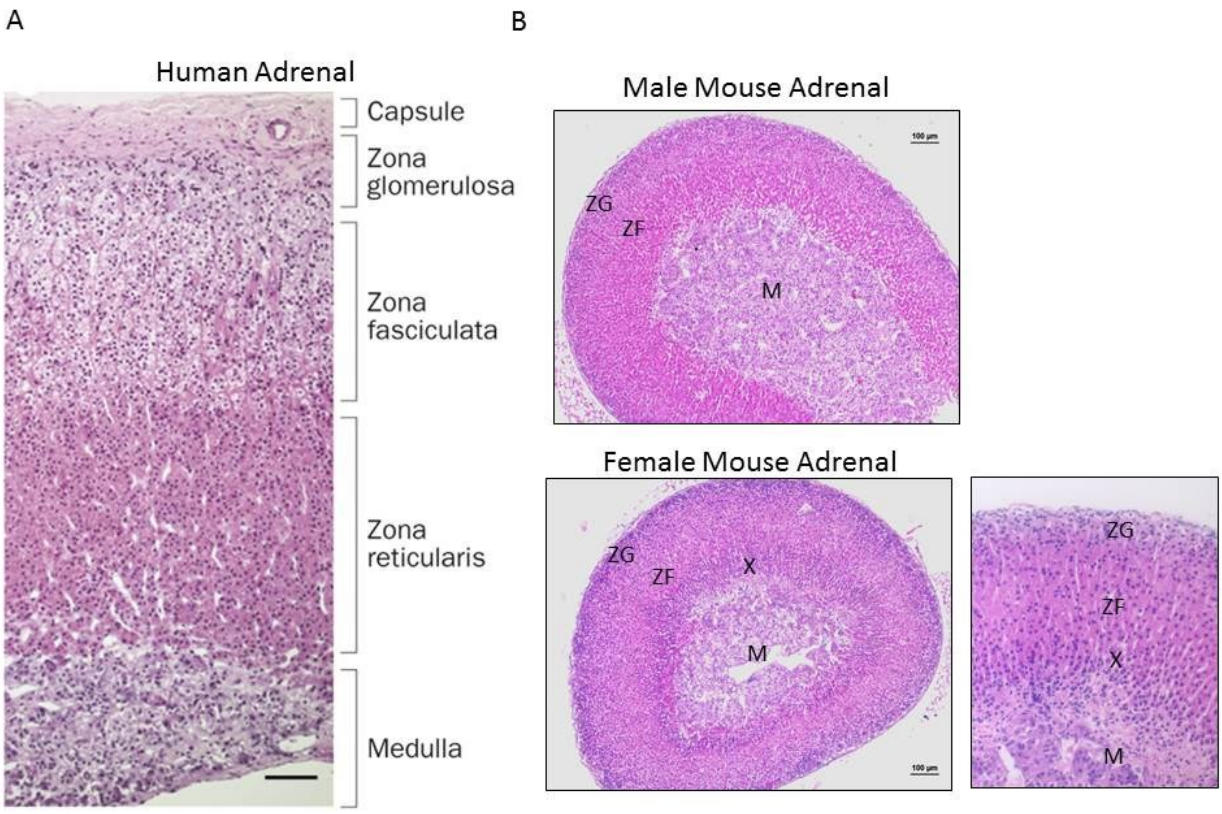

Figure 1.1. Histology of the adrenal cortex in humans and mice. (A) Human adrenal histology. The adrenal gland is surrounded by a mesenchymal capsule that contains stem/progenitor cells. The zona glomerulosa (ZG) is the outermost zone which secretes mineralocorticoids, and is characterized by tightly packed rosette-structured cells. The zona fasciculata (ZF) is more lipid-rich in histology and the largest zone. Finally, the zona reticularis (ZR) is highly eosinophilic with densely packed nuclei, and is the innermost zone of the cortex above the medulla (M). **(B)** Mouse adrenal histology. In mice, the ZF and ZF have similar morphologies to that of humans. However, there is not a ZR present. Instead, there is an X-zone (X), remnants of the fetal adrenal whose function is still not well understood. Pictured here is the adrenal from male and female adult mice, showing that there is a sex difference in the regression of the X-zone. In males, the X-zone disappears at puberty, and in females it regresses at first pregnancy.

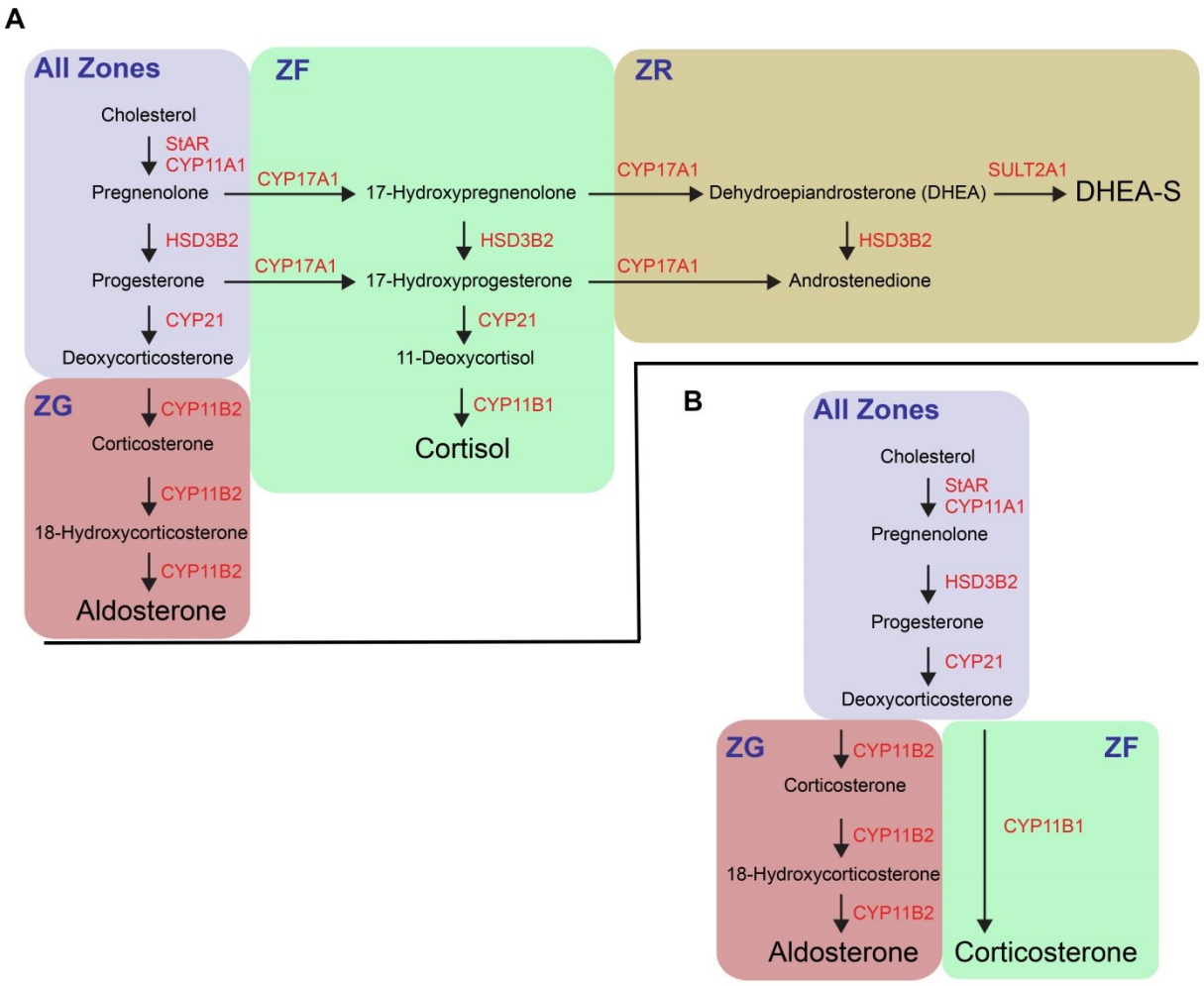

Figure 1.2. Adrenal steroid pathway in humans and mice. (A) Human adrenal steroid pathway. In all zones, the precursor for steroids is cholesterol, often derived from LDL in the cytoplasm. StAR is a transport protein that moves cholesterol from the outer mitochondrial membrane to the inner mitochondrial membrane. From there, several steroidogenic enzymatic reactions (denoted in red) occur. In the ZG, CYP11B2 carries out the final 3 steps of synthesis to aldosterone. In the ZF, 17α-hydroxylation pushes steroids down a path of glucocorticoid synthesis, where CYP11B1 carries out the final step to cortisol production. In the ZR, CYP17A1 not only has 17α-hydroxylation activity, but also 17, 20-lyase activity resulting in the production of the androgen precursor DHEA. Other androgen precursors such as androstenedion and DHEA-sulfate (DHEA-S) are also produced in the ZR. **(B)** Mouse adrenal steroid pathway. Mice differ from humans in a few respects related to steroidogenesis. First, mice do not express CYP17A1, so their primary glucocorticoid is corticosterone instead of cortisol. This is produced in one step by CYP11B1 in the ZF from deoxycorticosterone. Also, mice do not secrete adrenal androgens or contain a functional ZR.

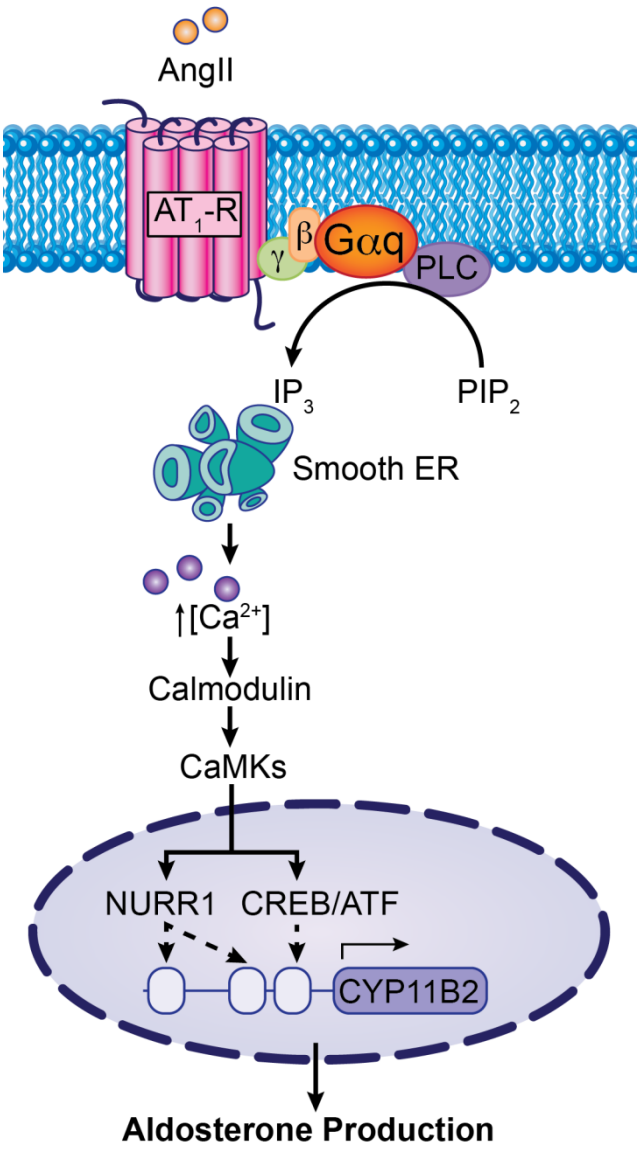

Figure 1.3. Gq signaling pathway activation by angiotensin II in adrenal ZG cells. The primary pathway activated by AT_1R upon binding of AngII is Gq signaling. Gαq cleaves phosphatidylinositol 4,5-bisphosphate into inositol 1,4,5-trisphosphate (IP3), which binds to its receptor at the smooth endoplasmic reticulum (ER). This elicits release of calcium (Ca^{2+}) into the cytosol, activating calmodulin, which activates calmodulin dependent protein kinases (CaMKs). CaMKs increase the transcription and activation of Nurr1, CREB, and ATF transcription factors in the nucleus that are important for activation of *Cyp11b2* transcription. Cyp11b2 transcription and translation then leads to increased aldosterone production within the cell.

PA Subtype	Description	Prevalence
Idiopathic hyperaldosteronism (IHA)	Bilateral hyperplasia of the adrenal cortex	50-70%
Aldosterone-producing adenoma (APA)	Benign aldosterone producing adrenocortical tumor; usually unilateral; common mutations: *KCNJ5, CACNA1D, ATP1A1, ATP2B3*	30-50%
Unilateral adrenal hyperplasia	IHA phenotype, unilateral disease	2%
Aldosterone-producing adrenocortical carcinoma (APACC)	Malignant tumor that secretes aldosterone	<1%
Familial hyperaldosteronism (FH) type I	Chimeric fusion of *CYP11B1* and *CYP11B2*; activated by ACTH; Glucocorticoid-remediable	<1%
FH type II	Inherited APA or IHA	<6%
FH type III	Germline *KCNJ5* mutation	<1%
FH type IV	Germline *CACNA1H* mutation	<0.1%
Ectopic APA or APACC	APA or APACC located in a tissue outside of adrenal cortex, such as the ovaries	<0.1%

Table 1.1. Subtypes of primary aldosteronism. Listed are the subtypes of PA with a description and prevalence of each subtype. Data reported from Young, 2018 (146) and El Ghorayeb et al. 2016 (147).

Types of Models	Mouse Model	Description	Phenotype
Potassium channel deletions	*Kcnk3*$^{-/-}$	Task1 (K^+ channel) knockout	High aldosterone and BP, disrupted Cyp11b2 zonation, decreased circulating renin
	Kcnk9$^{-/-}$	Task3 (K^+ channel) knockout	Milder phenotype of aldosterone increase and hypertension
	Kcnk3$^{-/-}$ *and Kcnk9*$^{-/-}$	Task1 and 3 knockout	No zonation defect, but markedly higher aldosterone, regardless of Na^+ diet level
	Kcnmb1$^{-/-}$	Ca^{2+}-activated potassium channel β-subunit deletion	High aldosterone, BP, increased vasorelaxation
	Kcnma1$^{-/-}$	Ca^{2+}-activated potassium channel α-subunit deletion	High aldosterone, small BP increase, low plasma K^+, increased vascular tone
Wnt/β-catenin pathway activation	*Apc*$^{min/+}$	Disruption of Apc, part of the β-catenin destruction complex	Hypertension, increase in plasma aldosterone and corticosterone, increased K^+/decreased Na^+ excretion
	ΔCat	Constitutive activation of β-catenin in the adrenal gland	Severe hyperplasia, disrupted zonation, increased aldosterone and corticosterone
***Cyp11b2* Stabilization**	*Cyp11b2*$^{hi/hi}$	Stabilization of 3' UTR of *Cyp11b2*	Mild phenotype of increased Cyp11b2 expression
	hAS$^{+/-}$	Insertion of human *CYP11B2* under control of human *CYP11B1* promoter	High plasma aldosterone, BP, and *CYP11B2* gene expression
Other Causes	*Tgfb1*$^{L/L}$	Knockdown of TGFβ1 expression	Highly increased aldosterone to renin ratio, high BP, impaired natriuresis
	Enu	Random mutagenesis screen	High aldosterone-to-renin ratio and Cyp11b2 expression
	Siah1a$^{-/-}$	Deletion of E3 ubiquitin ligase	Disrupted adrenal morphology, zonation defects, increased aldosterone, decreased plasma K^+
	Cry-null	Circadian rhythm disruption	Increased aldosterone production and hypertension as a result of high Hsd3b6

Table 1.2. Summary of previous mouse models of primary aldosteronism. Modified from Aragao-Santiago et al. 2017 (169). BP, blood pressure; UTR, untranslated region.

CHAPTER 2

Chemogenetic Gq Signaling Disrupts Adrenal Zonation and Causes Primary Aldosteronism

2.1 Abstract

The mineralocorticoid aldosterone is produced in the adrenal zona glomerulosa (ZG) under the control of the renin-angiotensin II (AngII) system. Primary aldosteronism (PA) results from renin-independent production of aldosterone, and is a common cause of hypertension.. PA is caused by dysregulated expression of the enzyme aldosterone synthase (Cyp11b2), which is normally restricted to ZG. Cyp11b2 expression and aldosterone production are predominantly regulated by AngII activation of the Gq signaling pathway. Here, we report the generation of transgenic mice with adrenal cortex expression of Gq-coupled designer receptors exclusively activated by designer drugs (DREADDs). We show that adrenal-wide ligand activation of Gq DREADD receptors triggered disorganization of adrenal functional zonation, with induction of Cyp11b2 in glucocorticoid-producing zona fasciculata cells. This result was consistent with increased renin-independent aldosterone production and hypertension. All parameters were reversible following termination of DREADD Gq signaling. These findings demonstrate that Gq signaling is sufficient for adrenocortical aldosterone production and implicate the pathway in adrenal zonation homeostasis. This transgenic mouse also provides an inducible and reversible model of hyperaldosteronism to

investigate PA therapeutics and the mechanisms leading to aldosterone's damaging effects on the cardiovascular system.

2.2 Introduction

The human adrenal glands synthesize and secrete steroid hormones that play critical roles in blood pressure regulation, stress mediation, and sexual maturation. To accomplish these roles, the adrenal cortex is organized into three functionally and histologically distinct zones. The outermost zona glomerulosa (ZG) is responsible for maintaining sodium and potassium balance through secretion of mineralocorticoids, predominantly aldosterone. Aldosterone synthesis and secretion are tightly controlled by the renin-angiotensin-aldosterone system (RAAS). The zona fasciculata (ZF) produces glucocorticoids and the zona reticularis (ZR) produces a variety of androgen precursors. This functional zonation is maintained through differential expression of the enzymes required for mineralocorticoid vs. glucocorticoid production. The adrenal zones undergo a cell renewal process that involves lineal centripetal conversion of steroidogenic cells from a ZG to ZF phenotype. This process initiates with subcapsular stem and progenitor cells differentiating into aldosterone-producing ZG cells. These cells are then displaced inward to the medullary border where they undergo apoptosis, changing their zone-specific steroidogenic enzyme expression pattern throughout the process (25, 28-30, 32-34, 36, 183). Most recently, a lineage-tracing study revealed that the outer ZG cells repopulate nearly the entire adrenal cortex within 3 months (28). Although adrenocortical centripetal migration has been experimentally demonstrated, there remains controversy as to what factors contribute to the cellular phenotypic switch that occurs at zonal boundaries.

Physiologic regulation of aldosterone production involves the binding of angiotensin II (AngII) to its receptor (angiotensin II receptor type 1, AT_1-R) resulting in activation of the Gq protein family. Gq signaling through phospholipase C increases cytosolic calcium, which then activates calmodulin/calmodulin-dependent kinases (CaMKs) (89-93, 184-186). CaMKs initiate the activity of transcription factors that are critical for *CYP11B2* transcription (114). Due to the ZG-specific expression of AT_1R and CYP11B2 within the adrenal gland, aldosterone production is limited to adrenal ZG cells (10).

Disruption of zone-specific expression of steroidogenic enzymes is one characteristic of diseases of steroid imbalance. One such disease is primary aldosteronism (PA), which is the most prevalent cause of secondary hypertension, affecting 5-10% of hypertensive patients and 20% of those with resistant hypertension (127-132, 187). Production of aldosterone that is independent of circulating renin causes inappropriate renal sodium retention and consequently high blood pressure. PA patients are therefore susceptible to severe cardiovascular risks and complications (134, 135, 137, 138, 188). In addition to PA causing hypertension, inappropriate aldosterone enhances deleterious effects on the cardiovascular system, including cardiac hypertrophy and fibrosis (136, 139-141). Despite the high prevalence and mortality associated with PA, animal models for this disease are limited (169).

Designer receptors exclusively activated by designer drugs (DREADDs) are modified G protein-coupled receptors that bind synthetic ligands (189). This transgenic technology allows for chemogenetic activation of G protein signaling pathways. DREADD technologies include a modified human M3 muscarinic receptor used to

modulate Gq signaling (hM3Dq) (190-193). The receptor exclusively binds a small molecule ligand (clozapine N-oxide, CNO), thereby initiating Gq signaling. In the current study, we developed transgenic mice with pan-adrenocortical expression of hM3Dq receptors. Activation of adrenal Gq signaling promoted ectopic expression of Cyp11b2 in the ZF. Mice also exhibited a PA phenotype with renin-independent aldosterone production and hypertension. Furthermore, beyond triggering aldosterone production, the presence of Gq signaling may contribute to maintenance of an adrenal ZG cellular phenotype.

2.3 Results

Generation of AS$^{+/Cre}$::hM3Dq mice. hM3Dq mice contain a transgene encoding the hM3Dq DREADD (190). The *hM3Dq* transgene is expressed exclusively in the presence of Cre expression, and contains an HA-tag sequence (190). Expression of *hM3Dq* was driven specifically to the adrenal cortex through crossing to the aldosterone synthase Cre (*AS*-Cre) mouse line (Figure 2.1). *AS*-Cre mice have Cre-recombinase inserted into the *Cyp11b2* locus (28). Mice were bred as heterozygous for *AS*-Cre (*AS$^{+/Cre}$::hM3Dq*), allowing them to maintain *Cyp11b2* expression (28). Expression of hM3Dq was confirmed by HA-tag immunofluorescence (IF) staining. Adrenal *Cyp11b2* expression arises after birth, therefore low-level adrenal hM3Dq expression was seen early in life at 3 weeks of age (Figure 2.8). Centripetal migration of Cre-recombined cells led to adrenocortical hM3Dq expression that increased through life (Figure 2.8). The majority of cortical cells contained hM3Dq by 20 weeks of age, with no expression in the medulla (Figure 2.1). Due to this caveat, experiments used *AS$^{+/Cre}$::hM3Dq* mice that

were 18-22 weeks of age. In mice that lacked Cre and were wild-type for AS (*AS*$^{+/+}$*::hM3Dq*), there was no expression of HA-tag stained hM3Dq (data not shown).

Cortical activation of Gq signaling results in hyperaldosteronism. Female *AS*$^{+/Cre}$*::hM3Dq* mice treated with CNO for 7 days significantly increased *Cyp11b2* transcript levels by 6.5-fold above vehicle (Veh) treated mice as assessed by quantitative RTPCR (qPCR) (Figure 2.2C). This correlated with a significant increase in Cyp11b2 protein expression and 3.1-fold higher circulating aldosterone levels in CNO-treated females (Figure 2.2, D and E). Interestingly, zonation of Cyp11b2 was disordered, as Cyp11b2 positive cells were found in the ZF as well as the ZG. Double IF suggested that some ZF cells co-expressed Cyp11b1 and Cyp11b2 with a smaller subset exclusively expressing Cyp11b2 (Figure 2.2D). The increase in aldosterone levels was variable, with some CNO-treated mice producing greater than 1000 pg/ml of aldosterone, while others had more moderate increases (Figure 2.2E). 18-hydroxycorticosterone (18OHB), the final steroid precursor for the synthesis of aldosterone, was also significantly increased following CNO treatment (2.6-fold), but there was no change in concentrations of the earlier precursor, 11-deoxycorticosterone (11DOC) (Table 2.1). Kidney RNA was isolated to detect *Ren1* mRNA, the mouse transcript that encodes renin in the juxtaglomerular renal cells. *Ren1* mRNA was significantly decreased in female CNO-treated mice, illustrating a suppression of the RAAS (Figure 2.2F). This verified that the hM3Dq-induced aldosterone production was renin independent, as seen in PA. Of the genes encoding adrenal steroidogenic enzymes, *Cyp11b2* was the only upregulated gene. Furthermore, *Star, Hsd3b1,* and *Cyp11b1* all had small but significant decreases in expression, with downward trends

also observed for transcripts encoding the other steroidogenic enzymes (Figure 2.2C). These data demonstrate that the increase in aldosterone secretion in CNO treated mice is a direct effect of increased Cyp11b2 transcript and protein levels, rather than targeted increases in other enzymatic steps in steroidogenesis. Despite the slight decrease in *Cyp11b1* transcription, there was not a significant decrease in plasma corticosterone levels (Figure 2.2E). It is worth noting that *AS*$^{+/+}$*::hM3Dq* control mice littermates did not have any significant responses (in steroids or steroidogenic enzyme mRNA expression) to 7 days of CNO treatment (data not shown).

Female *AS*$^{+/Cre}$*::hM3Dq* mice did not have a significant difference in body weight following 7 days of CNO treatment (Figure 2.9A). Interestingly, there was a minor but significant decrease in adrenal size relative to body weight in CNO-treated females in the left adrenal, and a trend for a decrease in the right adrenal (Figure 2.9C). Nevertheless, there were no obvious changes to adrenal morphology assessed by H&E staining after 7 days of CNO (Figure 2.9B).

Male mice did not exhibit the same phenotype as females. Although plasma aldosterone production was significantly upregulated 1.8-fold higher than control mice, there were no significant changes in *Cyp11b2* mRNA levels (Figure 2.10, A and C). Additionally, when IF was performed, the Cyp11b2 expression was largely sequestered to the ZG with less ZF expression compared to that of females (Figure 2.10B). The small increase in aldosterone did not inhibit renin production, as kidney *Ren1* transcript showed no significant difference between groups (Figure 2.10D). This sexual dimorphic response could partly be explained by the unequal hM3Dq expression at 20 weeks of age in males and females (Figure 1.1C). A previous mouse model that also utilized the

AS-Cre mouse line to drive adrenal cortex Cre expression exhibited a similar sex difference in adrenal remodeling, which led to a more robust phenotype in females at an earlier age (64).

Gq signaling contributes to the ZG cell phenotype. We also examined the expression of disabled homolog 2 (Dab2), a ZG-specific protein that participates in aldosterone production and is regulated by AngII (194). Following 7 days of CNO treatment, Dab2 was no longer restricted to the ZG in female mice, as several ZF cells were also positive for Dab2 (Figure 2.3A). This coincided with a 1.5-fold increase in *Dab2* transcript levels in adrenals of female $AS^{+/Cre}$*::hM3Dq* mice treated with CNO (Figure 2.3B).

Wnt/β-catenin signaling has implications in adrenal development, growth, cell replenishment, and is preferentially activated in the ZG compared to other cortical zones (38-42, 66). Therefore, we determined whether chemogenetic Gq signaling would be sufficient to induce active Wnt/β-catenin signaling in the ZF. IF for active β-catenin found localization to be limited to the ZG in both vehicle control and CNO-treated female mice, with only minor activation in the outer ZF cells (Figure 2.3C). Furthermore, qPCR for the canonical Wnt pathway target gene *Axin2* revealed no change between vehicle and CNO groups (Figure 2.3D). This suggests that the Cyp11b2 positive ZF cells have not undergone a complete phenotypic switch to a ZG cell. It also indicates that aldosterone production *per se* is not reliant on Wnt/β-catenin-signaling, as Cyp11b2 is able to turn on in the ZF following activation of Gq signaling.

hM3Dq-induced aldosterone production bypasses high sodium diet suppression of the RAAS. High sodium diets (HS) inactivate adrenal aldosterone synthesis through

suppression of renin under normal physiological conditions (111). This was apparent in *AS$^{+/Cre}$::hM3Dq* mice fed HS for 3 days prior to CNO treatment. To determine if CNO treatment could override RAAS suppression, mice were split into two groups: 1) HS + 2 days of CNO treatment and 2) HS + 7 days of CNO treatment (Figure 2.4A). Alongside these groups, we used littermates treated with HS + Veh as controls. The two time points allowed us to examine the temporal regulation of aldosterone synthesis by the hM3Dq system. In female mice administered HS + CNO for 2 days, we found that aldosterone significantly increased 2.6-fold, and *Cyp11b2* mRNA levels also increased 8.3-fold above HS + Veh treated controls (Figure 2.4, B and C). When IF staining was assessed, Cyp11b2 protein was detected in the ZG and in the ZF at variable levels (Figure 2.4D). On day 2 of treatment, ZF Cyp11b2 expression was almost exclusively in cells that co-expressed Cyp11b1 in the majority of mice. In comparison, mice that were treated with HS + CNO for 7 days robustly increased aldosterone production by 105-fold through an upregulation of *Cyp11b2* transcript levels by 44-fold relative to HS + Veh controls (Figure 2.4, B and C). The levels of aldosterone in these 7 day HS + CNO treated mice averaged 1949 pg/ml, a remarkable increase from the 285 pg/ml average of the 2 day HS + CNO mice. 18OHB also increased significantly in both the 2 day (1.8-fold) and 7 day cohorts (33-fold) (Table 2.1). No significant changes were observed in 11DOC or corticosterone under these protocols (Table 2.1). Moreover, the level and disorganization of Cyp11b2 protein expression was higher than in the 2 day treated samples (Figure 2.4D). These mice also had a subset of ZF cells with exclusive expression Cyp11b2 after 7 days of HS + CNO treatment (Figure 2.4D). These observations validate the ability of CNO to elevate aldosterone secretion independent of

renin, even at an early timepoint. In addition, these data suggest that prolonged activation of ZF Gq signaling can promote the development of an aldosterone-producing cellular phenotype.

Male *AS$^{+/Cre}$::hM3Dq* mice in this cohort were also assessed. At the 2 day timepoint, HS + CNO treated males displayed a 3.8-fold upregulation in circulating aldosterone, with an average of 289 pg/ml (Figure 2.10F). In addition, adrenal *Cyp11b2* transcripts increased by 9.7-fold (Figure 2.10E). The 2 day male response was similar to that seen in females, but in the 7 days HS + CNO treated group the response of males diverged from females with lower levels of circulating aldosterone (482 pg/ml average) and adrenal *Cyp11b2* (6.5-fold compared to controls) (Figure 2.10, E and F).

Washout of CNO normalizes the PA phenotype in AS$^{+/Cre}$::hM3Dq mice. To address whether the PA phenotype observed in the *AS$^{+/Cre}$::hM3Dq* was reversible, we designed a CNO washout experiment. All mice were administered HS for a 3 day period, and then given HS + CNO for 7 days. One group of mice was sacrificed, whereas another group was maintained on HS diet without CNO (Figure 2.5A). When analyzing mRNA and steroid data, we compared both groups to the previously described 7 day HS + Veh group (Figure 2.4). Mice treated with HS + CNO had robust elevations of both Cyp11b2 and aldosterone, with the same level of disorganization in Cyp11b2 expression as described above (Figure 2.5, B-D). Strikingly, upon CNO removal, 10 days was sufficient to reverse the phenotype for all parameters back to baseline levels (Figure 2.5, B-D).

hM3Dq activation causes hypertension. To ascertain whether the adrenal and steroid phenotype in the *AS$^{+/Cre}$::hM3Dq* mice recapitulated the hypertension seen in

PA, we evaluated the blood pressure. Radiotelemetry allowed continuous monitoring of blood pressure in real time. After recovery from surgery, mice were given a HS diet for 3 days, followed by 7 days of HS + CNO (Figure 2.6A). HS alone did not elevate mean arterial pressure (MAP), while HS combined with CNO increased blood pressure by an average of 11.2 mmHg compared to the HS alone across the full treatment period (Figure 2.6B). Treatment caused similar increases in both systolic and diastolic pressures. Hourly MAPs were increased within 24 hours of HS + CNO treatment, with significant increases observed within the animal's dark cycle and every hour of the subsequent light cycle (Figure 2.6C). Upon CNO removal, MAP decreased over the course of the 10-day washout (Figure 2.6D).

2.4 Discussion

The current study suggests that activation of Gq signaling is sufficient to cause glucocorticoid-producing ZF cells to regain the ability to produce aldosterone. The ectopic expression of Cyp11b2 leads to renin-independent hyperaldosteronism resulting in a significant increase of MAP. The *AS*$^{+/Cre}$*::hM3Dq* phenotype is reversible upon removal of the activating ligand, CNO. Taken together, targeted expression of hM3Dq to the adrenal cortex has provided new insights into adrenocortical cell plasticity and a new inducible/reversible model to study primary aldosteronism.

There are several features that define the adrenal ZG. These include the capacity to produce aldosterone as well as the capacity to provide cells needed to repopulate the adrenal cortex through centripetal migration. Activation of hM3Dq receptors partially reverted ZF cells to a ZG phenotype, particularly regarding aldosterone production. This is illustrated by the ZF localization of Cyp11b2, elevated

circulating aldosterone and suppression of renal Ren1 expression. We also found that the ZG-specific protein Dab2 (182, 194) could be detected in some ZF cells following CNO treatment, combined with a significant increase in its adrenal mRNA. These findings imply that ZF loss of AT_1-R expression, and consequently AngII-mediated Gq signaling might be a factor involved in the ZG to ZF cell transition. However, it appears that Gq signaling alone is not sufficient for a complete ZF to ZG cell transition. Our data suggest that activation of Gq signaling throughout the adrenal does not alter the localization of Wnt/β-catenin, which is primarily a ZG-restricted pathway. Wnt/β-catenin signaling has an important role in adrenal development and tissue homeostasis (39). Within the ZG most cells are both β-catenin and Cyp11b2 positive (40), and it has been suggested that Wnt/β-catenin signaling can control aldosterone production (41, 195). Activating mutations in *CTNNB1*, the gene that encodes β-catenin, have also been described in a small subset of aldosterone-producing adenomas (43, 45, 196, 197). Therefore, while it is clear that the Wnt/β-catenin pathway is involved in ZG aldosterone production, these data demonstrate that it may not be essential for the Gq signaling steps downstream of AT_1R binding of AngII. This aligns with the previously reported role of β-catenin in stimulating *AT_1R* expression (41), a mechanism that is upstream of the hM3Dq-induced Gq activation. It is also possible that Wnt/β-catenin signaling could activate aldosterone synthesis through a separate mechanism than regulating the potential for Gq signaling.

With the *$AS^{+/Cre}$::hM3Dq* model, we have created a novel tool for researchers to study PA, hypertension, and peripheral tissue damage caused by inappropriate aldosterone production. There have been several previous mouse models that exhibit a

PA phenotype. A series of papers have linked constitutive inactivation of various potassium channels to hyperaldosteronism in vivo (170-175, 198, 199). Disruption of the circadian clock through *Cry1/Cry2* knockout have also caused elevated plasma aldosterone and salt-sensitive high blood pressure (178). One study utilized a mutagenesis screen to link mutations to hyperaldosteronism phenotypes (179). Increasing aldosterone synthesis and salt-sensitive blood pressure has also been accomplished through transgeni stabilization of the 3' untranslated region of *Cyp11b2* or overexpression of the human *CYP11B2* gene (180, 181). Most recently, inactivation of an E3 ubiquitin ligase, Siah1, led to an increase of Cyp11b2 expression and aldosterone production (182). While previous findings have advanced the field, the aforementioned transgenic models of PA are associated with the onset of autonomous aldosterone production at birth. Thus, these models do not accurately recapitulate PA as it is typically an adult onset disease. Furthermore, the aldosterone excess seen in these mice is not reversible. Mice can also be treated with mineralocorticoids for the study of peripheral effects of mineralocorticoid receptor activation, but this does not address the impaired adrenal zonation that exists in cases of PA. In addition, the minipumps used for administration of aldosterone, as well as the cost of this steroid, limits this experimental approach. Therefore, the *AS*$^{+/Cre}$*::hM3Dq* mouse model provides an attractive transgenic PA model that is inducible and reversible, and is the first use of DREADD technology in the adrenal gland.

Future studies will be needed to determine the cause of the sexual dimorphism observed in the *AS*$^{+/Cre}$*::hM3Dq* mouse line. This can partially be attributed to a slower rate of adrenocortical cell turnover in males compared to females, resulting in lower

expression of the hM3Dq receptor in males until late in life. However, the rather large disparity between male and female response implies that additional underlying factors may be at play. Sexual dimorphism in the mouse adrenal is well established with clear sex differences in gene expression observed within the adrenal gland (200). Several previous mouse models of adrenal dysfunction have had varying results between sexes (64, 170, 172, 179, 198, 201). This further argues for a sex-dependent mechanism of adrenal regulation, possibly driven by androgens or estrogens.

In summary, this study supports a role for Gq signaling in adrenocortical functional zonation and the induction of an aldosterone-producing cell phenotype. Our findings indicate that the Gq signaling pathway is sufficient to trigger Cyp11b2 expression in non-aldosterone producing ZF cells. This suggests that adrenocortical cells possess plasticity in steroidogenic potential, and their steroidogenic role can be transformed when exposed to a stimulus such as Gq signaling. Nevertheless, further work will be needed to address whether Gq signaling is necessary for physiologic maintenance of a ZG cellular identity. Future studies with the *AS*$^{+/Cre}$*::hM3Dq* mouse line will also aid in defining the mechanisms whereby sustained inappropriate aldosterone production causes deleterious effects in peripheral tissues, and provide a -preclinical model to for potential PA therapeutic targets.

2.5 Methods

Mice. Both the *AS*-Cre (28) and *hM3Dq* (190) lines have been previously described. *AS*$^{+/Cre}$*::hM3Dq* mice were maintained on a mixed background, with littermate controls used when possible to control for genetic variability. Mice in all experiments were 18-22 weeks old at the start of each experimental protocol. CNO

(Tocris Bioscience, Bristol, United Kingdom) was dissolved in dimethyl sulfoxide (DMSO) at 30 mg/ml. CNO treated mice were administered 50 µg/ml CNO in drinking water in addition to 5 mM saccharin for taste. Vehicle treated mice were administered 5 mM saccharin and 0.17% DMSO (the same as CNO animals). The water was provided ad libitum, and replaced every 2 days. Mice were fed ad libitum with a standard chow diet (Research Diets, New Brunswick, NJ) or high sodium diet (Envigo, Huntington, United Kingdom) that contained 4% NaCl. All mice were maintained under a 12-hour light/12-hour dark cycle. Mice were housed in the Unit for Laboratory Animal Management facility at University of Michigan.

Real-time PCR analysis. RNA was isolated from whole adrenals using bead homogenization method and the RNEasy Plus Mini Kit (Qiagen, Hilden, Germany). In kidney experiments, frozen kidneys were first pulverized into a frozen powder that was used for RNA extraction. Reverse transcription was performed using the High Capacity cDNA Reverse Transcription Kit (Applied Biosystems, Foster City, CA). qPCR was performed using Taqman or SYBR green primer sets and data was analyzed as relative expression using the delta/delta CT method. Taqman primers from Applied Biosystems were: *Cyp11a1* (Mm00490735_m1), Cyp21a1 (Mm00487230_g1), *Hsd3b1* (Mm01261921_mH), *Ppia* (Rn00690933_m1), *Ren1* (Mm02342887_mH), *Star* (Mm00441558_m1). Taqman primers designed through Integrated DNA Technologies (Coralville, IA) were: *Cyp11b1* F (5'– GTCCTCAATGTGAATCTGTATTCCA – 3'), *Cyp11b1* R (5'-CCAGCGCTGAGGCATATAGC-3'), *Cyp11b1* probe (5'-56-FAM/ CCGGAACCCTGCAGTG-3'), *Cyp11b2* F (5-TGCTGGGACATTGGTCCTACT-3'), *Cyp11b2* R (5'-CTTGGGAACACTGCAGGGTT-3'), *Cyp11b2* probe (5'-56-FAM/

TATCTCTAC /ZEN/ TCCATGGGC-3'). SYBR green primer sets from Integrated DNA Technologies were: *Axin2* F (GAGGATGCTGAAGGCTCAAA), *Axin2* R (GCAGGCAAATTCGTCACTC), *Dab2* F (TGTTGGCCAGGTTCAAAGGT) *Dab2* R (GCACATCATCAATACCGATTAGCT).

Immunofluorescence and histology analysis. Whole adrenal glands were fixed in 4% paraformaldehyde for 1 hour. These tissues were processed, embedded in paraffin, and sectioned at 5 μm thickness. Antibodies used were anti-HA High Affinity (1/500, Roche, Basel, Switzerland, 11867423001) anti-Cyp11b2 (1/200, gift from C. Gomez-Sanchez, University of Mississippi), anti-Cyp11b1 (1/100, gift from C. Gomez-Sanchez, University of Mississippi), anti-Dab2 (1/500, BD Biosciences, San Jose, CA, #610464), and anti-β-Catenin (1/500, Cell Signaling, Danvers, MA, #8814). Histologic analysis of tissues was assessed on H&E stained sections.

Steroid Measurements. Trunk blood from decapitated mice was collected in sodium heparin tubes, and plasma was isolated by centrifugation. We quantified 4 C_{18} steroids using LC-MS/MS: 11-deoxycorticosterone, corticosterone, 18-hydroxycorticosterone, and aldosterone. Unlabeled and deuterium-labeled steroids were obtained from Sigma-Aldrich, Cerilliant and C/D/N isotopes (Table 2.2). Steroid extraction by liquid-liquid extraction and quantitation was carried out as previously described (202).

Samples (10 μL) were injected via autosampler and resolved with a pair of Agilent 1260/1290 binary pump HPLCs via 2D liquid chromatography, first on a 10 mm x 3 mm, 3 μm particle size Hypersil Gold C4 loading column (Thermo Scientific, Waltham, Massachusetts) followed by a Kinetex 50 mm x 2.1 mm, 2.6 μm particle size

biphenyl resolving column (Phenomenex, Torrance, CA). The mobile phases consisted of 0.2 mmol/L aqueous ammonium fluoride (mobile phase A) and methanol with 0.2 mmol/L ammonium fluoride (mobile phase B). Steroids were eluted using gradient specifications as described in Table 2.3. The column effluent was directed into the source of an Agilent 6495 triple quadrupole mass spectrometer using electrospray ionization in positive ion mode for Δ4 and analyzed using multiple reaction monitoring (MRM) mode (Table 2.3). Quantitation was accomplished by comparing ion currents for the monitored ions with weighted (1/x) 12-point linear external calibration curves (r2 was >0.995) and corrected for specimen dilution and recovery of internal standards using ChemStation and MassHunter software (Agilent, Santa Clara, CA). Intra-assay and inter-assay coefficients of variation (CV) were assessed by measuring quality control pooled serum samples five times within a run and across five different runs, respectively, and they were < 12% for all steroids. The lower limit of detection (LOD) for each steroid was defined by the minimum concentration achieving an extrapolated signal-to-noise ratio of 3, and it ranged from 3.0 pg/mL for aldosterone to 44.4 pg/mL for corticosterone (Table 2.2).

Radiotelemetry. Mice were surgically implanted with a telemetric blood pressure transducer (Data Sciences International, St. Paul, MN) by the University of Michigan Physiology Phenotyping Core, as previously described (203). The catheter of the device was passed into the carotid artery and the transducer was placed in the abdominal cavity. Mice were monitored postoperatively and were given 2 weeks to recover from surgery prior to treatment. Mice were individually housed in cages atop receiver pads allowing for real-time measurements of blood pressure. As stated by DSI, the mean

pressure parameter value was calculated by averaging the pressure values over 50 sub-segments of the segment length.

Statistics. Data is represented as mean ± SEM. The box and whisker plots in Figure 6 B and D depict the interquartile range between the 25th and 75th percentile with the median (box), along with the maximum and minimum (whiskers). For groups of two, an unpaired two-tailed Student's t-test was used for comparison. One-way ANOVA with a Bonferroni post-hoc analysis was used for groups of three or more. Figure 2.6B used a repeated measures one-way ANOVA with a Bonferroni Correction for multiple comparisons. Comparison of hourly blood pressure values (Figure 2.6C) used a repeated measures two-way ANOVA with a Bonferroni correction. Direct comparison of HS + CNO and CNO washout blood pressures (Figure 2.6D) used a paired two-tailed Student's t-test. All immunofluorescent experiments were performed in n ≥ 5 animals. Statistical tests were calculated using GraphPad Prism 7.0 software. Data was considered statistically significant with a *P* value of less than 0.05.

Study approval. All animal procedures were approved by the Institutional Animal Care and Use Committee at University of Michigan.

2.6 Acknowledgments

This project was supported by grants from the NIH (DK043140 to William E. Rainey, and GM008322 to Matthew J. Taylor) and the AHA (16PRE29620010 to Matthew J. Taylor). We would like to thank Steven E. Whitesall and Daniel E. Michele from the University of Michigan Phenotyping Core for their collaboration on the radiotelemetry surgeries, experiments, and data analysis.

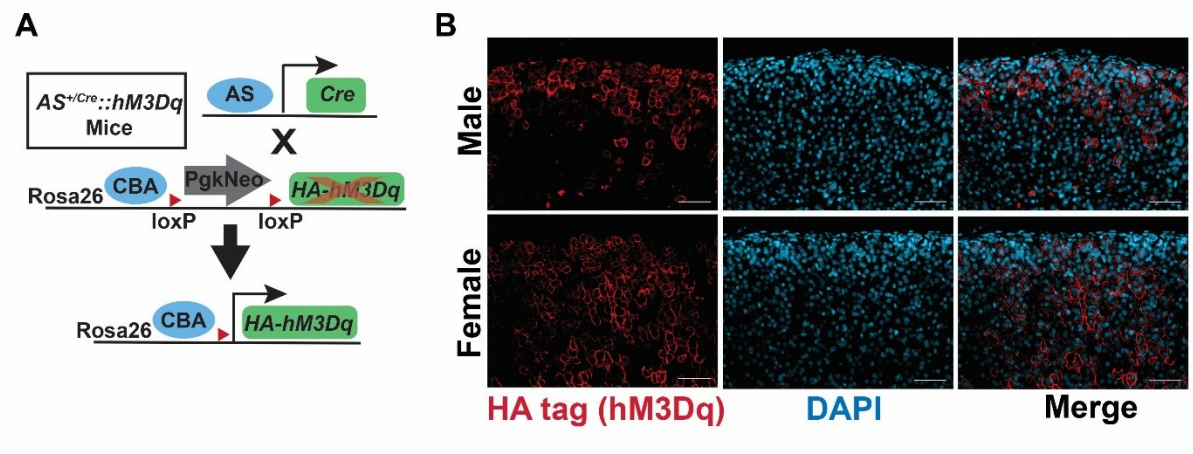

Figure 2.1. Adrenocortical specific expression of hM3Dq driven by *AS*-Cre. (A) *AS*$^{+/Cre}$*::hM3Dq* mouse cross. *AS*-Cre mice were bred as heterozygous for the Cre allele (*AS*$^{+/Cre}$) and crossed to the *hM3Dq* line. Mice were bred on a homozygous *hM3Dq* background. Cre recombination resulted in an excision of the upstream Pgk-neomycin cassette at the loxP sites, allowing transcription of *hM3Dq* in Cre positive cells. (B) Immunofluorescent labeling of hM3Dq. The *hM3Dq* transgene has an HA tag, allowing for detection of the receptor via HA tag immunofluorescence. Adrenals pictured are from 20 week old mice. DAPI (blue) marks the nuclei. Scale bars: 50 μm.

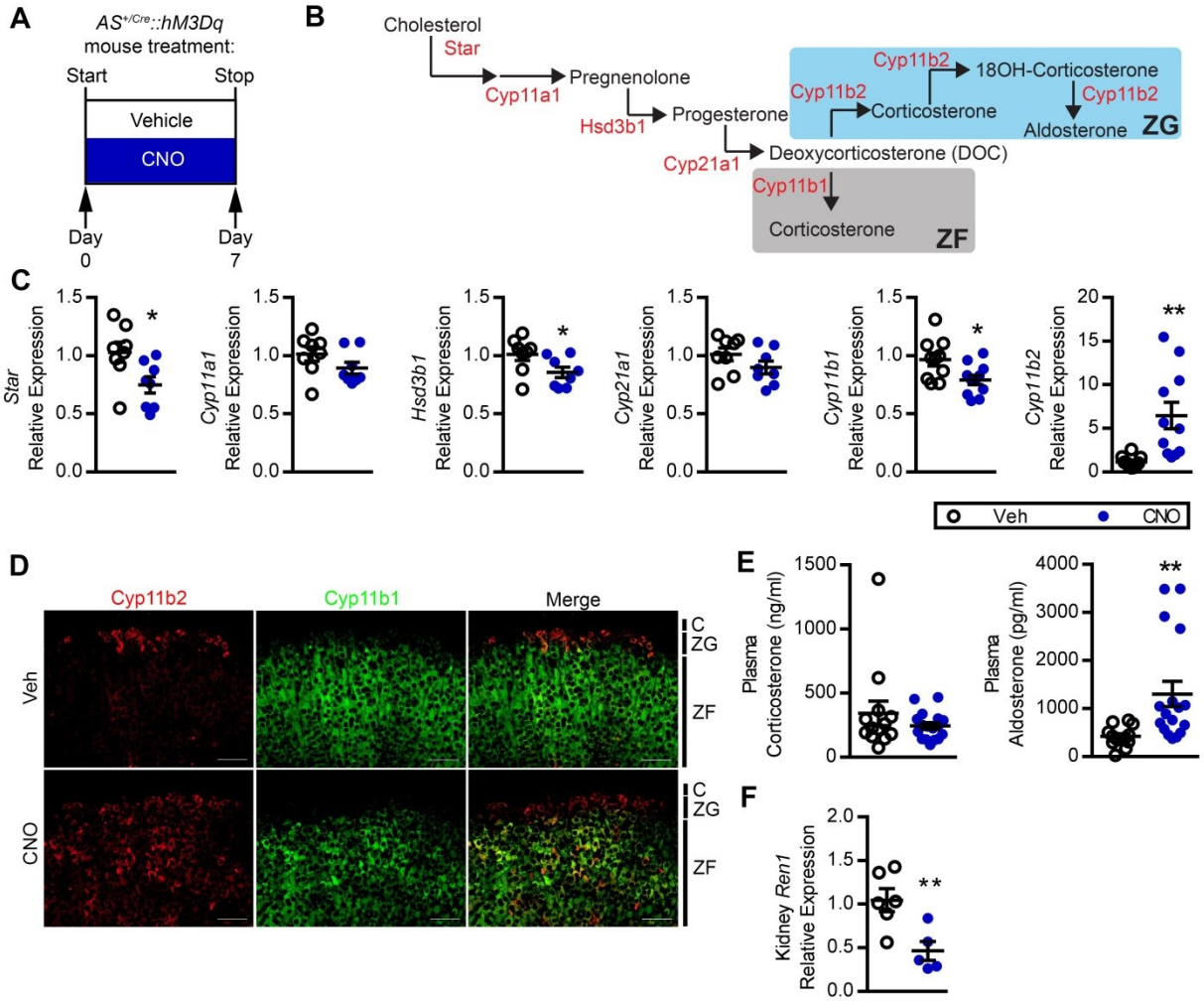

Figure 2.2. CNO activation of adrenal-hM3Dq upregulates Cyp11b2 expression and aldosterone production. **(A)** Experimental protocol. 18-20 week old female *AS*$^{+/Cre}$*::hM3Dq* mice were treated with either CNO (50 µg/ml) or vehicle in their drinking water *ad libitum* for 7 days prior to sacrifice. **(B)** Mouse adrenal steroidogenic pathway. Star transports cholesterol to the inner mitochondrial membrane where it is converted to pregnenolone prior to downstream conversions to either glucocorticoids (ZF) or mineralocorticoids (ZG) by steroidogenic enzymes. **(C)** qPCR analysis of steroidogenic enzyme mRNA in whole adrenal tissue. For steroidogenic enzymes, n = 8 for both groups, except for *Cyp11b1* and *Cyp11b2*, where n = 10 for vehicle and n = 11 for CNO. **(D)** Immunofluorescence of Cyp11b2 and Cyp11b1. **(E)** Steroid measurements measured by LC-MS/MS. For steroids, n = 13 for vehicle, n = 17 for CNO. **(F)** qPCR analysis of kidney *Ren1*. For *Ren1* analysis, n = 6 for vehicle, n = 5 for CNO. C, capsule; ZG, zona glomerulosa; ZF, zona fasciculata; Veh, vehicle. Bars in dot plots represent mean ± SEM. Scale bars = 50 µm. Statistical analysis used for dot plots was unpaired two-tailed Student's *t* test. **P* < 0.05, ***P* < 0.01.

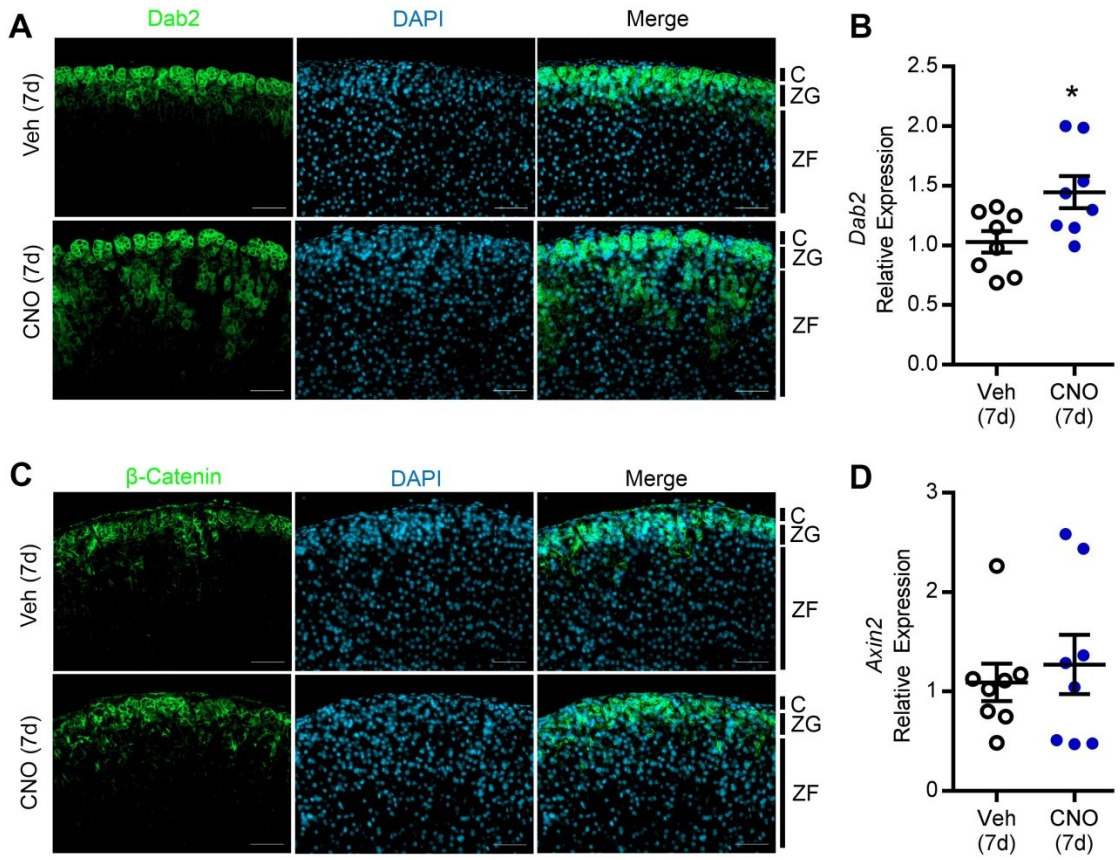

Figure 2.3. *AS*$^{+/Cre}$*::hM3Dq* mice have increased expression of ZG marker Dab2 with no changes in the ZG specific Wnt pathway. (A) Immunofluorescent staining for the ZG-specific Dab2 protein (green). **(B)** qPCR analysis for whole adrenal *Dab2* mRNA. **(C)** Immunofluorescent staining for active β-Catenin (green). **(D)** qPCR analysis for whole adrenal mRNA expression of the Wnt pathway target gene *Axin2*. C, capsule; ZG, zona glomerulosa; ZF, zona fasciculata; Veh, vehicle; 7d, 7 days. For qPCR analysis, n = 8 for both groups. Bars in dot plots represent mean ± SEM. Scale bars = 50 μm. DAPI (blue) stained the nuclei in both A and C. Statistical analysis used for dot plots was unpaired two-tailed Student's *t* test. *$P < 0.05$.

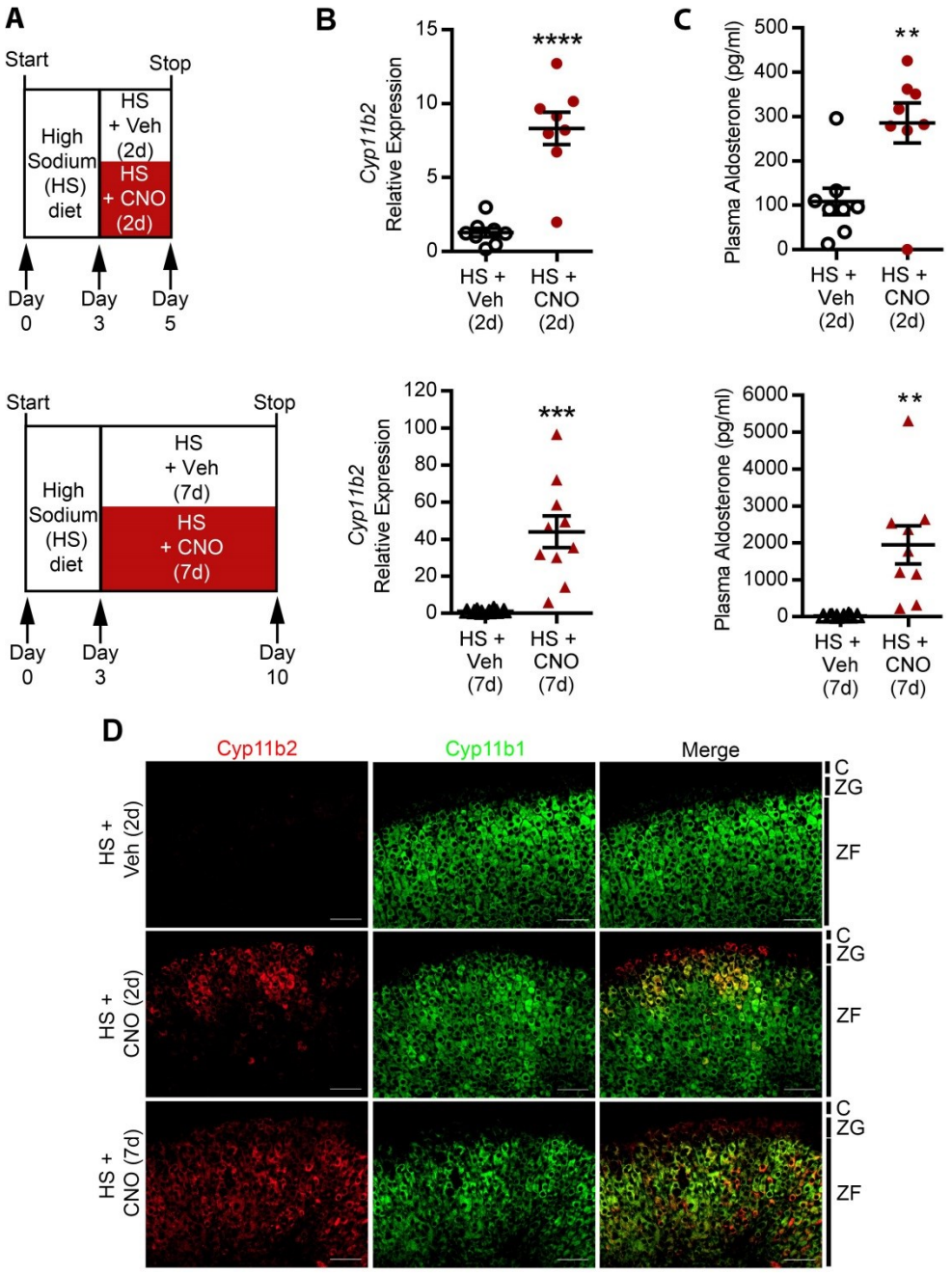

Figure 2.4. *AS*$^{+/Cre}$*::hM3Dq* mice activate Cyp11b2 and aldosterone production in the presence of high sodium. (A) *AS*$^{+/Cre}$*::hM3Dq* female 20-22 week old mice were fed a high sodium (HS) diet for 3 days. One group then received HS + CNO or HS + vehicle for 2 days and the other HS + CNO or HS + vehicle for 7 days prior to sacrifice. **(B)** qPCR analysis for whole adrenal *Cyp11b2* mRNA. **(C)** LC-MS/MS analysis of plasma aldosterone concentration. **(D)** Immunofluorescent staining of Cyp11b2 (red) and Cyp11b1 (green). C, capsule; ZG, zona glomerulosa; ZF, zona fasciculata; Veh, vehicle; 7d, 7 days. For steroids and qPCR, n = 8 for all groups except HS + CNO (7d), where n = 10. Bars in dot plots represent mean ± SEM. Scale bars = 50 µm. Statistical analysis used for dot plots was unpaired two-tailed Student's *t* test. ***P* < 0.01, ****P* < 0.001, *****P* < 0.001.

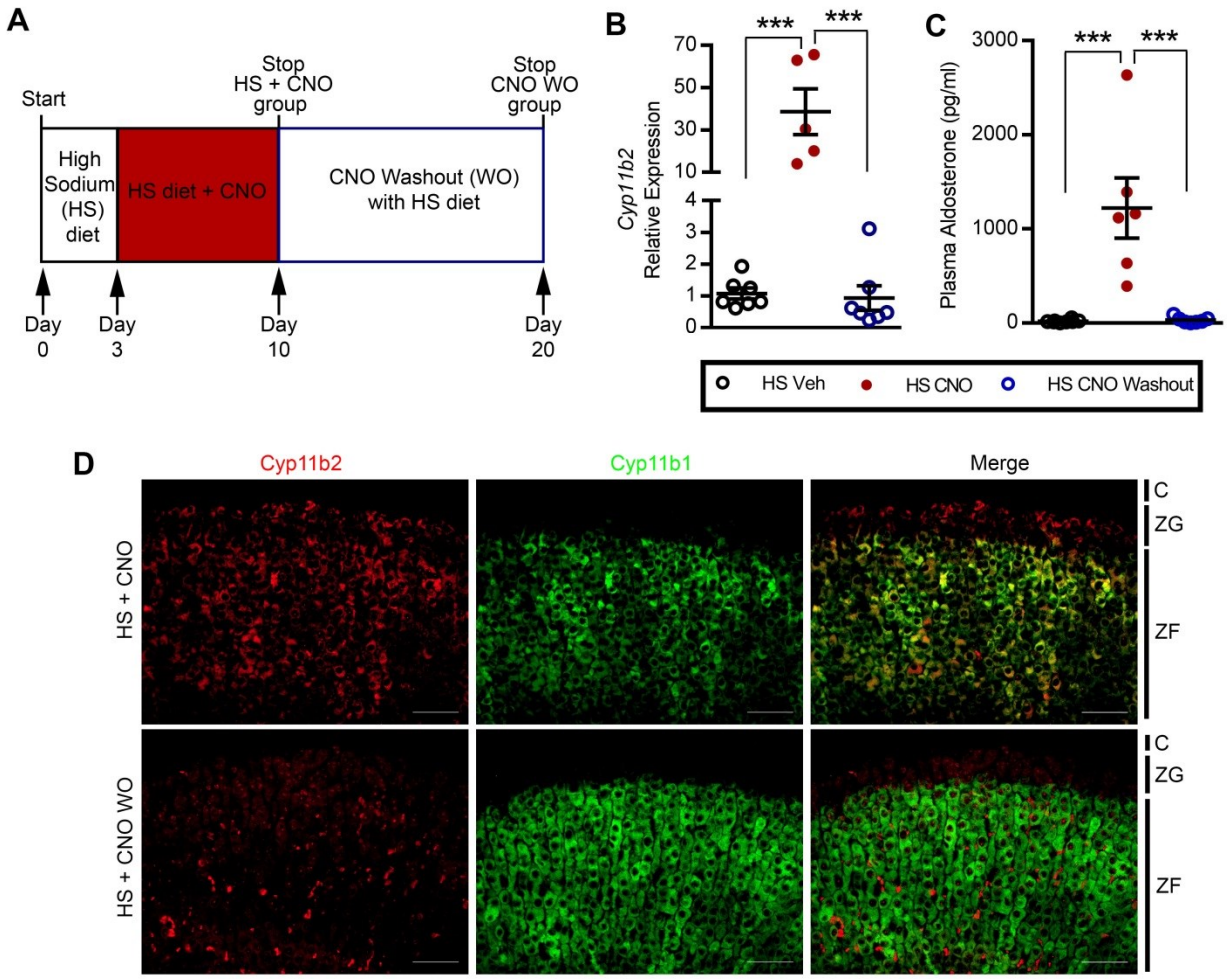

Figure 2.5. CNO washout causes reversal of the PA phenotype in *AS$^{+/Cre}$::hM3Dq* mice. (A) Experimental protocol. 20-22 week old *AS$^{+/Cre}$::hM3Dq* female mice were treated with high sodium (HS) diet for 3 days. All mice were then administered HS + CNO for 7 days. One group was sacrificed at 7 days (HS + CNO group) while the other initiated a washout protocol for an additional 10 days with HS diet but without CNO (HS + CNO WO group). **(B)** qPCR analysis of whole adrenal *Cyp11b2* mRNA. For qPCR, HS Veh, n = 7, for HS CNO, n = 5, and for HS CNO washout, n = 7. **(C)** LC-MS/MS measurement of plasma aldosterone. For steroids, HS Veh, n = 8, for HS CNO, n = 6, and for HS CNO washout, n = 7. **(D)** Immunofluorescent staining of Cyp11b2 (red) and Cyp11b1 (green). For (B) and (C), mice from both groups were compared to previously described HS + Veh controls (Figure 4). C, capsule; ZG, zona glomerulosa; ZF, zona fasciculata. Bars in dot plots represent mean ± SEM. Scale bars = 50 μm. Statistical analysis used for dot plots was one-way ANOVA with a Bonferroni correction. ***$P < 0.001$.

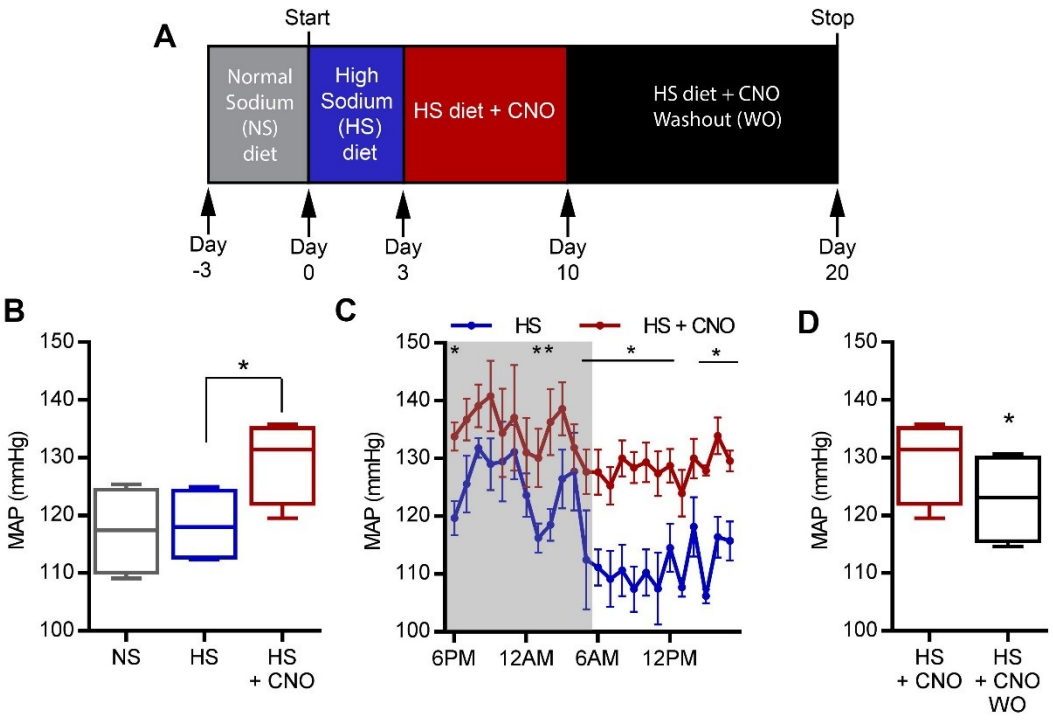

Figure 2.6 High sodium diet plus CNO increases blood pressure in *AS$^{+/Cre}$::hM3Dq* mice. (A) Experimental protocol. 20 week old *AS$^{+/Cre}$::hM3Dq* female mice (n = 4) were implanted with a radiotelemetry device and given 2 weeks for recovery. The final 4 days prior to treatment were analyzed as the baseline (normal sodium diet, NS). Mice then received a high sodium (HS) diet for 3 days followed by HS + CNO for 7 days. CNO washout then lasted 10 days. HS was maintained during washout. Mean arterial pressure (MAP) was continuously recorded throughout the experiment. **(B)** MAP in NS, HS, and HS + CNO complete treatment periods. **(C)** Hourly MAP overlaid for the same mice using the final 24 hours of HS alone (blue), and the 24 hours of the 2nd day of CNO treatment (Day 4 in panel A). Gray box signifies dark (active) period. The 2nd day was chosen to allow orally given CNO to raise aldosterone levels. **(D)** MAP in HS + CNO and HS CNO washout complete treatment periods. Data in (B) and (D) represented as the interquartile range with median (box) and the minimum/maximum (whiskers). Data in (C) represented as mean ± SEM of the mice within each hour. Statistical analysis used for (B) was repeated measures one-way ANOVA with a Bonferroni correction. Statistical analysis used for (C) was a repeated measures two-way ANOVA with a Bonferroni correction. Statistical analysis used for (D) was a paired two-tailed Student's t-test. *$P < 0.05$.

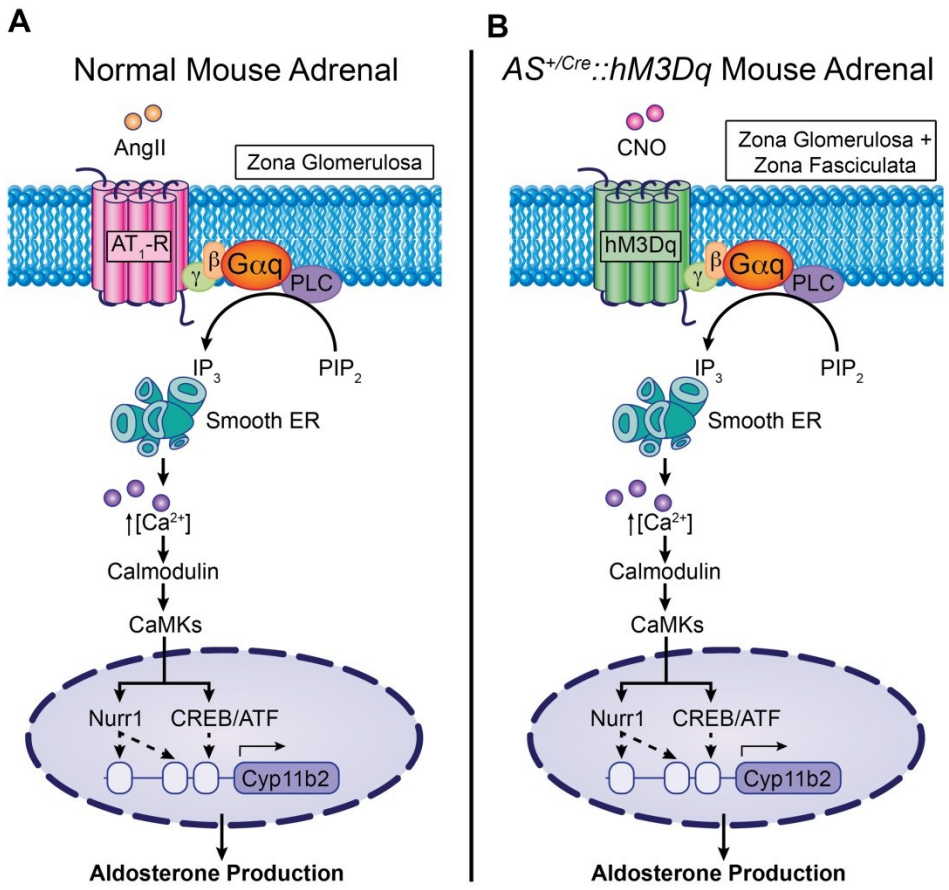

Figure 2.7. Activation of Gq signaling in both the normal and *AS*$^{+/Cre}$*::hM3Dq* mouse adrenal cells. (A) Angiotensin II (AngII) binding to its receptor (AT_1-R) specifically on the cellular membrane of zona glomerulosa (ZG) cells activates the Gq protein family, leading to *Cyp11b2* transcription and aldosterone production. **(B)** Rationale for the use of DREADD technology. hM3Dq is a modified human muscarinic M3 receptor that binds CNO and not endogenous ligands. This receptor can couple to Gq proteins in the same manner as AT_1-R and activate Gq signaling.

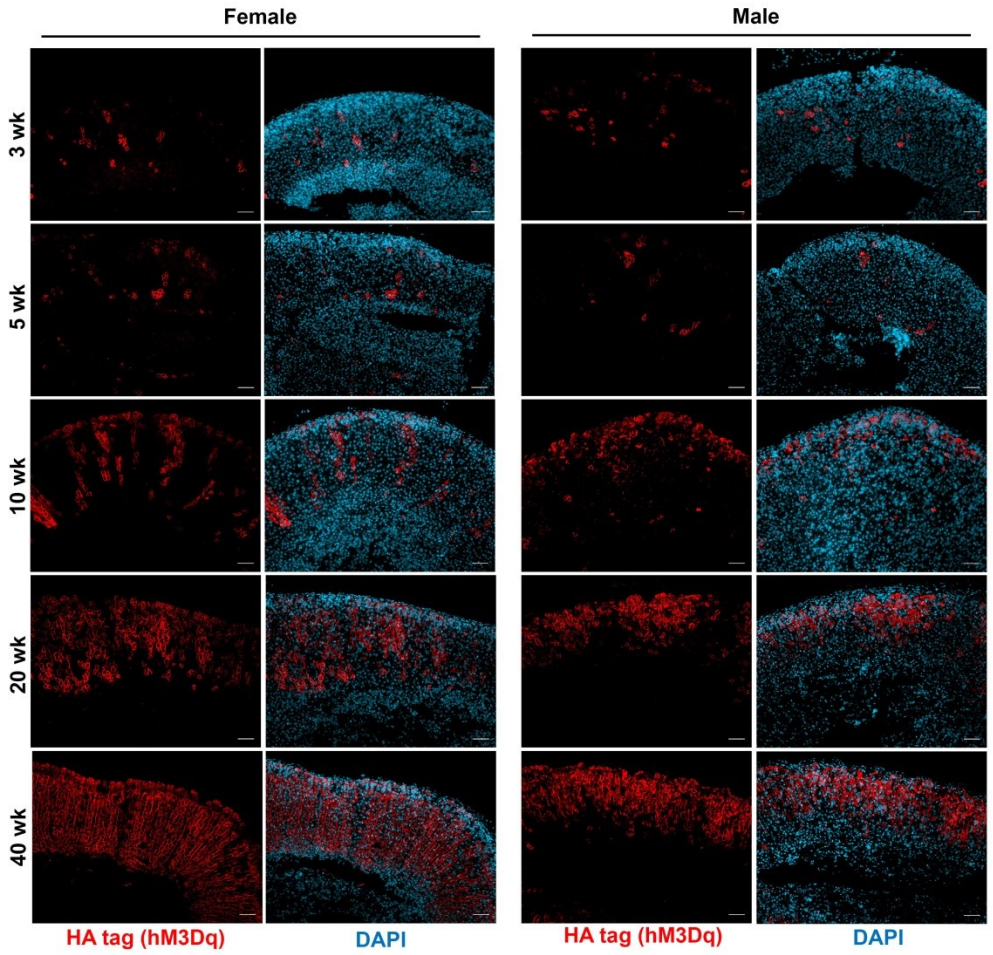

Figure 2.8. Expression of hM3Dq increases with age in the *AS$^{+/Cre}$::hM3Dq* model. Untreated male and female *AS$^{+/Cre}$::hM3Dq* mice were sacrificed at the indicated ages and stained for HA tag (hM3Dq) (red) by immunofluorescence. DAPI (blue) marks the nuclei. Scale bars = 50 µm.

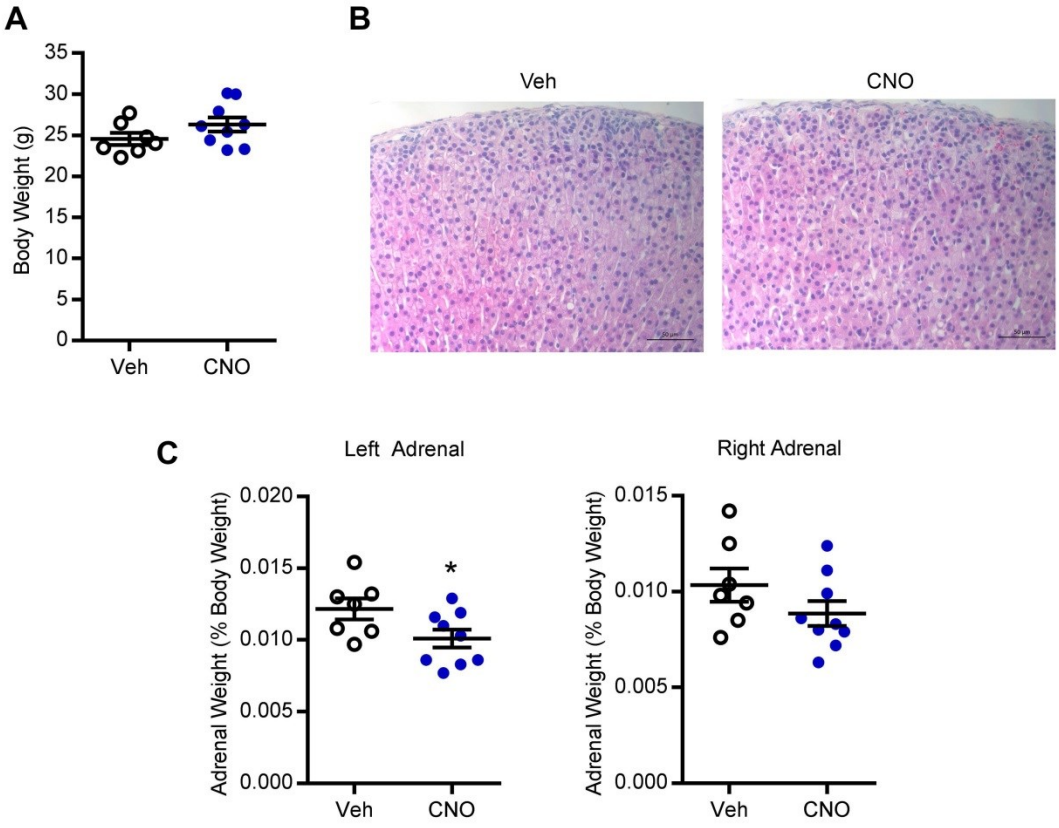

Figure 2.9. Additional phenotyping of *AS$^{+/Cre}$::hM3Dq* mice. (A) In 20-21 week old post- treatment females, body weight was measured prior to sacrifice and showed no significant difference between CNO and vehicle. **(B)** The histology of the adrenal glands was examined by H&E staining. **(C)** Adrenal weights were measured and then normalized to each animal's body weight as a percentage of body weight. For weights, n = 7 for vehicle and n = 9 for CNO. Bars in dot plots represent mean ± SEM. Scale bars = 50μm. Statistical analysis used for dot plots was unpaired two-tailed Student's *t* test. *$P < 0.05$.

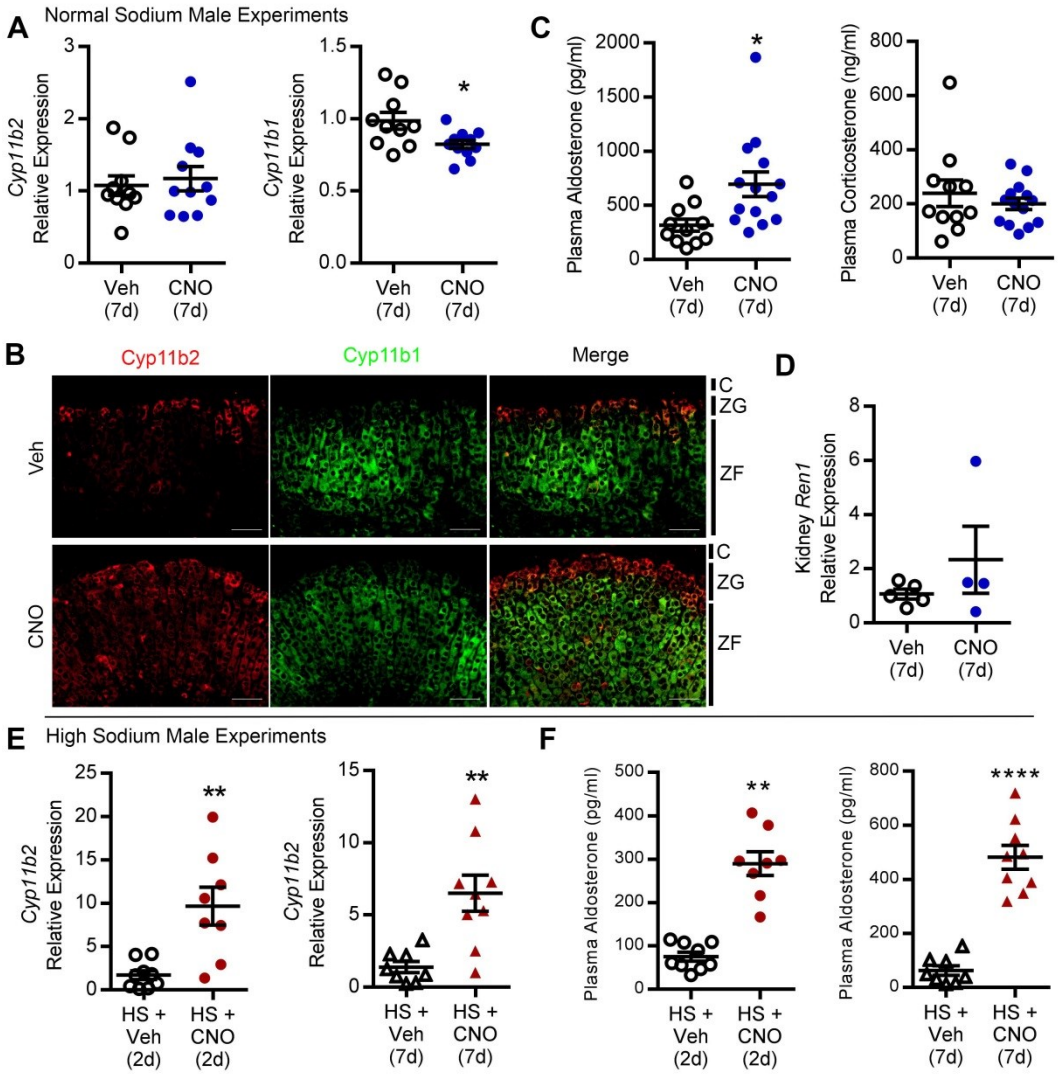

Figure 2.10. CNO treated 20 week old male *AS$^{+/Cre}$::hM3Dq* mice exhibit a moderate response in aldosterone production. (A) Whole adrenal mRNA expression of *Cyp11b2* and *Cyp11b1* in vehicle (n = 10) or CNO treated (n = 11) males. **(B)** Immunofluorescence of Cyp11b2 (red) and Cyp11b1 (green). **(C)** LC-MS/MS steroid measurements in vehicle (n = 11) and CNO treated (n = 14) males **(D)** qPCR analysis of kidney *Ren1* mRNA expression showed no difference between vehicle (n = 5) and CNO treated (n = 4) male mice. **(E)** High sodium diet plus CNO *Cyp11b2* expression. 20-22 week old male mice were treated under the same 2 day and 7 day protocols described in Figure 4. Male HS + CNO mice had significantly upregulated *Cyp11b2* mRNA expression at both 2 days and 7 days **(F)** HS + CNO plasma aldosterone concentration. Male HS + CNO mice had significantly elevated concentrations of aldosterone compared to HS + vehicle at both 2 days and 7 days. For 2 and 7 day experiments, n = 9 for both HS + vehicle (2d) and HS + CNO (7d), and n = 8 for both HS + CNO (2d) and HS + vehicle (7d). Bars in dot plots represent mean ± SEM. C, capsule; ZG, zona glomerulosa; ZF, zona fasciculata; Veh, vehicle; 2d, 2 days; 7d, 7 days. Scale bars = 50 µm. Statistical analysis used for dot plots was unpaired two-tailed Student's *t* test. **P* < 0.05, ***P* < 0.01, *****P* < 0.0001.

Sex	Treatment	*n*	11DOC (ng/ml)	Corticosterone (ng/ml)	18OHB (pg/ml)	Aldosterone (pg/ml)
F	Veh (7d)	13	19.3 ± 3.3	342.0 ± 95.1	987.2 ± 145.0	418.8 ± 58.3
	CNO (7d)	17	19.9 ± 4.3	243.4 ± 25.9	2544.5 ± 620.9*	1302.4 ± 265.1**
	HS + Veh (2d)	8	26.4 ± 7.2	288.8 ± 42.8	273.7 ± 54.3	108.8 ± 30.0
	HS + CNO (2d)	8	11.9 ± 4.5	230.3 ± 36.4	488.6 ± 68.5*	285.8 ± 44.9**
	HS + Veh (7d)	8	39.4 ± 9.7	356.4 ± 42.3	110.5 ± 20.4	18.5 ± 5.6
	HS + CNO (7d)	10	20.0 ± 5.0	305.0 ± 28.4	3655.3 ± 1046.0**	1935.2 ± 461.3**
M	Veh (7d)	11	12.4 ± 2.8	239.6 ± 48.5	641.2 ± 128.4	318.2 ± 56.1
	CNO (7d)	14	10.2 ± 2.3	200.5 ± 20.8	1140.5 ± 166.7*	696.1 ± 113.6*
	HS + Veh (2d)	9	23.5 ± 5.2	212.0 ± 27.0	179.5 ± 17.5	75.1 ± 10.2
	HS + CNO (2d)	8	6.0 ± 2.6*	147.4 ± 22.2	466.6 ± 42.7****	289.9 ± 27.6****
	HS + Veh (7d)	8	8.8 ± 2.3	202.5 ± 26.5	170.2 ± 55.0	62.8 ± 17.5
	HS + CNO (7d)	9	6.9 ± 2.4	210.4 ± 30.8	699.7 ± 62.6****	481.9 ± 44.0****

Table 2.1. Concentrations of adrenal steroids in *AS$^{+/Cre}$::hM3Dq* under various treatment protocols. LC-MS/MS was performed to detect steroid concentrations in mice from the various treatment protocols. Data for Veh/CNO (7d) corticosterone is presented as dot plots in Figure 2.4 and Figure 2.10. Data for aldosterone under all conditions is presented as dot plots in Figures 2.2 and 2.4, and Supplemental Figure 4. Data is represented as mean ± SEM. Unpaired two-tailed Student's t-test was performed within each sex/treatment regimen group. *P<0.05, **P<0.01, ****P<0.0001. F, female; M, male; 11DOC, 11-deoxycorticosterone; 18OHB, 18-hydroxycorticosterone; HS, high sodium; Veh, vehicle; 2d, 2 days; 7d, 7 days.

Steroid	Steroid Manufacturer	Precursor/ Product Ions (m/z)	RT (min)	LOD (pg/ml)	Internal Standard	Internal Standard Manufacturer
11DOC	Cerilliant	331.2 / 109.0	8.6	11.2	11DOC-d_8	Sigma-Aldrich
B	Cerilliant	347.2 / 329.2	6.8	44.4	B-d_8	C/D/N Isotopes
18OHB	Cerilliant	363.2 / 269.3	4.7	23.0	Cortisol-d_4	Cerilliant
Aldo	Cerilliant	361.2 / 343.1	5.6	3.0	Aldo-d_8	Sigma-Aldrich

Table 2.2. Steroids standards used for LC-MS/MS. m/z, mass to charge ratio; RT, retention time; LOD, limit of detection (calculated by measuring a signal-to-noise ratio of 3). Steroid abbreviations: 11DOC, 11-deoxycorticosterone; B, corticosterone; 18OHB, 18-hydroxycorticosterone; Aldo, aldosterone.

(A) 1260 HPLC Pump - C4 loading column

Mobile Phase A: 0.2 mmol/L Ammonium fluoride (NH_4F)

Mobile Phase B: Methanol + 0.2 mmol/L NH_4F

Time (min)	A (%)	B (%)	Flow (mL/min)	Pressure (bar)
Δ4				
1.00	81.0	19.0	0.500	435
1.20	0.0	100.0	0.500	435
2.50	0.0	100.0	0.500	435
2.51	0.0	100.0	0.000	435
3.90	0.0	100.0	0.000	435
3.91	0.0	100.0	0.100	435
7.20	0.0	100.0	0.100	435
7.40	0.0	100.0	0.100	435
7.41	0.0	100.0	0.500	435
8.99	0.0	100.0	0.500	435
9.00	81.0	19.0	0.500	435
12.00	81.0	19.0	0.500	435
12.10	81.0	19.0	0.500	435

(B) 1290 HPLC Pump - Biphenyl resolution column

Mobile Phase A: 0.2 mmol/L Ammonium fluoride (NH_4F)

Mobile Phase B: Methanol + 0.2 mmol/L NH_4F

Time (min)	A (%)	B (%)	Flow (mL/min)	Pressure (bar)
Δ4				
0.99	81.0	19.0	0.500	480
1.00	55.0	45.0	0.500	480
1.80	55.0	45.0	0.500	480
2.00	40.0	60.0	0.200	480
3.01	40.0	60.0	0.200	480
7.50	23.0	77.0	0.200	460
8.90	23.0	77.0	0.200	460
9.80	10.0	90.0	0.700	600
10.20	0.0	100.0	0.700	600
11.20	0.0	100.0	0.700	600
11.30	81.0	19.0	0.700	600
11.50	81.0	19.0	0.500	600

Table 2.3. Gradient specifications of the Agilent LC system.

CHAPTER 3

Synthetic High Density Lipoprotein (sHDL) Inhibits Steroid Production in Adrenal HAC15 Adrenal Cells

Modified from: Taylor MJ, Sanjanwala AR, Morin EE, Rowland-Fisher E, Anderson K, Schwendeman A, et al. Synthetic High-Density Lipoprotein (sHDL) Inhibits Steroid Production in HAC15 Adrenal Cells. *Endocrinology.* 2016;157(8):3122-9.

3.1 Abstract

Background: High density lipoprotein (HDL) transported cholesterol represents one of the sources of substrate for adrenal steroid production. Synthetic HDL (sHDL) particles represent a new therapeutic option to reduce atherosclerotic plaque burden by increasing cholesterol efflux from macrophage cells. The effects of the sHDL particles on steroidogenic cells have not been explored.

Methods: sHDL, specifically ETC-642, was studied in HAC15 adrenocortical cells. Cells were treated with sHDL, forskolin, 22R-hydroxycholesterol (22OHC), or pregnenolone. Experiments included time and concentration response curves, followed by steroid assay. Quantitative-RT PCR (qPCR) was used to study mRNA of 3-hydroxy-3-methyl-glutaryl-CoA reductase (HMGCR), lanosterol 14 -α- methylase (CYP51A1), cholesterol side-chain cleavage enzyme (CYP11A1), and steroid acute regulatory protein (StAR). Cholesterol assay was performed using media and cell lipid extracts from a dose response experiment.

Results: sHDL significantly inhibited production of cortisol. Inhibition occurred in a concentration- and time-dependent manner and in a concentration range of 3-50 μM.

Forskolin (10 μM) stimulated cortisol production was also inhibited. Incubation with 22OHC (10 μM) and pregnenolone (10 μM) increased cortisol production, which was unaffected by sHDL treatment. sHDL increased transcript levels for the rate-limiting cholesterol biosynthetic enzyme, HMGCR. Extracellular cholesterol assayed in culture media showed a positive correlation with increasing concentration of sHDL, while intracellular cholesterol decreased following treatment with sHDL.

Conclusion: The current study suggests that sHDL inhibits HAC15 adrenal cell steroid production by efflux of cholesterol, leading to an overall decrease in steroid production and an adaptive rise in adrenal cholesterol biosynthesis.

3.2 Introduction

Low and high density lipoproteins (LDL and HDL) are extracellular carriers that deliver cholesterol to steroidogenic tissues such as the ovaries, testes and adrenal glands. Low density lipoprotein receptor (LDL-R) and scavenger receptor BI (SR-BI) are highly expressed in adrenal tissue allowing the adrenal gland to efficiently take up cholesterol from lipoprotein particles (204-208). Both LDL and HDL have been shown to provide cholesterol for steroidogenesis (204, 209-211). In addition, the lipoprotein cholesterol levels (LDL-C and HDL-C) are indicators of cardiovascular health and ischemic event risk (212). HDL inhibits atherosclerotic development through reverse cholesterol transport, a mechanism by which nascent HDL effluxes cholesterol from peripheral tissue and delivers it to the liver for elimination (213).

Strong epidemiological evidence for the cardio protective properties of HDL prompted development of several therapeutic agents to either increase HDL-C or to

stimulate reverse lipid transport. While niacin is FDA approved to elevate HDL levels, the clinical efficacy is somewhat controversial. Additionally, inhibiting cholesteryl-ester transfer protein (CETP) with torcetrapib or anacetrapib increased HDL-C levels clinically, but did not show either plaque or event reduction (214). Of interest, torcetrapib increased adrenal aldosterone production through non-specific activity of this CETP's chemical structure, and not through the resultant increase in HDL-C (215).

Infusion therapy with nascent, cholesterol free synthetic HDL (sHDL) represents an alternative strategy to stimulate reverse cholesterol transport through targeted increase of efflux capacity, rapid mobilization, and elimination of cholesterol (216). There is strong *in vitro* evidence that sHDL enhances cholesterol efflux from foam macrophages (217). Several of these products are clinically tested including ETC-216 (218), CSL-111 (219), ETC-642 (220), CSL-112 and CER-001 (221). While ETC-216 and CSL-111 were shown to reduce atheroma burden (218, 219), CER-001 failed to show efficacy (221). CSL-112 was shown to be effective in initiating cholesterol efflux in patients(222) and a larger safety and efficacy Phase 2 trial is ongoing (223).

Though sHDL may lower intracellular cholesterol and its clinical use is being expanded, the effects of sHDL on steroidogenic tissues, which use cholesterol as a substrate for steroid hormone synthesis, have not been investigated. Therefore, the current study defined the effects of sHDL on adrenal cell steroidogenesis using the forskolin responsive human adrenocortical cell line (HAC15) as a model (224). HAC15 cells are a clonal cell line derived from the non-clonal H295R human adrenocortical cancer cells. HAC15 cells have a modest response to ACTH which is not found in the original H295R line (224, 225). Herein, the HAC15 cell line was used to define the

effects of sHDL on steroidogenesis. Our results demonstrate a broad inhibition of steroid production that is associated with sHDL depletion of cellular cholesterol.

3.3 Materials and Methods

Materials. Apolipoprotein A-I mimic peptide was synthesized by Genscript (Piscataway, NJ) using solid-phase flourenylmethyloxycarbonyl (FMOC) chemistry. Peptide purity was > 95 % as determined by high performance liquid chromatography (HPLC). Egg sphingomyelin and 1,2-dipalmitoyl-*sn*-glycero-3-phosphocholine (DPPC) were generously donated by Nippon Oil and Fat (Osaka, Japan). All other materials were obtained from commercial sources.

Preparation of sHDL. ETC-642, a model sHDL nanoparticle, was prepared using homogenization method as follows: the composition of sHDL was apolipoprotein A-I mimetic peptide (ESP 24218) combined with sphingomyelin and DPPC at 1:3.75:3.75 molar ratio (226). Phospholipids were dispersed in phosphate buffered saline (PBS) by sonication. Peptide was dissolved in PBS mixed with lipid suspension. The mixture was heated to 50°C and incubated for 15 min until the solution became clear indicating sHDL formation. The resulting sHDL solution concentration was 7.5 mg/mL of ESP24218 peptide corresponding to approximately 3 mM sHDL concentration. The solution was sterile filtered and stored frozen at -20°C until use. The purity and size of sHDL remained unchanged after three freeze-thaw cycles.

Characterization of sHDL. The size distribution of sHDL was assessed by dynamic light scattering (DLS) using a Zetasizer Nano, Malvern Instruments (Westborough, MA). The number and intensity average values were reported. The

purity of sHDL was analyzed by gel permeation chromatography with UV detection at 220 nm using a Tosoh TSK gel G3000SWxl column (Tosoh Bioscience, King of Prussia, PA) on a Waters Breeze Dual Pump system. The samples were diluted to a 200 μM concentration and a 50 μL injection volume was used.

Transmission electron microscopy (TEM) images were obtained using a Tecnai T12 electron microscope (JEOL USA) equipped with a Gatan US4000 CCD camera. Images were acquired at 120 kV in low dose mode with a defocus of approximately –0.96 μm. The samples were negatively stained with uranyl formate solution.

Cell Culture and Treatment. HAC15 cells were plated at a density of 100,000 cells per well in a 48 well plate (Figures 3.1, 3.2, 3.4, and 3.5A), 200,000 cells per well in a 24 well plate (Figure 3.5B and C), or 400,000 cells per well in a 12 well plate (Figures 3.3 and 3.6). Cells were plated in DMEM/F12 media supplemented with 10% Cosmic Calf serum (Hyclone, Logan, Utah), 1% insulin/transferrin/selenium Premix (ITS, BD Biosciences), 1% Penicillin/Streptamicin, and 0.01% Gentamicin and were given 48 h to adhere to the plate. Prior to treatment with sHDL, the cells were cultured in experimental media (0.1% Cosmic Calf serum and antibiotics) for 18 h. Cells were then treated with varying concentrations and times with sHDL as well as steroidogenesis substrates (22R-hydroxycholesterol [22OHC], pregnenolone, or forskolin).For cholesterol flux experiments, cells were treated in phenol free DMEM/F12 media in order to not interfere with the colorimetric cholesterol assay.

Protein Extraction and Protein Assay. Cells were lysed in mammalian protein extraction buffer (Pierce Chemic Co., Rockford, IL). Protein content in wells was determined by bicinchoninic acid (BCA) protein assay using the micro BCA protocol

(Pierce Chemical Co.). Samples were read on an Epoch Microtiter Spectrophotometer (Sugar Land, TX) at 562 nm absorbance.

mRNA Isolation and qPCR Analysis. RNA was extracted from cells using the RNA isolation kit (Qiagen Sciences, Valencia, CA) according to manufacturer recommendations. Briefly, RNA was extracted using proprietary RLT lysis buffer and isolated using spin columns provided in the kit. Total RNA was re-suspended in nuclease free water (Qiagen Sciences, Valencia, CA) and reverse transcribed using random primers (Life Sciences, Carlsbad, CA). Quantitative polymerase chain reactions (RT-qPCR) were performed with Taqman primer probes for 3-hydroxy-3-methyl-glutaryl-CoA reductase (*HMGCR*) (Life Technologies, Hs00168352_m1) and lanosterol 14 -α-methylase (*CYP51A1*) (Life Technologies, Hs00426415_m1). Primer probes for steroid acute regulatory protein (*StAR*) and cholesterol side-chain cleavage enzyme (*CYP11A1*) were designed by the Rainey laboratory and purchased through IDT. The following primer sequences were used: *StAR* forward, 5'-ATGAGTAAAGTGGTCCCAGATG-3', reverse 5'-ACCTTGATCTCCTTGACATTGG-3', and probe, 5'-/56-FAM/ATCCGGCTGGAGGTCGTGGTGGA-3'; *CYP11A1* forward 5'-GAGATGGCACGCAACCTGAAG-3', reverse 5'-CTTAGTGTCTCCTTGATGCTGGC-3', and probe 5'-/56-FAM/CGATCTGCCGCGCAGCCAAGACC-3'.

Steroid Assays. Cortisol immunoassay was performed according to the manufacturer's recommendations (Alpco, Salem, New Hampshire). The standard curve was prepared using cortisol standards dissolved in the cell culture media. Briefly, 20 µL of experimental media was incubated on antibody-coated plates, in proprietary assay buffer, for 45 min at room temperature. Following incubation, the cells were washed with

1x wash buffer. Tetramethylbenzidine substrate was added followed by 20 min incubation with shaking. Stop buffer was then added and absorbance was measured at 450 nm on a microtiter spectrophotometer.

Aldosterone and androstenedione radioimmunoassays (Coat-a-Count) were performed according to the manufacturer's recommendations (Siemens, Washington D.C). Steroid standard curves were prepared using aldosterone and androstenedione dissolved in cell culture media. Radioactivity was measured on a Wallac Wizard 1470 multicrystal gamma counter (Perkin Elmer, Waltham, MA).

Intracellular Cholesterol Extraction and Colorimetric Cholesterol Assay. Intracellular cholesterol was extracted from cells using a 2:1 mixture of chloroform:methanol. Purified water was then added, and upon centrifugation, the organic, bottom phase was taken and dried by vacuum centrifugation. The resulting lipid pellet was re-suspended in 1X cholesterol assay buffer from the kit described below.

Extracellular cholesterol assay (Cell Biolabs, San Diego, CA) was performed, according to manufacturer's directions with phenol-free experimental cell culture media. The intracellular assay was performed with the suspended pellet described above. In short, 50 µL of sample was added to 50 µL of cholesterol reaction reagent containing cholesterol esterase, cholesterol oxidase, colorimetric probe, and horseradish peroxidase diluted in assay buffer. Following an incubation step, absorbance was read at 562 nm. Cholesterol standards were prepared in phenol free experimental cell culture media for extracellular cholesterol and in 1X assay buffer for intracellular cholesterol.

Statistical Analysis. Studies were replicated in a minimum of three independent experiments. Results are expressed as means ± SD. Statistics were calculated using a one-way ANOVA with pairwise analysis, when necessary (Sigma Plot 12.5, San Jose, CA). $p < 0.05$ was considered statistically significant.

3.4 Results

sHDL Characterization. Analysis of sHDL nanoparticles by gel permeation chromatography revealed formation of a mono-dispersed nanoparticle and absence of unbound apolipoprotein A-I peptide or liposomes (Supplementary Figure 3.1A). The size distribution by DLS confirmed the presence of mono-dispersed particles of 8.3 nm in average diameter (number averaged distribution was used for DLS data fitting) (Supplementary Figure 3.1B). Electron microscopy showed a discoidal shape of sHDL that is characteristic of nascent or cholesterol free HDL (Supplementary Figure 3.1C).

Steroid Production. Treatment of HAC15 adrenal cells with increasing concentrations of sHDL for 24 h caused a decrease in aldosterone, cortisol, and androstenedione (Supplementary Figure 3.2). Compared to basal steroid levels, sHDL profoundly inhibited cortisol production in a concentration dependent manner. Inhibition of cortisol production plateaued at 80% with a 30 μM concentration with no additional effects seen at 50 μM sHDL (Figure 3.1). Importantly, 48 h sHDL treatments as high as 100 μM did not have cytotoxic effects on the HAC15 cells (data not shown). To establish the time-dependence of sHDL effect on cortisol production, cells were incubated in the presence of 30 μM sHDL for up to 24 h (Figure 3.2). Cortisol production dropped to

approximately 20% of basal levels after 6 h of treatment and steroidogenesis was consistently inhibited through all time points examined.

Cortisol production was also examined in cells that were untreated, treated with forksolin (10 μM), an activator of cAMP production, alone, and forskolin with sHDL (50 μM) for 3, 6, 12, 24 h (Figure 3.3). Compared with basal levels, forskolin significantly increased cortisol production at each time point (ranging from approximately 1.7-fold above basal at 3 h, to 2.6-fold at 24 h) (Figure 3.3). However, in the presence of sHDL, the forskolin effect was significantly abrogated, as the production of cortisol was decreased to near basal levels for each time point (1.1-fold at 6h, 0.8-fold at 12 h, and 0.7-fold at 24 h compared to basal levels) (Figure 3). This highlights the ability of sHDL to inhibit both basal and agonist stimulated cortisol production.

The rate-limiting step in adrenal cell steroid production can be bypassed by incubation of cells with 22OHC or pregnenolone. Addition of 22OHC (10 μM) or pregnenolone (10 μM) increased basal cortisol production significantly (approximately 2.5 and 3-fold respectively). As noted above, treatment with sHDL (30 μM) alone inhibited cortisol production to 20% of that seen in control cells. Co-incubation of sHDL with 22OHC or pregnenolone showed no significant difference when compared to treatment groups without sHDL (Figure 4). The lack of sHDL inhibition of 22OHC metabolism to cortisol suggests that sHDL is not cytotoxic and likely acts prior to mitochondrial pregnenolone production.

Transcript levels. The enzymes required for cholesterol biosynthesis are increased in response to experimental manipulations that cause depletion of cellular cholesterol levels. *HMGCR* and *CYP51A1* represent two cholesterol biosynthetic

enzyme transcripts that increase following depletion of cellular cholesterol levels. Adrenal cells responded to sHDL with a time-dependent increase in *HMGCR* which peaked with a 2.6-fold increase at 6 h (Figure 3.5A). *HMGCR* transcripts remained significantly elevated at 12 and 24 h. *CYP51A1* encodes a cholesterol biosynthetic enzyme responsible for removing the 14-α-methyl group from lanosterol. *CYP51A1* mRNA was also significantly increased at 3 h, 6 h, 12 h, and peaked at 24 h (approximately 2.5-fold), further illustrating the induction of the cholesterol biosynthetic pathway. In contrast, the transcripts for both *CYP11A1* and *StAR*, two important proteins in the early steroidogenesis pathway, were not significantly changed after 6 h of incubation with sHDL (Figure 3.5C).

Cholesterol Efflux. Extracellular cholesterol was measured in HAC15 cell experimental media following 24 h incubation of untreated cells, as well as from cells treatment with 10 μM and 50 μM sHDL (Figure 3.6). Intracellular cholesterol was measured in the same cells of the respective experiments following cell lysis and lipid extraction. While basal levels of extracellular cholesterol were undetectable, the cells incubated with 50 μM sHDL effluxed approximately 100 nmol/mg cell protein after 24 h of incubation (Figure 3.6). Intracellular cholesterol was significantly depleted compared to basal at the 50 μM concentration of sHDL (approximately 40 nmol cholesterol/mg protein compared to the 65 nmol/mg protein at basal), while no significant effect was observed at the 10 μM concentration (Figure 3.6).

3.5 Discussion

The adrenal gland produces considerable amounts of steroid hormones using cholesterol as a precursor. Sources for adrenal cholesterol include *de novo* synthesis,

LDL, and HDL (206, 209-211, 227). As an indication of the important roles for each of these cholesterol sources, the adrenal expresses high levels of the enzymes needed for cholesterol synthesis, as well as the receptors for both HDL (SR-BI) and LDL (LDLR) (204, 228-230). Because of the beneficial cardio-protective effects of HDL, several groups have developed synthetic versions of HDL as potential therapeutics. Despite the fact that the adrenal cortex has the highest tissue expression of SR-BI, the effects of sHDL on adrenal steroid hormone production have not been previously reported.

There have been numerous studies directed at defining the role of native HDL and LDL in the adrenal using human, bovine, rat and mouse adrenal models (209, 210, 231, 232), (233, 234). Evidence for the steroidogenic role of LDL is fairly consistent. LDL has been demonstrated to increase steroidogenesis in murine Y1 cells in the presence of agonist ACTH (231). *En suite*, in the 1980s, several studies demonstrated the ability of LDL to increase steroidogenesis in the human adrenal cell (207, 235, 236). On the other hand, the role of HDL in human steroidogenesis has not been as clearly defined. While a stimulatory effect on cortisol and aldosterone production has been documented on adult adrenal cells (209, 210), HDL had little effect on fetal adrenal cell steroidogenesis (211, 227). So far, there have been no studies indicating an inhibitory role for either native LDL or HDL. Our findings clearly demonstrated that sHDL inhibited cortisol, aldosterone, and androstenedione. This effect may be attributed to the difference in composition between synthetic and mature native HDL. Unlike native HDL, sHDL does not have a cholesterol component. The lack of cholesterol in sHDL and its ability to efficiently take up cholesterol may explain its inhibitory effects on steroid production.

As opposed to steroidogenesis, sHDL appeared to increase HAC15 adrenal cell cholesterol biosynthesis. To assess cellular cholesterol synthesis we monitored HMGCR and CYP51A1, two key enzymes in its synthetic pathway. HMGCR is the rate controlling enzyme for cholesterol biosynthesis and acts to convert acetyl–CoA to the sterol precursor melavonate. Rainey *et al.* demonstrated that adrenocorticotropic hormone (ACTH), in the absence of an extracellular source of cholesterol, significantly increased levels of HMGCR activity in primary adrenal cells (237). The induction of HMGCR appears directly related to increased cellular needs for cholesterol. Studies in the 1970s by Balasubramanian and Brown *et al.* demonstrated an inverse relationship between HMGCR activity and plasma cholesterol levels in rats (238, 239). When the plasma cholesterol levels were low, the adrenal gland increased cholesterol synthesis through activity of HMGCR by almost 30 fold to maintain steroidogenesis. Herein, we found that transcripts for *CYP51A1* and *HMGCR* significantly increased in HAC15 cells following treatment with sHDL, suggesting that sHDL activates cholesterol biosynthesis. This observation was in direct contrast to the inhibitory effects on steroid production.

As a possible explanation for the activation of cholesterol synthesis but inhibition of steroid production, we tested the hypothesis that sHDL caused a loss of steroid substrate as a result of cholesterol efflux from the cells. This concept is based on previous findings in macrophage cells where formulations of sHDL cause dose- and time-dependent cholesterol efflux through interaction with ATP-binding cassette transporter sub-family G member 1 (ABCA1) (240). In addition kidney cells transfected with SR-BI, ATP-binding cassette transporter sub-family G member 1 (ABCG1), and ABCA1 also demonstrate cholesterol efflux when treated with sHDL (241, 242). We

observed that sHDL caused a dose-dependent increase in the cell culture media levels of cholesterol. Inversely, intracellular cholesterol was significantly decreased at higher doses of sHDL treatment. The activation of cholesterol efflux appeared to parallel the activation of cholesterol synthesis. Taken together, our study suggests that sHDL inhibits HAC15 cell steroidogenesis through its efflux of cholesterol, causing an increase in cholesterol synthesis in an attempt to maintain output of steroid hormones.

There are potential concerns regarding the study that we attempted to resolve. One potential concern of the study was a possible cytotoxic effect of sHDL that might inhibit steroid production and raise extracellular cholesterol. To address this issue we did not see any effect on viability of cells treated with doses as high as 100 μM of sHDL over 48 h (data not shown). It is also important to note that the concentrations of sHDL used in the current in vitro study are within the levels generated *in vivo* during sHDL therapy. A recent study using 10-30 mg/kg of the sHDL particle, ETC-642, caused peak plasma concentrations of 0.250 mg/ml (243). Our experiments were conducted with doses up to 0.130 mg/mL (50 μM). This is significantly lower than the peak plasma concentration of the lowest dose of the ETC-642 trial. Finally, the experiments of this study were performed in the HAC15 adrenal cell line. This represents the only available human steroidogenic adrenal cell model, but this model originated from an adrenocortical tumor. Therefore additional studies using primary cultures of human adrenal cells and/or *in vivo* animal model studies are warranted to confirm the current findings.

In summary, sHDL inhibits HAC15 adrenal cell steroidogenesis in both a dose and time-dependent manner through its effects on the efflux of cholesterol. Decreased

availability of cholesterol causes a compensatory rise in adrenal cell cholesterol biosynthesis that allows the cells to partially maintain steroid output. sHDL therapeutics have great potential for treating cardiovascular disease. However, as sHDL clinical trials move forward, it will be important to monitor the adrenal hormonal axis as a potential unanticipated target.

3.6 Acknowledgements

The authors wish to acknowledge Anne Dosey and Dr. Georgios Skiniotis of Life Science Institute, University of Michigan for electron microscopy imaging. We would like to acknowledge Nippon Oil and Fat for the phospholipid gift. This research was funded in part by AHA 13PRE16670022 Fellowship to A.R.S., NIH DK069950 to W.E.R. and both AHA 13SDG17230049 and R01GM113832 to A.S. M.J.T. was supported by a Systems and Integrative Biology Training Program GM008322. E.E.M. was supported by a Cellular Biotechnology Training Program GM008353.

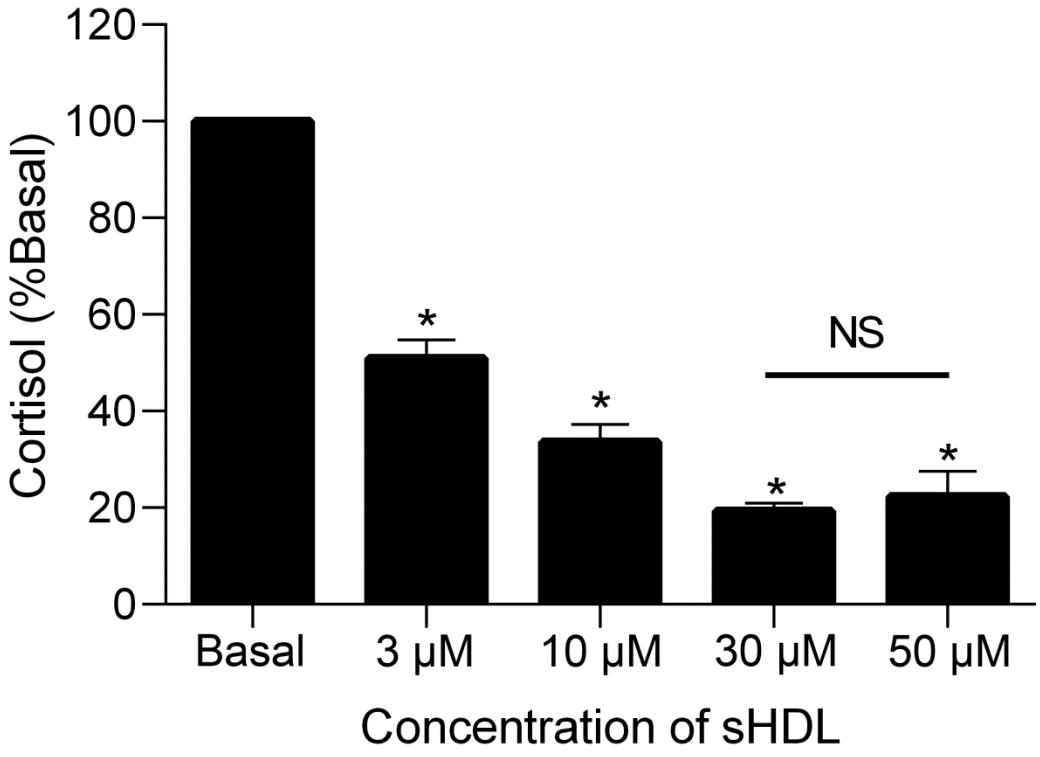

Figure 3.1. Concentration-dependent effects of sHDL (ETC-642) on adrenal cell cortisol production. HAC15 adrenocortical cells were incubated for 24 h with increasing amounts of ETC-642. Cortisol from the media was then measured and normalized to cell protein. Values shown are the mean ± SD from 3 independent experiments. (* denotes $p < 0.05$ compared to basal)

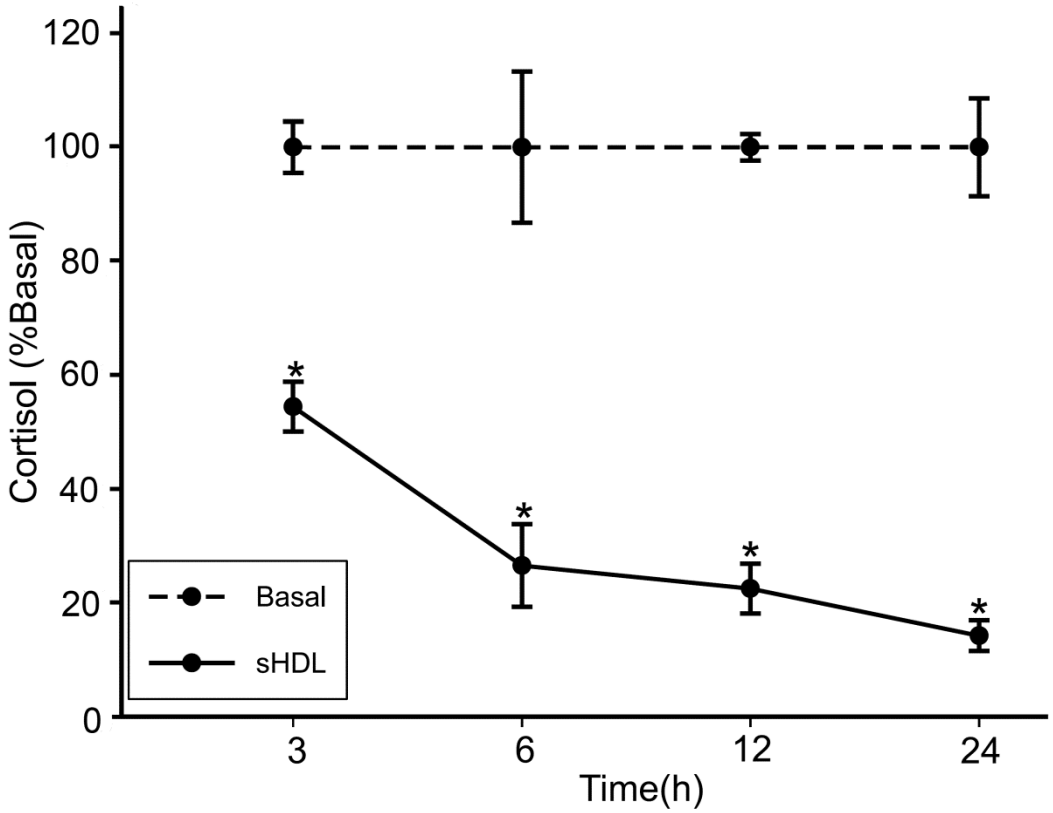

Figure 3.2. Time-dependent effects of sHDL (ETC-642) on adrenal cell cortisol production. HAC15 adrenal cells were incubated for the indicated times with or without ETC-642 (30 μM). Cortisol was measured in medium and normalized to cell protein. Results represent means ± SD from 3 independent experiments. (* denotes $p < 0.001$ compared to basal)

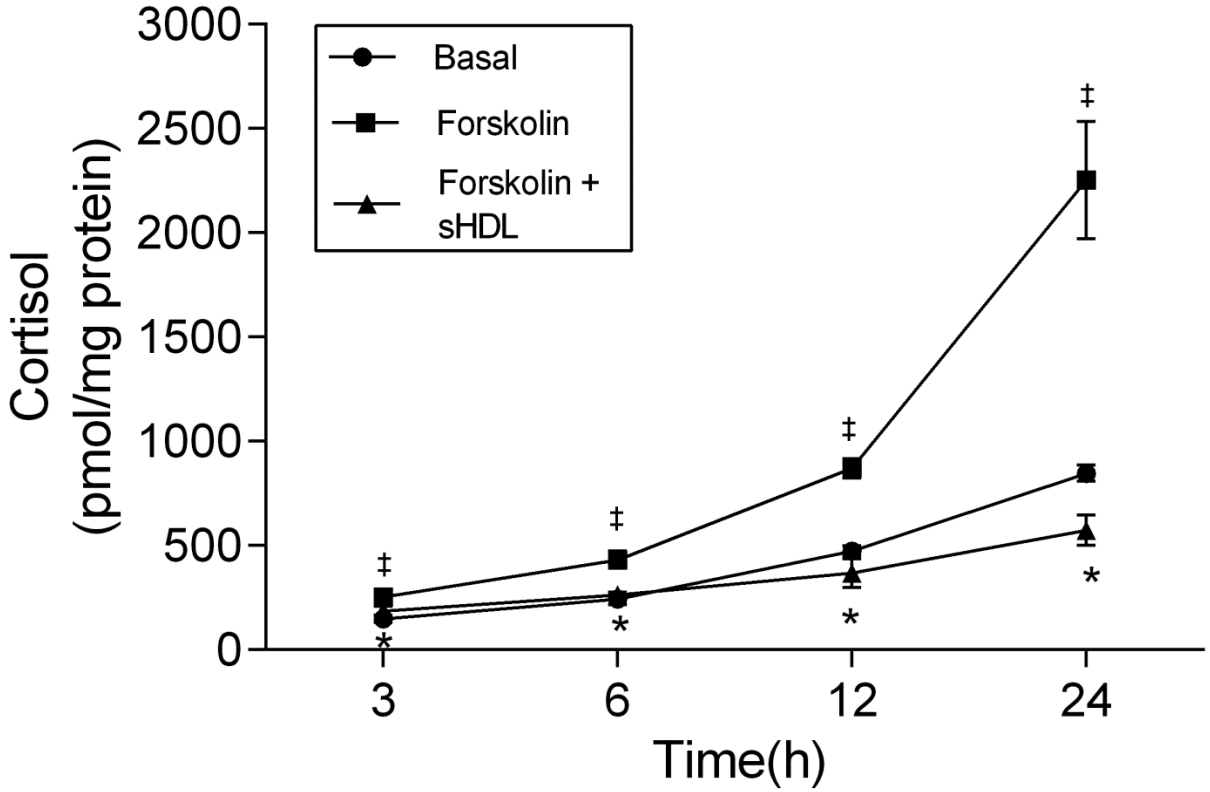

Figure 3.3. Time-dependent effect of sHDL (ETC-642) on agonist-stimulated adrenal cell cortisol production. HAC15 adrenal cells were incubated for the indicated times with or without forskolin (10 μM), as well as forskolin + ETC-642 (50 μM). Cortisol production was measured in the experimental media and normalized to protein. Results represent means ± SD from 3 independent experiments. (‡ denotes $p < 0.05$ for forskolin compared to basal, and * denotes $p < 0.05$ for forskolin + sHDL compared to forskolin)

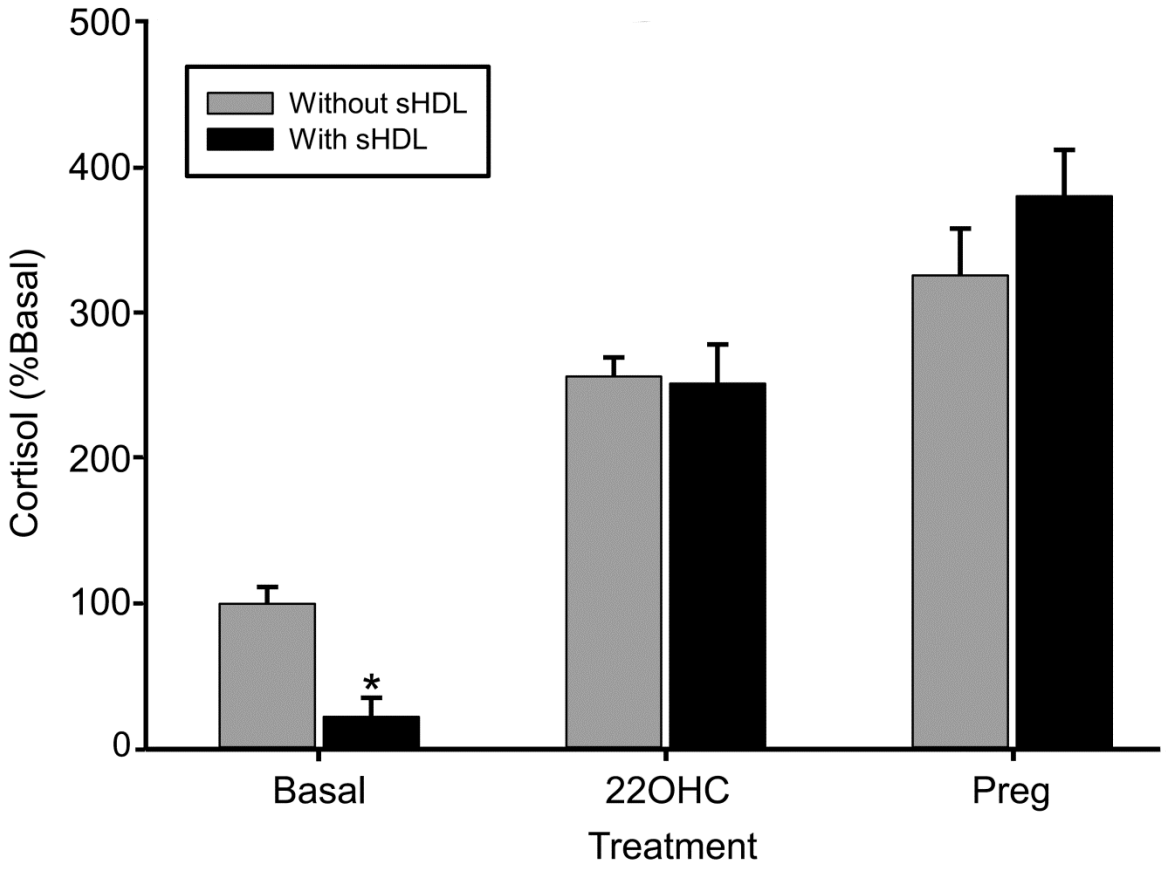

Figure 3.4. Effect of sHDL (ETC-642) on 22R-hydroxycholesterol (22OHC) and pregnenolone stimulated cortisol production. HAC15 cells were treated for 24 h with and without ETC-642 (30 μM). Samples were then incubated for 6 h with and without 22OHC (10 μM) and pregnenolone (10 μM). Cortisol production was measured in media and normalized to protein. Results represent means ± SD from 3 independent experiments. (* denotes $p < 0.001$, pairwise analysis comparing treatment group with and without sHDL)

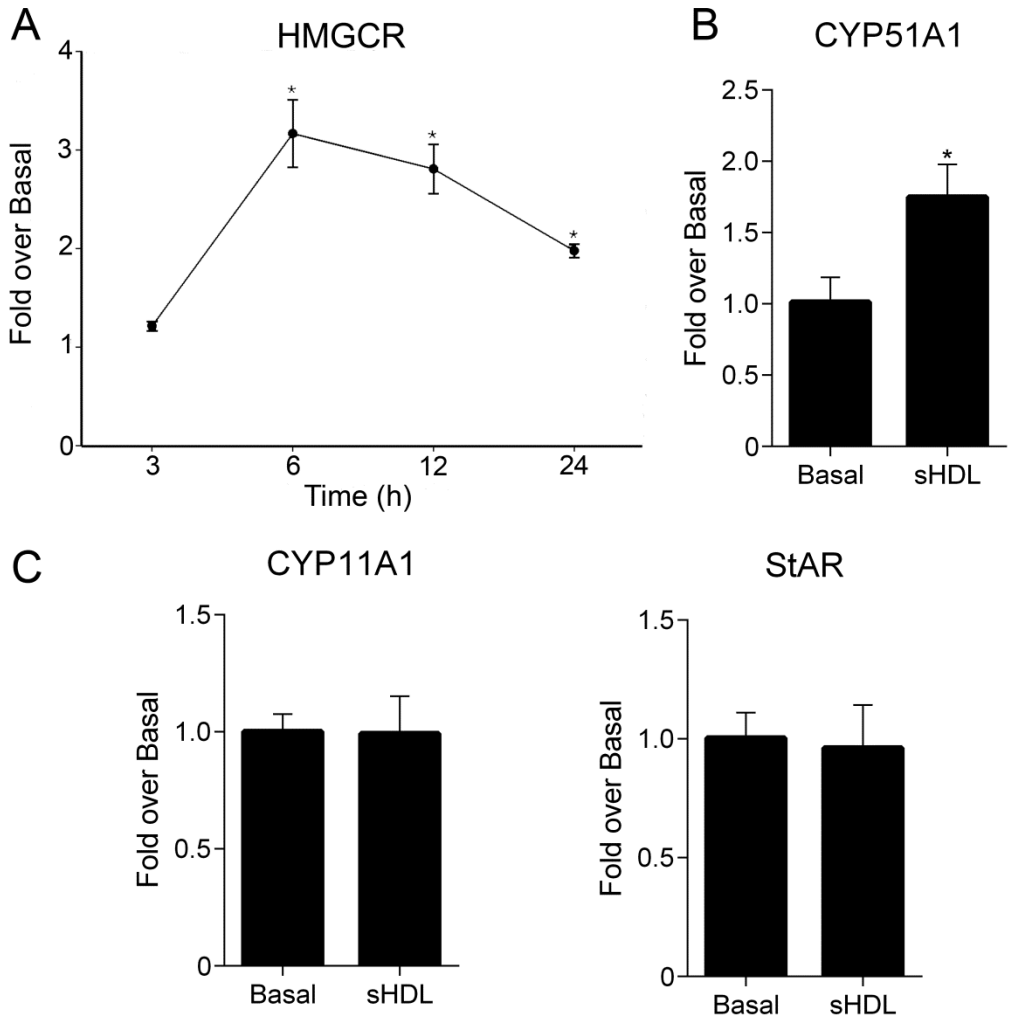

Figure 3.5. Effect of sHDL (ETC-642) on cholesterol biosynthesis and steroidogenic genes. (A) Time-dependent effects of sHDL on HMG-CoA-Reductase (*HMGCR*) gene expression. **(B)** Time-dependent effects of sHDL on the cholesterol biosynthetic gene, *CYP51A1*. **(C)** Effect of sHDL on the expression of key steroidogenesis genes, cholesterol side-chain cleavage enzyme (*CYP11A1*) and steroid acute regulatory protein (*StAR*). For all experiments, HAC15 cells were incubated with or without ETC-642 (50 μM, for the times indicated in A and B, and 6 h - the peak of HMGCR expression - in C). For A and B, results represent means ± SD from 2 independent experiments with 3 replicates within each experiment. For C, results represent means ± SD from 3 independent experiments. (* denotes $p < 0.05$ compared to basal)

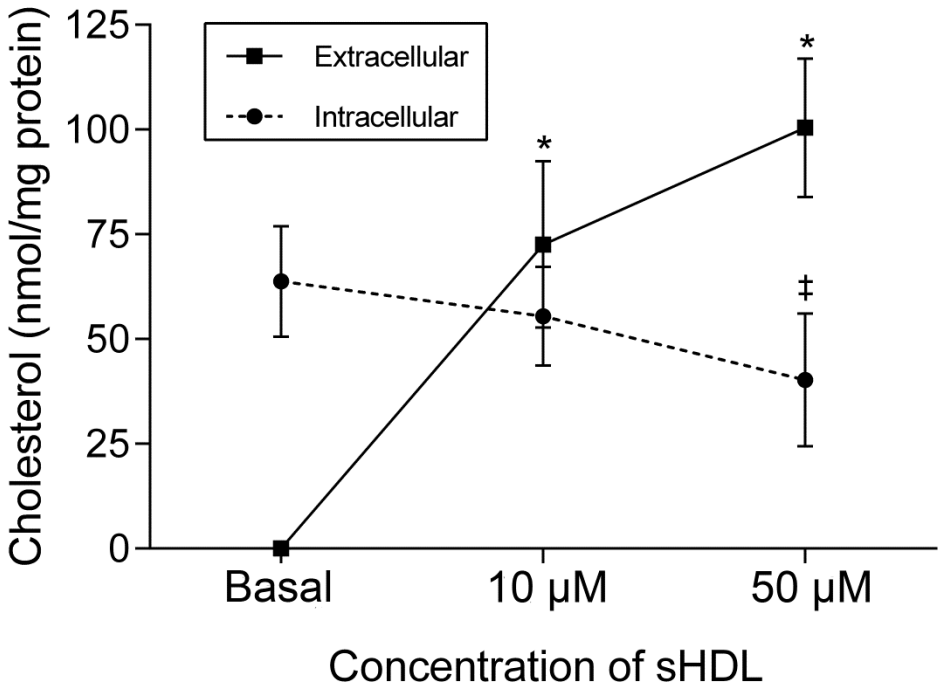

Figure 3.6. Increasing concentration of sHDL leads to cholesterol efflux from adrenocortical cells. HAC15 adrenocortical cells were incubated for 24 h with or without ETC-642 at the indicated concentration. Extracellular cholesterol was measured in the media. Intracellular cholesterol was measured from the cell lysate as described in the methods section. Both were normalized to total cell protein. Results represent means ± SD from 3 independent experiments. (* denotes $p < 0.05$ compared to extracellular basal, ‡ denotes $p < 0.05$ compared to intracellular basal)

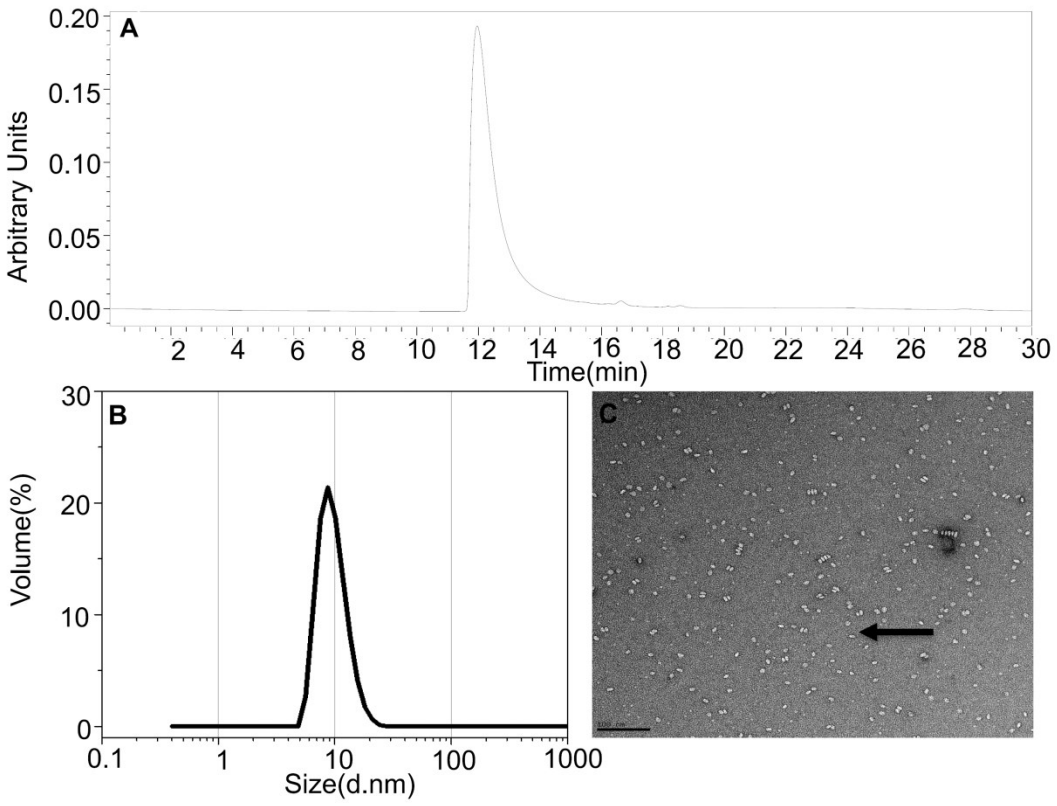

Figure 3.7. sHDL (ETC-642) characteristics. (A) Gel permeation chromatography profile of sHDL (ETC-642). Single peak at the HDL retention time indicates purity of sHDL and absence of free peptide or liposome impurities. **(B)** Dynamic light scattering analysis of sHDL. Mono-model peak indicates formation of homogeneous sHDL with an average diameter of 8.3 nm. **(C)** Electron microscopy image of sHDL. ETC-642 was stained with uranyl formate and imaged using a Tecnai T12 electron microscope at 120 kV. Individual nano-discs indicated with a bold arrow.

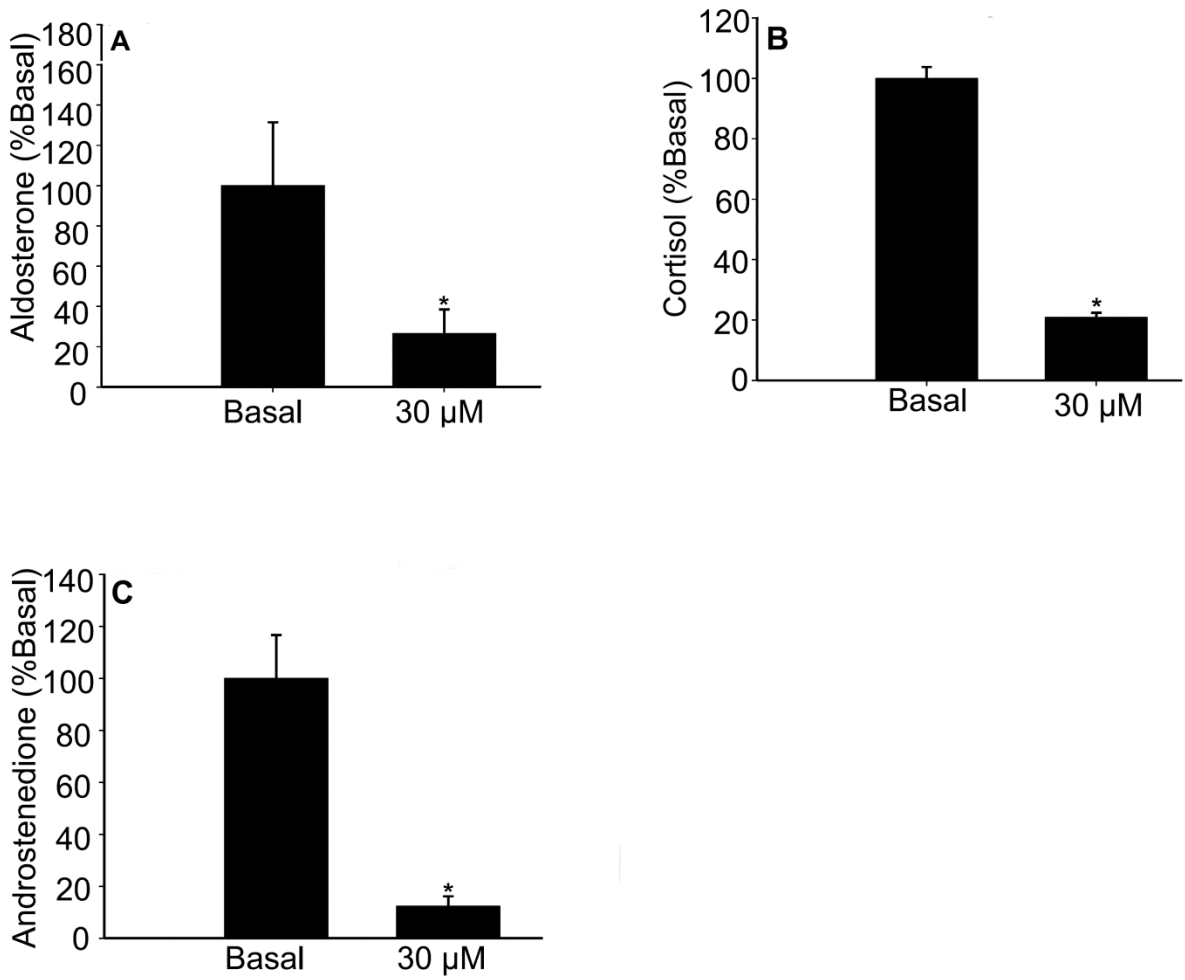

Figure 3.8. Effect of sHDL (ETC-642) on adrenal steroid production. Cells were treated for 24 h with and without sHDL at the concentration indicated in the figure. At the end of treatment, cell media was assayed for **(A)** aldosterone, **(B)** cortisol, and **(C)** androstenedione. Results represent means ± SD from 3 independent experiments. (* denotes $p < 0.05$ compared to basal)

CHAPTER 4
Conclusions and Future Directions

4.1 Summary

This dissertation project used transgenic mouse modeling to define the role of Gq signaling in adrenocortical aldosterone production. The *AS$^{Cre/+}$::hM3Dq* mouse model demonstrated a dominant role of Gq in controlling both ZG (physiologic) and ZF (aberrant) aldosterone production. Specifically, this model suggests that ZF cells have the capacity to make aldosterone if the stimulus of Gq signaling is present. This brings forth new questions regarding the influence of Gq signaling on adrenal cell fate that need to be addressed through future work. In addition this model provides the first transgenic in vivo model of aldosterone excess and hypertension that is both inducible and reversible.

The *AS$^{Cre/+}$::hM3Dq* model represents the first use of DREADD technology in the adrenal gland. This chemogenetic in vivo technology used to modulate G protein pathways was first developed in 2007 and predominantly applied to research in the neuroscience field (193). Now, DREADD technology and the field of chemogenetics have moved beyond neurons (244), into glia (245), hepatocytes (246), triple-negative breast cancer cells (247), transformed fibroblasts (248), and induced pluripotent stem cells (249). DREADDs have even recently been used in the endocrinology field, within

pancreatic β cells (191, 250). However, the work described in Chapter 2 marked the first use of DREADD technology within a steroidogenic tissue, allowing for future applications in studies of G protein pathways in steroidogenic tissues.

4.2 *AS$^{Cre/+}$::hM3Dq* Mice as a Model for Primary Aldosteronism

The *AS$^{Cre/+}$::hM3Dq* model harbored several characteristics of PA after chronic CNO treatment. Activation of the GqDREADD receptor resulted in elevated plasma aldosterone concentrations and Cyp11b2 expression. The increase in aldosterone production even in with the presence of a HS diet, indicates that the aldosterone secretion was RAAS independent. CNO treated mice displayed a significant decrease in the transcript levels of kidney *Ren1* as well, further supporting aldosterone production that was independent of renin, as seen in PA. Finally, mice developed hypertension when CNO was combined with HS, which was reversed upon CNO washout.

The excess aldosterone production in the *AS$^{Cre/+}$::hM3Dq* mouse model occurs through activation of Gq proteins. As discussed previously, the downstream events in the Gq signaling pathway result in an increase in cytosolic calcium. This elevation in cytosolic calcium concentration is the main catalyst in increasing the transcript levels of intracellular *CYP11B2* in physiologic human aldosterone production. Furthermore, the most common molecular mechanisms of PA onset involve various gene mutations that also increase intracellular calcium. Mutations in genes that encode calcium channels and transport proteins (*CACNA1D, CACNA1H, ATP2B3*) alter the encoded protein function, thereby directly increasing calcium concentration. Other mutations (*KCNJ5, ATP1A1*) cause depolarization of the cellular membrane, indirectly leading to elevated

cytosolic calcium through the opening of calcium channels. Thus, while the *AS$^{Cre/+}$::hM3Dq* mouse model does not completely resemble genetic causes of PA, the calcium signaling mechanism through which it acts recapitulates many forms of the disease. Moreover, perhaps the subtype of PA that the *AS$^{Cre/+}$::hM3Dq* mice most closely represent is FH type I. This rare subtype is characterized by a chimeric fusion of the *CYP11B1* and *CYP11B2* genes, allowing for *CYP11B2* transcription driven by ACTH binding to its receptor in ZF cells. This receptor-ligand interaction that controls aldosterone production in ZF cells is reminiscent of the mechanism in the *AS$^{Cre/+}$::hM3Dq* model. Therefore, this model may be used to further probe the molecular mechanisms contributing to aldosterone production that underlie several forms of PA.

The *AS$^{Cre/+}$::hM3Dq* mouse model will also facilitate future research on peripheral effects of high circulating aldosterone. Previous studies have illustrated that elevated aldosterone exerts deleterious effects such as inflammation and fibrosis on peripheral tissues, including the renal (251-255) and cardiovascular (74, 134-141, 188) systems. There are questions that remain regarding the mechanisms that lead to this aldosterone-mediated peripheral damage and the possible recovery after treating this disease. In this dissertation project, the longest reported CNO treatment was 7 days. It is possible that there is an upregulation of pro-inflammatory cytokines at this time point. However, it is likely that a more chronic treatment regimen, such as 1-2 months on CNO plus HS diet, would be needed to observe end organ damage such as renal or cardiac fibrosis. The *AS$^{Cre/+}$::hM3Dq* mouse model can be used to study the effects on other tissues as it has the benefit of being inducible. This model also has a lower financial

cost, less hands-on work, and provides less stress to the animal compared to exogenous mineralocorticoid treatments. Additionally, in the *AS$^{Cre/+}$::hM3Dq* mouse model, the mineralocorticoids are derived endogenously from a dysfunctional adrenal cortex, as in PA. The model can also be reversed, which can be used to mimic the phenotype of a successful treatment that reverses the effects of excessive aldosterone. In summary, while this project has established *AS$^{Cre/+}$::hM3Dq* mice as an accurate model of PA, there are still several questions to be addressed regarding the role of Gq signaling in adrenal aldosterone production and the effects of aldosterone action on target organs.

4.3 Gq Signaling in Adrenal Functional Zonation

AS$^{Cre/+}$::hM3Dq mice treated with CNO exhibited a disruption of the zonal expression of Cyp11b2, an enzyme normally restricted to ZG cells. Many cells in the ZF expressed Cyp11b2, with some cells exclusively expressing this enzyme rather than the typical ZF-related enzyme Cyp11b1. Other cells exhibited co-expression of both Cyp11b1 and Cyp11b2. The localization of Cyp11b2 was variable at 2 days following CNO plus HS diet treatment. Some mice responded with robust Cyp11b2 expression throughout their cortex, whereas others displayed Cyp11b2 localization predominantly in the ZG and outer ZF (with Cyp11b1 co-expression). Nevertheless, the findings at this early time point strongly suggests that ZF cells have initiated Cyp11b2 expression, as opposed to the alternative explanation that CNO caused Cyp11b2 positive ZG cells to migrate into the ZF. After 1 week of CNO plus HS diet, all mice had Cyp11b2 localization in the ZF, with some cells still harboring co-expression of both enzymes.

Taken together, these data imply that possibly there is a slower transition from a Cyp11b1^{+} to Cyp11b2^{+} state in some cells. Additionally, cells that are exclusively Cyp11b2^{+} at the early time point of 2 days suggests that these cells were more primed for a transition to an aldosterone-producing phenotype. Further work is needed to understand the factors that contribute to the plasticity of a ZF cell to revert to aldosterone production. It is possible that the presence of Gq signaling dominates over the ACTH-induced glucocorticoid-producing signal present in ZF cells. Therefore, in physiological conditions, loss of the AT_1R and Gq signaling may be a critical regulatory event in the transition from a ZG to ZF cell state. Measuring circulating ACTH concentration in these mice will be an important next step to understand how the GqDREADD activation influences the ZF-specific HPA axis.

Immunofluorescent staining also revealed that DREADD-induced Gq signaling activation upregulated the expression of the ZG marker Dab2, with localization in the ZG and ZF. This was confirmed with an increase in *Dab2* mRNA. In vitro studies have shown that Dab2 plays a role in aldosterone production, as transfection of a *Dab2* plasmid increased AngII-mediated aldosterone production (194). Furthermore, Dab2 has been characterized as a ZG protein that mirrors the expansion of Cyp11b2 under low sodium conditions (194). However, in conditions of high sodium when Cyp11b2 expression regresses, Dab2 expression remains stable in the ZG (194), suggesting that it does not always follow Cyp11b2 expression but remains a ZG marker. Taken together, this suggests that Gq signaling may regulate additional ZG-specific factors beyond Cyp11b2.

Conversely, we observed no significant changes in the expression or localization of active β-catenin, part of the ZG-enriched Wnt signaling pathway. There was also no significant change in the mRNA expression of *Axin2*, a β-catenin responsive gene. Wnt/β-catenin signaling has been suggested to influence aldosterone production (41, 199). Our data indicate that this pathway is not necessary for Cyp11b2 expression if the cell has active Gq signaling. It is likely that the Wnt pathway still has a role in aldosterone production, perhaps upstream of activated Gq, such as the upregulation of ZG AT_1R expression (41).

In order to address the impact of Gq signaling on the ZG to ZF cell transition, further analysis is needed. A detailed transcriptome analysis, such as microarray or single-cell RNA-seq, would help characterize the broad transcriptome changes in mice treated with CNO vs. control water. Our preliminary microarray analysis using mice on a normal sodium diet treated with CNO or control water yielded variable results. Therefore, in future studies it might be beneficial to focus on groups with a HS diet which helped minimize variability for aldosterone production and adrenal Cyp11b2 expression. Comparing these groups to mice on a sodium deficient diet would provide a physiological control for the upregulation of ZG-related genes.

Another important future direction of this work would be to better define the mechanism through which GqDREADD can activate aldosterone production in non-aldosterone producing cells. To address this question, in vitro mechanistic studies with GqDREADD viral transduction might allow targeted cell signaling and molecular studies. During this dissertation project, we attempted the transduction of a GqDREADD viral construct under a CMV promoter control into the HAC15 adrenocortical carcinoma cell

line (225). Despite observing expression of the mCherry fluorescent tag in a subset of cells, we saw a minimal increase of *Cyp11b2* mRNA in response to CNO, compared to the normal HAC15 agonist AngII (data not shown). Cell sorting for a purer population of GqDREADD-expressing cells did not lead to an increase in CNO response. The rational for these findings is not clear, but future studies might consider use of a different GqDREADD constructs (available through Addgene) or alternative cell model. An additional possibility would be to study Gq signaling in the context of the transgenic GqDREADD mouse primary cultures. These platforms would enable research into a possible molecular mechanism for Gq signaling induced differentiation of glucocorticoid-producing cells to a mineralocorticoid producing phenotype.

Interestingly, there was a minor decrease in adrenal weight (significant in the left adrenal and a trend in the right adrenal) following 1 week of CNO treatment. Additional experiments involving long-term treatments of CNO (>1 month) would be useful to determine if Gq signaling activation causes adrenal hypoplasia. Preliminary data suggested that cellular proliferation was decreased as assessed by Ki67 staining. Moreover, our preliminary microarray data revealed the downregulation of several cell cycle genes following 1 week of CNO treatment. These data will need to be confirmed by qPCR and reassessed in long-term treated mice. This could lead to additional studies to determine whether Gq signaling regulates cell growth and proliferation in the adrenal gland.

Regarding potential future mouse models, this project suggests that DREADD technology can be applied to the adrenal and possibly other endocrine glands. As mentioned previously, AngII also activates the inhibitory G protein (Gi) signaling

pathway. Future studies using a GiDREADD (256) in the adrenal cortex could be additive to our findings in the GqDREADD system. Together, these mice could aid in the understanding of the specific roles played by each pathway activated through AngII binding to adrenal AT_1R. Beyond the adrenal ZG, a recently developed GsDREADD system could be valuable for researchers studying ZF cell signaling and glucocorticoid synthesis. This DREADD activates the cAMP pathway and protein kinase A activity (257), the predominant pathway in glucocorticoid production. The adrenal use of this inducible transgenic technology would allow further elucidation of several critical signaling pathways in normal adrenal function and adrenal disease.

Finally, a follow-up to this dissertation work would be the inverse in vivo manipulation – by inactivation of Gq signaling in the adrenal cortex. One way to accomplish this would be to ablate the Gαq protein specifically in the adrenal cortex. This would also address the importance of this signaling pathway over other pathways in the synthesis of aldosterone. The *gnaq*^{flox} mice are available and characterized (258). This mouse line could be crossed to the *AS*-Cre line to specifically delete Gαq in aldosterone producing cells after birth. This project would address two important unanswered questions related to this dissertation research: 1) the importance of Gq signaling in adrenal aldosterone production relative to the other routes to aldosterone synthesis and 2) the role for Gq signaling in the establishment of the postnatal ZG and the maintenance of a ZG cellular state in adult life. While this project has demonstrated that Gq signaling is sufficient for aldosterone production, this future study would determine whether Gq signaling is a necessary factor.

4.4 Sex Differences in *AS*$^{Cre/+}$*::hM3Dq* Mice

An interesting finding of this project was the sexual dimorphism that exists in response to CNO treatment. Males exhibited less expression of the GqDREADD receptor and slower rates of adrenocortical cell turnover. This was expected given similar findings in a previous report using the same *AS*-Cre line (64). However, our preliminary studies have demonstrated that in aged mice (40 weeks) that have high GqDREADD in both males and females (Supplemental Figure 2.2), there is still a substantial sex difference in response to CNO treatment. As mentioned previously, other models of adrenal disease have exhibited a more robust phenotype in females compared to males (64, 170, 172, 179, 198, 201). This includes sex differences in previous models of hyperaldosteronism (170, 172, 179, 198). This study provides further evidence for a possible molecular mechanism that prevents males from excess aldosterone production and ectopic Cyp11b2 expression in the adrenal cortex. Alternatively, there may be unknown factors that cause females to be more susceptible to dysregulated Cyp11b2 expression. Additional experiments directed at defining the mechanisms leading to this differential response between sexes will be required.

We propose that this sexual dimorphism is an androgen driven event in males. The male adrenal has a high expression of androgen receptors throughout the adrenal cortex (259). Likewise, the male adrenal gland has high tissue expression of 5α-reductase type 2 (Srd5a2) (200), the enzyme that converts testosterone to DHT and also is a gene target of AR. The presence of AR and ability to generate DHT suggests that the adrenal is an androgen responsive tissue. We have confirmed this result in wild-type mice in preliminary experiments. The transgenic adrenal-specific ablation of AR in

adrenocortical cells would be a possible future approach to define the role of AR in the adrenal cortex. Crossing the *AR^{flox}* mouse line (260) to the *AS*-Cre line would achieve the transgenic deletion of AR. As previously reported, the transcriptional regulator Dax1 is suppressed by the androgen receptor, leading to a sexually dimorphic expression pattern of Dax1 (259), where it is only expressed in the ZG of males. We hypothesize that Dax1 is necessary for the expression of Cyp11b2 in the ZF of female GqDREADD mice, and that its expression is repressed by adrenal AR in males. Therefore, in the adrenal AR knockout mice, assessing Dax1 expression patterns might also aid in defining the causes of mouse adrenal sex differences. Ablating AR on an *AS$^{Cre/+}$::hM3Dq* background would determine if disruption of AR increases the male response to CNO, causing a more 'female-like' phenotype.

4.5 Final Thoughts

This dissertation research examined the ability of Gq signaling to activate aldosterone production in vivo. The findings of this dissertation project outline a role for Gq signaling in maintenance of an aldosterone-producing cellular state, and suggest that Gq pathway activation is enough to drive adrenocortical cells (both ZG and ZF) to produce aldosterone. These data also imply that loss of Gq signaling might be a factor that impacts the ZG to ZF cell transition during adrenal centripetal displacement. This dissertation project has also created a novel tool in the *AS$^{Cre/+}$::hM3Dq* mouse model for researchers in the PA, aldosterone action, and hypertension fields. Future work using this model will attempt to further uncover the role of Gq signaling in maintenance of adrenal functional zonation, the deleterious actions of circulating aldosterone on

peripheral tissues, and sex differences that may be present in adrenal physiology. This dissertation project combined with future studies using the newly developed mouse model may lead to improved therapeutic interventions of adrenal disease.

REFERENCES

1. Miller WL. A brief history of adrenal research: steroidogenesis - the soul of the adrenal. *Mol Cell Endocrinol.* 2013;371(1-2):5-14.
2. Mezzogiorno A, and Mezzogiorno V. Bartolomeo Eustachio: A pioneer in morphological studies of the kidney. *Am J Nephrol.* 1999;19(2):193-8.
3. Walczak EM, and Hammer GD. Regulation of the adrenocortical stem cell niche: implications for disease. *Nat Rev Endocrinol.* 2014.
4. Arnold J. Ein Beitrag zu der feineren Struktur und dem Chemismus der Nebennieren [German]. *Arch Pathol Anat Physiol Klin Med.* 1866;35:64–107.
5. Willenberg HS, and Bornstein SR. Adrenal Cortex; Development, Anatomy, Physiology. 2000.
6. Brown-Séquard CE. Recherches expérimentales sur la physiologie et la pathologie des capsules surrénales. *Arch Gen Med.* 1856;8:385-401.
7. Selye H. The general adaptation syndrome and the diseases of adaptation. *J Clin Endocrinol Metab.* 1946;6:117-230.
8. Conn JW. Presidential address. I. Painting background. II. Primary aldosteronism, a new clinical syndrome. *J Lab Clin Med.* 1955;45(1):3-17.
9. Mornet E, Dupont J, Vitek A, and White PC. Characterization of two genes encoding human steroid 11 beta-hydroxylase (P-450(11) beta). *J Biol Chem.* 1989;264(35):20961-7.
10. Breault L, Lehoux JG, and Gallo-Payet N. Angiotensin II receptors in the human adrenal gland. *Endocr Res.* 1996;22(4):355-61.
11. Margioris AN, and Tsatsanis C. ACTH Action on the Adrenals. 2000.
12. Chan LF, Metherell LA, and Clark AJ. Effects of melanocortins on adrenal gland physiology. *Eur J Pharmacol.* 2011;660(1):171-80.
13. Mukai K, Imai M, Shimada H, and Ishimura Y. Isolation and characterization of rat CYP11B genes involved in late steps of mineralo- and glucocorticoid syntheses. *J Biol Chem.* 1993;268(12):9130-7.
14. Mukai K, Mitani F, Agake R, and Ishimura Y. Adrenocorticotropic hormone stimulates CYP11B1 gene transcription through a mechanism involving AP-1 factors. *Eur J Biochem.* 1998;256(1):190-200.
15. Havelock JC, Auchus RJ, and Rainey WE. The rise in adrenal androgen biosynthesis: adrenarche. *Semin Reprod Med.* 2004;22(4):337-47.
16. Hui XG, Akahira J, Suzuki T, Nio M, Nakamura Y, Suzuki H, et al. Development of the human adrenal zona reticularis: morphometric and immunohistochemical studies from birth to adolescence. *J Endocrinol.* 2009;203(2):241-52.
17. Rege J, and Rainey WE. The steroid metabolome of adrenarche. *J Endocrinol.* 2012;214(2):133-43.
18. Rainey WE, and Nakamura Y. Regulation of the adrenal androgen biosynthesis. *J Steroid Biochem Mol Biol.* 2008;108(3-5):281-6.

19. Reiter EO, Fuldauer VG, and Root AW. Secretion of the adrenal androgen, dehydroepiandrosterone sulfate, during normal infancy, childhood, and adolescence, in sick infants, and in children with endocrinologic abnormalities. *J Pediatr.* 1977;90(5):766-70. 20. Rosenfield RL, Grossman BJ, and Ozoa N. Plasma 17-ketosteroids and testosterone in prepubertal children before and after ACTH administration. *J Clin Endocrinol Metab.* 1971;33(2):249-53.
21. Turcu AF, and Auchus RJ. Adrenal steroidogenesis and congenital adrenal hyperplasia. *Endocrinol Metab Clin North Am.* 2015;44(2):275-96.
22. Greep RO, and Deane HW. Histological, cytochemical and physiological observations on the regeneration of the rat's adrenal gland following enucleation. *Endocrinology.* 1949;45(1):42-56.
23. Kim AC, and Hammer GD. Adrenocortical cells with stem/progenitor cell properties: recent advances. *Mol Cell Endocrinol.* 2007;265-266:10-6.
24. Walczak EM, and Hammer GD. Regulation of the adrenocortical stem cell niche: implications for disease. *Nat Rev Endocrinol.* 2015;11(1):14-28.
25. Chang SP, Morrison HD, Nilsson F, Kenyon CJ, West JD, and Morley SD. Cell proliferation, movement and differentiation during maintenance of the adult mouse adrenal cortex. *PLoS One.* 2013;8(12):e81865.
26. Miyamoto H, Mitani F, Mukai K, Suematsu M, and Ishimura Y. Studies on cytogenesis in adult rat adrenal cortex: Circadian and zonal variations and their modulation by adrenocorticotropic hormone. *J Biochem.* 1999;126(6):1175-83.
27. Pihlajoki M, Dorner J, Cochran RS, Heikinheimo M, and Wilson DB. Adrenocortical zonation, renewal, and remodeling. *Front Endocrinol (Lausanne).* 2015;6:27.
28. Freedman BD, Kempna PB, Carlone DL, Shah M, Guagliardo NA, Barrett PQ, et al. Adrenocortical zonation results from lineage conversion of differentiated zona glomerulosa cells. *Dev Cell.* 2013;26(6):666-73.
29. Iannaccone P, Morley S, Skimina T, Mullins J, and Landini G. Cord-like mosaic patches in the adrenal cortex are fractal: implications for growth and development. *FASEB J.* 2003;17(1):41-3.
30. Morley SD, Viard I, Chung BC, Ikeda Y, Parker KL, and Mullins JJ. Variegated expression of a mouse steroid 21-hydroxylase/beta- galactosidase transgene suggests centripetal migration of adrenocortical cells. *Mol Endocrinol.* 1996;10(5):585-98.
31. Stachowiak A, Nussdorfer GG, and Malendowicz LK. Proliferation and distribution of adrenocortical cells in the gland of ACTH- or dexamethasone-treated rats. *Histol Histopathol.* 1990;5(1):25-9.
32. McNicol AM, and Duffy AE. A study of cell migration in the adrenal cortex of the rat using bromodeoxyuridine. *Cell Tissue Kinet.* 1987;20(5):519-26.
33. Zajicek G, Ariel I, and Arber N. The streaming adrenal cortex: direct evidence of centripetal migration of adrenocytes by estimation of cell turnover rate. *J Endocrinol.* 1986;111(3):477-82.
34. Bertholet JY. Proliferative activity and cell migration in the adrenal cortex of fetal and neonatal rats: an autoradiographic study. *J Endocrinol.* 1980;87(1):1-9.

35. Mitani F, Mukai K, Miyamoto H, Suematsu M, and Ishimura Y. Development of functional zonation in the rat adrenal cortex. *Endocrinology.* 1999;140(7):3342-53.
36. Kataoka Y, Ikehara Y, and Hattori T. Cell proliferation and renewal of mouse adrenal cortex. *J Anat.* 1996;188 (Pt 2):375-81.
37. King P, Paul A, and Laufer E. Shh signaling regulates adrenocortical development and identifies progenitors of steroidogenic lineages. *Proc Natl Acad Sci U S A.* 2009;106(50):21185-90.
38. Finco I, Lerario AM, and Hammer GD. Sonic Hedgehog and WNT Signaling Promote Adrenal Gland Regeneration in Male Mice. *Endocrinology.* 2018;159(2):579-96.
39. Kim AC, Reuter AL, Zubair M, Else T, Serecky K, Bingham NC, et al. Targeted disruption of beta-catenin in Sf1-expressing cells impairs development and maintenance of the adrenal cortex. *Development.* 2008;135(15):2593-602.
40. Walczak EM, Kuick R, Finco I, Bohin N, Hrycaj SM, Wellik DM, et al. Wnt signaling inhibits adrenal steroidogenesis by cell-autonomous and non-cell-autonomous mechanisms. *Mol Endocrinol.* 2014;28(9):1471-86.
41. Berthon A, Drelon C, Ragazzon B, Boulkroun S, Tissier F, Amar L, et al. WNT/beta-catenin signalling is activated in aldosterone-producing adenomas and controls aldosterone production. *Hum Mol Genet.* 2014;23(4):889-905.
42. Berthon A, Sahut-Barnola I, Lambert-Langlais S, de Joussineau C, Damon-Soubeyrand C, Louiset E, et al. Constitutive beta-catenin activation induces adrenal hyperplasia and promotes adrenal cancer development. *Hum Mol Genet.* 2010;19(8):1561-76.
43. Akerstrom T, Maharjan R, Sven Willenberg H, Cupisti K, Ip J, Moser A, et al. Activating mutations in CTNNB1 in aldosterone producing adenomas. *Sci Rep.* 2016;6:19546.
44. Maharjan R, Backman S, Akerstrom T, Hellman P, and Bjorklund P. Comprehensive analysis of CTNNB1 in adrenocortical carcinomas: Identification of novel mutations and correlation to survival. *Sci Rep.* 2018;8(1):8610.
45. Wu VC, Wang SM, Chueh SJ, Yang SY, Huang KH, Lin YH, et al. The prevalence of CTNNB1 mutations in primary aldosteronism and consequences for clinical outcomes. *Sci Rep.* 2017;7:39121.
46. Vidal V, Sacco S, Rocha AS, da Silva F, Panzolini C, Dumontet T, et al. The adrenal capsule is a signaling center controlling cell renewal and zonation through Rspo3. *Genes Dev.* 2016;30(12):1389-94.
47. Laufer E, Kesper D, Vortkamp A, and King P. Sonic hedgehog signaling during adrenal development. *Mol Cell Endocrinol.* 2012;351(1):19-27.
48. Ching S, and Vilain E. Targeted disruption of Sonic Hedgehog in the mouse adrenal leads to adrenocortical hypoplasia. *Genesis.* 2009;47(9):628-37.
49. Huang CC, Miyagawa S, Matsumaru D, Parker KL, and Yao HH. Progenitor cell expansion and organ size of mouse adrenal is regulated by sonic hedgehog. *Endocrinology.* 2010;151(3):1119-28.
50. Mitani F, Miyamoto H, Mukai K, and Ishimura Y. Effects of long term stimulation of ACTH and angiotensin II-secretions on the rat adrenal cortex. *Endocr Res.* 1996;22(4):421-31.

51. McEwan PE, Vinson GP, and Kenyon CJ. Control of adrenal cell proliferation by AT1 receptors in response to angiotensin II and low-sodium diet. *Am J Physiol.* 1999;276(2 Pt 1):E303-9.
52. Tian Y, Balla T, Baukal AJ, and Catt KJ. Growth responses to angiotensin II in bovine adrenal glomerulosa cells. *Am J Physiol.* 1995;268(1 Pt 1):E135-44.
53. Tian Y, Smith RD, Balla T, and Catt KJ. Angiotensin II activates mitogen-activated protein kinase via protein kinase C and Ras/Raf-1 kinase in bovine adrenal glomerulosa cells. *Endocrinology.* 1998;139(4):1801-9.
54. Nishimoto K, Harris RB, Rainey WE, and Seki T. Sodium deficiency regulates rat adrenal zona glomerulosa gene expression. *Endocrinology.* 2014;155(4):1363-72.
55. Deane HW, Shaw JH, and Greep RO. The effect of altered sodium or potassium intake on the width and cytochemistry of the zona glomerulosa of the rat's adrenal cortex. *Endocrinology.* 1948;43(3):133-53.
56. Shelton JH, and Jones AL. The fine structure of the mouse adrenal cortex and the ultrastructural changes in the zona glomerulosa with low and high sodium diets. *Anat Rec.* 1971;170(2):147-81.
57. McEwan PE, Lindop GB, and Kenyon CJ. Control of cell proliferation in the rat adrenal gland in vivo by the renin-angiotensin system. *Am J Physiol.* 1996;271(1 Pt 1):E192-8.
58. Ulrich-Lai YM, Figueiredo HF, Ostrander MM, Choi DC, Engeland WC, and Herman JP. Chronic stress induces adrenal hyperplasia and hypertrophy in a subregion-specific manner. *Am J Physiol Endocrinol Metab.* 2006;291(5):E965-73.
59. Nussdorfer GG, Rebuffat P, Mazzocchi G, Belloni AS, and Meneghelli V. Ivestigations on adrenocortical mitochondria turnover. I. Effect of chronic treatment with ACTH on the size and number of rat zona fasciculata mitochondria. *Cell Tissue Res.* 1974;150(1):79-94.
60. Wright NA, and Appleton D. The action of dexamethasone on the adrenal cortex. *J Endocrinol.* 1972;53(3):xxxvii.
61. Cote M, Guillon G, Payet MD, and Gallo-Payet N. Expression and regulation of adenylyl cyclase isoforms in the human adrenal gland. *J Clin Endocrinol Metab.* 2001;86(9):4495-503.
62. Gorrigan RJ, Guasti L, King P, Clark AJ, and Chan LF. Localisation of the melanocortin-2-receptor and its accessory proteins in the developing and adult adrenal gland. *J Mol Endocrinol.* 2011;46(3):227-32.
63. Sahut-Barnola I, de Joussineau C, Val P, Lambert-Langlais S, Damon C, Lefrancois-Martinez AM, et al. Cushing's syndrome and fetal features resurgence in adrenal cortex-specific Prkar1a knockout mice. *PLoS Genet.* 2010;6(6):e1000980.
64. Dumontet T, Sahut-Barnola I, Septier A, Montanier N, Plotton I, Roucher-Boulez F, et al. PKA signaling drives reticularis differentiation and sexually dimorphic adrenal cortex renewal. *JCI Insight.* 2018;3(2).
65. Kirschner LS, Carney JA, Pack SD, Taymans SE, Giatzakis C, Cho YS, et al. Mutations of the gene encoding the protein kinase A type I-alpha regulatory subunit in patients with the Carney complex. *Nat Genet.* 2000;26(1):89-92.

66. Drelon C, Berthon A, Sahut-Barnola I, Mathieu M, Dumontet T, Rodriguez S, et al. PKA inhibits WNT signalling in adrenal cortex zonation and prevents malignant tumour development. *Nat Commun.* 2016;7:12751.
67. Howard-Miller E. A transitory zone in the adrenal cortex which shows age and sex relationships. *American Journal of Anatomy.* 1927;40(2):251-93.
68. Hirokawa N, and Ishikawa H. Electron microscopic observations on postnatal development of the X zone in mouse adrenal cortex. *Z Anat Entwicklungsgesch.* 1974;144(1):85-100.
69. Morohashi K, and Zubair M. The fetal and adult adrenal cortex. *Mol Cell Endocrinol.* 2011;336(1-2):193-7.
70. Holmes PV, and Dickson AD. X-zone degeneration in the adrenal glands of adult and immature female mice. *J Anat.* 1971;108(Pt 1):159-68.
71. Hershkovitz L, Beuschlein F, Klammer S, Krup M, and Weinstein Y. Adrenal 20alpha-hydroxysteroid dehydrogenase in the mouse catabolizes progesterone and 11-deoxycorticosterone and is restricted to the X-zone. *Endocrinology.* 2007;148(3):976-88.
72. Sucheston ME, and Cannon MS. Development of zonular patterns in the human adrenal gland. *J Morphol.* 1968;126(4):477-91.
73. Ishimoto H, and Jaffe RB. Development and function of the human fetal adrenal cortex: a key component in the feto-placental unit. *Endocr Rev.* 2011;32(3):317-55.
74. Spencer SJ, Mesiano S, Lee JY, and Jaffe RB. Proliferation and apoptosis in the human adrenal cortex during the fetal and perinatal periods: implications for growth and remodeling. *J Clin Endocrinol Metab.* 1999;84(3):1110-5.
75. Lee O, Chang CC, Lee W, and Chang TY. Immunodepletion experiments suggest that acyl-coenzyme A:cholesterol acyltransferase-1 (ACAT-1) protein plays a major catalytic role in adult human liver, adrenal gland, macrophages, and kidney, but not in intestines. *J Lipid Res.* 1998;39(8):1722-7.
76. LaPensee CR, Mann JE, Rainey WE, Crudo V, Hunt SW, 3rd, and Hammer GD. ATR-101, a Selective and Potent Inhibitor of Acyl-CoA Acyltransferase 1, Induces Apoptosis in H295R Adrenocortical Cells and in the Adrenal Cortex of Dogs. *Endocrinology.* 2016;157(5):1775-88.
77. Clark BJ, Wells J, King SR, and Stocco DM. The purification, cloning, and expression of a novel luteinizing hormone-induced mitochondrial protein in MA-10 mouse Leydig tumor cells. Characterization of the steroidogenic acute regulatory protein (StAR). *J Biol Chem.* 1994;269(45):28314-22.
78. Turcu AF, Nanba AT, Chomic R, Upadhyay SK, Giordano TJ, Shields JJ, et al. Adrenal-derived 11-oxygenated 19-carbon steroids are the dominant androgens in classic 21-hydroxylase deficiency. *Eur J Endocrinol.* 2016;174(5):601-9.
79. Auchus RJ, Lee TC, and Miller WL. Cytochrome b5 augments the 17,20-lyase activity of human P450c17 without direct electron transfer. *J Biol Chem.* 1998;273(6):3158-65.
80. Miller WL, and Auchus RJ. The molecular biology, biochemistry, and physiology of human steroidogenesis and its disorders. *Endocr Rev.* 2011;32(1):81-151.
81. Beuschlein F, Galac S, and Wilson DB. Animal models of adrenocortical tumorigenesis. *Mol Cell Endocrinol.* 2012;351(1):78-86.

82. Castrop H, Hocherl K, Kurtz A, Schweda F, Todorov V, and Wagner C. Physiology of kidney renin. *Physiol Rev.* 2010;90(2):607-73.
83. Bollag WB. Regulation of aldosterone synthesis and secretion. *Compr Physiol.* 2014;4(3):1017-55.
84. Atlas SA. The renin-angiotensin aldosterone system: pathophysiological role and pharmacologic inhibition. *J Manag Care Pharm.* 2007;13(8 Suppl B):9-20.
85. Hattangady NG, Olala LO, Bollag WB, and Rainey WE. Acute and chronic regulation of aldosterone production. *Mol Cell Endocrinol.* 2012;350(2):151-62.
86. Cherradi N, Pardo B, Greenberg AS, Kraemer FB, and Capponi AM. Angiotensin II activates cholesterol ester hydrolase in bovine adrenal glomerulosa cells through phosphorylation mediated by p42/p44 mitogen-activated protein kinase. *Endocrinology.* 2003;144(11):4905-15.
87. Stocco DM, Wang X, Jo Y, and Manna PR. Multiple signaling pathways regulating steroidogenesis and steroidogenic acute regulatory protein expression: more complicated than we thought. *Mol Endocrinol.* 2005;19(11):2647-59.
88. Arakane F, King SR, Du Y, Kallen CB, Walsh LP, Watari H, et al. Phosphorylation of steroidogenic acute regulatory protein (StAR) modulates its steroidogenic activity. *J Biol Chem.* 1997;272(51):32656-62.
89. Barrett PQ, Bollag WB, Isales CM, McCarthy RT, and Rasmussen H. Role of calcium in angiotensin II-mediated aldosterone secretion. *Endocr Rev.* 1989;10(4):496-518.
90. Bird IM, Hanley NA, Word RA, Mathis JM, McCarthy JL, Mason JI, et al. Human NCI-H295 adrenocortical carcinoma cells: a model for angiotensin-II-responsive aldosterone secretion. *Endocrinology.* 1993;133(4):1555-61.
91. Bollag WB, Barrett PQ, Isales CM, and Rasmussen H. Angiotensin-II-induced changes in diacylglycerol levels and their potential role in modulating the steroidogenic response. *Endocrinology.* 1991;128(1):231-41.
92. Farese RV, Larson RE, Sabir MA, and Gomez-Sanchez C. Effects of angiotensin-II and potassium on phospholipid metabolism in the adrenal zona glomerulosa. *J Biol Chem.* 1981;256(21):11093-7.
93. Kojima I, Kojima K, Kreutter D, and Rasmussen H. The temporal integration of the aldosterone secretory response to angiotensin occurs via two intracellular pathways. *J Biol Chem.* 1984;259(23):14448-57.
94. Aptel HB, Johnson EI, Vallotton MB, Rossier MF, and Capponi AM. Demonstration of an angiotensin II-induced negative feedback effect on aldosterone synthesis in isolated rat adrenal zona glomerulosa cells. *Mol Cell Endocrinol.* 1996;119(1):105-11.
95. Burnay MM, Python CP, Vallotton MB, Capponi AM, and Rossier MF. Role of the capacitative calcium influx in the activation of steroidogenesis by angiotensin-II in adrenal glomerulosa cells. *Endocrinology.* 1994;135(2):751-8.
96. Rossier MF, Burnay MM, Vallotton MB, and Capponi AM. Distinct functions of T- and L-type calcium channels during activation of bovine adrenal glomerulosa cells. *Endocrinology.* 1996;137(11):4817-26.
97. Ganguly A, Chiou S, Fineberg NS, and Davis JS. Greater importance of Ca(2+)-calmodulin in maintenance of ang II- and K(+)-mediated aldosterone secretion:

lesser role of protein kinase C. *Biochem Biophys Res Commun.* 1992;182(1):254-61.
98. Pezzi V, Clark BJ, Ando S, Stocco DM, and Rainey WE. Role of calmodulin-dependent protein kinase II in the acute stimulation of aldosterone production. *J Steroid Biochem Mol Biol.* 1996;58(4):417-24.
99. Kapas S, Purbrick A, and Hinson JP. Role of tyrosine kinase and protein kinase C in the steroidogenic actions of angiotensin II, alpha-melanocyte-stimulating hormone and corticotropin in the rat adrenal cortex. *Biochem J.* 1995;305 (Pt 2):433-8.
100. Hajnoczky G, Varnai P, Buday L, Farago A, and Spat A. The role of protein kinase-C in control of aldosterone production by rat adrenal glomerulosa cells: activation of protein kinase-C by stimulation with potassium. *Endocrinology.* 1992;130(4):2230-6.
101. Manna PR, Huhtaniemi IT, and Stocco DM. Mechanisms of protein kinase C signaling in the modulation of 3',5'-cyclic adenosine monophosphate-mediated steroidogenesis in mouse gonadal cells. *Endocrinology.* 2009;150(7):3308-17.
102. Betancourt-Calle S, Calle RA, Isales CM, White S, Rasmussen H, and Bollag WB. Differential effects of agonists of aldosterone secretion on steroidogenic acute regulatory phosphorylation. *Mol Cell Endocrinol.* 2001;173(1-2):87-94.
103. Bollag WB, Barrett PQ, Isales CM, Liscovitch M, and Rasmussen H. A potential role for phospholipase-D in the angiotensin-II-induced stimulation of aldosterone secretion from bovine adrenal glomerulosa cells. *Endocrinology.* 1990;127(3):1436-43.
104. Bollag WB, Jung E, and Calle RA. Mechanism of angiotensin II-induced phospholipase D activation in bovine adrenal glomerulosa cells. *Mol Cell Endocrinol.* 2002;192(1-2):7-16.
105. Zheng X, and Bollag WB. AngII induces transient phospholipase D activity in the H295R glomerulosa cell model. *Mol Cell Endocrinol.* 2003;206(1-2):113-22.
106. Spat A, and Hunyady L. Control of aldosterone secretion: a model for convergence in cellular signaling pathways. *Physiol Rev.* 2004;84(2):489-539.
107. Clyne CD, Zhang Y, Slutsker L, Mathis JM, White PC, and Rainey WE. Angiotensin II and potassium regulate human CYP11B2 transcription through common cis-elements. *Mol Endocrinol.* 1997;11(5):638-49.
108. Sculptoreanu A, Scheuer T, and Catterall WA. Voltage-dependent potentiation of L-type Ca2+ channels due to phosphorylation by cAMP-dependent protein kinase. *Nature.* 1993;364(6434):240-3.
109. Gallo-Payet N, Grazzini E, Cote M, Chouinard L, Chorvatova A, Bilodeau L, et al. Role of Ca2+ in the action of adrenocorticotropin in cultured human adrenal glomerulosa cells. *J Clin Invest.* 1996;98(2):460-6.
110. Bassett MH, White PC, and Rainey WE. The regulation of aldosterone synthase expression. *Mol Cell Endocrinol.* 2004;217(1-2):67-74.
111. Holland OB, and Carr B. Modulation of aldosterone synthase messenger ribonucleic acid levels by dietary sodium and potassium and by adrenocorticotropin. *Endocrinology.* 1993;132(6):2666-73.
112. Tremblay A, Parker KL, and Lehoux JG. Dietary potassium supplementation and sodium restriction stimulate aldosterone synthase but not 11 beta-hydroxylase P-

450 messenger ribonucleic acid accumulation in rat adrenals and require angiotensin II production. *Endocrinology.* 1992;130(6):3152-8.
113. Adler GK, Chen R, Menachery AI, Braley LM, and Williams GH. Sodium restriction increases aldosterone biosynthesis by increasing late pathway, but not early pathway, messenger ribonucleic acid levels and enzyme activity in normotensive rats. *Endocrinology.* 1993;133(5):2235-40.
114. Bassett MH, Suzuki T, Sasano H, White PC, and Rainey WE. The orphan nuclear receptors NURR1 and NGFIB regulate adrenal aldosterone production. *Mol Endocrinol.* 2004;18(2):279-90.
115. Bassett MH, Zhang Y, White PC, and Rainey WE. Regulation of human CYP11B2 and CYP11B1: comparing the role of the common CRE/Ad1 element. *Endocr Res.* 2000;26(4):941-51.
116. Bassett MH, Zhang Y, Clyne C, White PC, and Rainey WE. Differential regulation of aldosterone synthase and 11beta-hydroxylase transcription by steroidogenic factor-1. *J Mol Endocrinol.* 2002;28(2):125-35.
117. Ye P, Nakamura Y, Lalli E, and Rainey WE. Differential effects of high and low steroidogenic factor-1 expression on CYP11B2 expression and aldosterone production in adrenocortical cells. *Endocrinology.* 2009;150(3):1303-9.
118. Chen X, Li W, Yoshida H, Tsuchida S, Nishimura H, Takemoto F, et al. Targeting deletion of angiotensin type 1B receptor gene in the mouse. *Am J Physiol.* 1997;272(3 Pt 2):F299-304.
119. Okubo S, Niimura F, Nishimura H, Takemoto F, Fogo A, Matsusaka T, et al. Angiotensin-independent mechanism for aldosterone synthesis during chronic extracellular fluid volume depletion. *J Clin Invest.* 1997;99(5):855-60.
120. Hartroft PM, and Sowa E. Effect of Potassium on Juxtaglomerular Cells and the Adrenal Zona Glomerulosa of Rats. *J Nutr.* 1964;82:439-42.
121. Crivello JF, and Gill GN. Induction of cultured bovine adrenocortical zona glomerulosa cell 17-hydroxylase activity by ACTH. *Mol Cell Endocrinol.* 1983;30(1):97-107.
122. Fuchs-Hammoser R, Schweiger M, and Oelkers W. The effect of chronic low-dose infusion of ACTH (1-24) on renin, renin-substrate, aldosterone and other corticosteroids in sodium replete and deplete man. *Acta Endocrinol (Copenh).* 1980;95(2):198-206.
123. Hausdorff WP, Sekura RD, Aguilera G, and Catt KJ. Control of aldosterone production by angiotensin II is mediated by two guanine nucleotide regulatory proteins. *Endocrinology.* 1987;120(4):1668-78.
124. Schteingart DE. The 50th anniversary of the identification of primary aldosteronism: a retrospective of the work of Jerome W. Conn. *J Lab Clin Med.* 2005;145(1):12-6.
125. Gomez-Sanchez CE, Qi X, Velarde-Miranda C, Plonczynski MW, Parker CR, Rainey W, et al. Development of monoclonal antibodies against human CYP11B1 and CYP11B2. *Mol Cell Endocrinol.* 2014;383(1-2):111-7.
126. Nishimoto K, Nakagawa K, Li D, Kosaka T, Oya M, Mikami S, et al. Adrenocortical zonation in humans under normal and pathological conditions. *J Clin Endocrinol Metab.* 2010;95(5):2296-305.

127. Monticone S, Burrello J, Tizzani D, Bertello C, Viola A, Buffolo F, et al. Prevalence and Clinical Manifestations of Primary Aldosteronism Encountered in Primary Care Practice. *J Am Coll Cardiol.* 2017;69(14):1811-20.
128. Rossi GP, Bernini G, Caliumi C, Desideri G, Fabris B, Ferri C, et al. A prospective study of the prevalence of primary aldosteronism in 1,125 hypertensive patients. *J Am Coll Cardiol.* 2006;48(11):2293-300.
129. Lim PO, Dow E, Brennan G, Jung RT, and MacDonald TM. High prevalence of primary aldosteronism in the Tayside hypertension clinic population. *J Hum Hypertens.* 2000;14(5):311-5.
130. Fardella CE, Mosso L, Gomez-Sanchez C, Cortes P, Soto J, Gomez L, et al. Primary hyperaldosteronism in essential hypertensives: prevalence, biochemical profile, and molecular biology. *J Clin Endocrinol Metab.* 2000;85(5):1863-7.
131. Strauch B, Zelinka T, Hampf M, Bernhardt R, and Widimsky J, Jr. Prevalence of primary hyperaldosteronism in moderate to severe hypertension in the Central Europe region. *J Hum Hypertens.* 2003;17(5):349-52.
132. Calhoun DA, Nishizaka MK, Zaman MA, Thakkar RB, and Weissmann P. Hyperaldosteronism among black and white subjects with resistant hypertension. *Hypertension.* 2002;40(6):892-6.
133. Gallay BJ, Ahmad S, Xu L, Toivola B, and Davidson RC. Screening for primary aldosteronism without discontinuing hypertensive medications: plasma aldosterone-renin ratio. *Am J Kidney Dis.* 2001;37(4):699-705.
134. Savard S, Amar L, Plouin PF, and Steichen O. Cardiovascular complications associated with primary aldosteronism: a controlled cross-sectional study. *Hypertension.* 2013;62(2):331-6.
135. Mulatero P, Monticone S, Bertello C, Viola A, Tizzani D, Iannaccone A, et al. Long-term cardio- and cerebrovascular events in patients with primary aldosteronism. *J Clin Endocrinol Metab.* 2013;98(12):4826-33.
136. Hayashi H, Kobara M, Abe M, Tanaka N, Gouda E, Toba H, et al. Aldosterone nongenomically produces NADPH oxidase-dependent reactive oxygen species and induces myocyte apoptosis. *Hypertens Res.* 2008;31(2):363-75.
137. Catena C, Colussi G, Nadalini E, Chiuch A, Baroselli S, Lapenna R, et al. Cardiovascular outcomes in patients with primary aldosteronism after treatment. *Arch Intern Med.* 2008;168(1):80-5.
138. Milliez P, Girerd X, Plouin PF, Blacher J, Safar ME, and Mourad JJ. Evidence for an increased rate of cardiovascular events in patients with primary aldosteronism. *J Am Coll Cardiol.* 2005;45(8):1243-8.
139. Tsybouleva N, Zhang L, Chen S, Patel R, Lutucuta S, Nemoto S, et al. Aldosterone, through novel signaling proteins, is a fundamental molecular bridge between the genetic defect and the cardiac phenotype of hypertrophic cardiomyopathy. *Circulation.* 2004;109(10):1284-91.
140. Qin W, Rudolph AE, Bond BR, Rocha R, Blomme EA, Goellner JJ, et al. Transgenic model of aldosterone-driven cardiac hypertrophy and heart failure. *Circ Res.* 2003;93(1):69-76.
141. Lijnen P, and Petrov V. Induction of cardiac fibrosis by aldosterone. *J Mol Cell Cardiol.* 2000;32(6):865-79.

142. Gomez-Sanchez CE, Kuppusamy M, Reincke M, and Williams TA. Disordered CYP11B2 Expression in Primary Aldosteronism. *Horm Metab Res.* 2017;49(12):957-62.
143. Perez-Rivas LG, Williams TA, and Reincke M. Inherited Forms of Primary Hyperaldosteronism: New Genes, New Phenotypes and Proposition of A New Classification. *Exp Clin Endocrinol Diabetes.* 2018.
144. Sutherland DJ, Ruse JL, and Laidlaw JC. Hypertension, increased aldosterone secretion and low plasma renin activity relieved by dexamethasone. *Can Med Assoc J.* 1966;95(22):1109-19.
145. Scholl UI, Stolting G, Schewe J, Thiel A, Tan H, Nelson-Williams C, et al. CLCN2 chloride channel mutations in familial hyperaldosteronism type II. *Nat Genet.* 2018;50(3):349-54.
146. Young WF, Jr. Diagnosis and treatment of primary aldosteronism: practical clinical perspectives. *J Intern Med.* 2018.
147. El Ghorayeb N, Bourdeau I, and Lacroix A. Role of ACTH and Other Hormones in the Regulation of Aldosterone Production in Primary Aldosteronism. *Front Endocrinol (Lausanne).* 2016;7:72.
148. Nanba K, Vaidya A, Williams GH, Zheng I, Else T, and Rainey WE. Age-Related Autonomous Aldosteronism. *Circulation.* 2017;136(4):347-55.
149. Nishimoto K, Seki T, Hayashi Y, Mikami S, Al-Eyd G, Nakagawa K, et al. Human Adrenocortical Remodeling Leading to Aldosterone-Producing Cell Cluster Generation. *Int J Endocrinol.* 2016;2016:7834356.
150. Omata K, Anand SK, Hovelson DH, Liu CJ, Yamazaki Y, Nakamura Y, et al. Aldosterone-Producing Cell Clusters Frequently Harbor Somatic Mutations and Accumulate With Age in Normal Adrenals. *J Endocr Soc.* 2017;1(7):787-99.
151. Monticone S, Castellano I, Versace K, Lucatello B, Veglio F, Gomez-Sanchez CE, et al. Immunohistochemical, genetic and clinical characterization of sporadic aldosterone-producing adenomas. *Mol Cell Endocrinol.* 2015;411:146-54.
152. Nanba K, Vaidya A, and Rainey WE. Aging and Adrenal Aldosterone Production. *Hypertension.* 2018;71(2):218-23.
153. Fernandes-Rosa FL, Williams TA, Riester A, Steichen O, Beuschlein F, Boulkroun S, et al. Genetic spectrum and clinical correlates of somatic mutations in aldosterone-producing adenoma. *Hypertension.* 2014;64(2):354-61.
154. Zheng FF, Zhu LM, Nie AF, Li XY, Lin JR, Zhang K, et al. Clinical characteristics of somatic mutations in Chinese patients with aldosterone-producing adenoma. *Hypertension.* 2015;65(3):622-8.
155. Williams TA, Monticone S, and Mulatero P. KCNJ5 mutations are the most frequent genetic alteration in primary aldosteronism. *Hypertension.* 2015;65(3):507-9.
156. Xie CB, Shaikh LH, Garg S, Tanriver G, Teo AE, Zhou J, et al. Regulation of aldosterone secretion by Cav1.3. *Sci Rep.* 2016;6:24697.
157. Azizan EA, Poulsen H, Tuluc P, Zhou J, Clausen MV, Lieb A, et al. Somatic mutations in ATP1A1 and CACNA1D underlie a common subtype of adrenal hypertension. *Nat Genet.* 2013;45(9):1055-60.

158. Scholl UI, Goh G, Stolting G, de Oliveira RC, Choi M, Overton JD, et al. Somatic and germline CACNA1D calcium channel mutations in aldosterone-producing adenomas and primary aldosteronism. *Nat Genet.* 2013;45(9):1050-4.
159. Tan GC, Negro G, Pinggera A, Tizen Laim NMS, Mohamed Rose I, Ceral J, et al. Aldosterone-Producing Adenomas: Histopathology-Genotype Correlation and Identification of a Novel CACNA1D Mutation. *Hypertension.* 2017;70(1):129-36.
160. Nishimoto K, Tomlins SA, Kuick R, Cani AK, Giordano TJ, Hovelson DH, et al. Aldosterone-stimulating somatic gene mutations are common in normal adrenal glands. *Proc Natl Acad Sci U S A.* 2015;112(33):E4591-9.
161. Scholl UI, Stolting G, Nelson-Williams C, Vichot AA, Choi M, Loring E, et al. Recurrent gain of function mutation in calcium channel CACNA1H causes early-onset hypertension with primary aldosteronism. *Elife.* 2015;4:e06315.
162. Beuschlein F, Boulkroun S, Osswald A, Wieland T, Nielsen HN, Lichtenauer UD, et al. Somatic mutations in ATP1A1 and ATP2B3 lead to aldosterone-producing adenomas and secondary hypertension. *Nat Genet.* 2013;45(4):440-4, 4e1-2.
163. Mulatero P, Monticone S, Burrello J, Veglio F, Williams TA, and Funder J. Guidelines for primary aldosteronism: uptake by primary care physicians in Europe. *J Hypertens.* 2016;34(11):2253-7.
164. Rossi E, Perazzoli F, Negro A, and Magnani A. Diagnostic rate of primary aldosteronism in Emilia-Romagna, Northern Italy, during 16 years (2000-2015). *J Hypertens.* 2017;35(8):1691-7.
165. Young WF, Stanson AW, Thompson GB, Grant CS, Farley DR, and van Heerden JA. Role for adrenal venous sampling in primary aldosteronism. *Surgery.* 2004;136(6):1227-35.
166. Lim V, Guo Q, Grant CS, Thompson GB, Richards ML, Farley DR, et al. Accuracy of adrenal imaging and adrenal venous sampling in predicting surgical cure of primary aldosteronism. *J Clin Endocrinol Metab.* 2014;99(8):2712-9.
167. Nanba AT, Nanba K, Byrd JB, Shields JJ, Giordano TJ, Miller BS, et al. Discordance between imaging and immunohistochemistry in unilateral primary aldosteronism. *Clin Endocrinol (Oxf).* 2017;87(6):665-72.
168. Gomez-Sanchez EP. Third-generation Mineralocorticoid Receptor Antagonists: Why Do We Need a Fourth? *J Cardiovasc Pharmacol.* 2016;67(1):26-38.
169. Aragao-Santiago L, Gomez-Sanchez CE, Mulatero P, Spyroglou A, Reincke M, and Williams TA. Mouse Models of Primary Aldosteronism: From Physiology to Pathophysiology. *Endocrinology.* 2017;158(12):4129-38.
170. Heitzmann D, Derand R, Jungbauer S, Bandulik S, Sterner C, Schweda F, et al. Invalidation of TASK1 potassium channels disrupts adrenal gland zonation and mineralocorticoid homeostasis. *EMBO J.* 2008;27(1):179-87.
171. Bandulik S, Penton D, Barhanin J, and Warth R. TASK1 and TASK3 potassium channels: determinants of aldosterone secretion and adrenocortical zonation. *Horm Metab Res.* 2010;42(6):450-7.
172. Penton D, Bandulik S, Schweda F, Haubs S, Tauber P, Reichold M, et al. Task3 potassium channel gene invalidation causes low renin and salt-sensitive arterial hypertension. *Endocrinology.* 2012;153(10):4740-8.

173. Guagliardo NA, Yao J, Hu C, Schertz EM, Tyson DA, Carey RM, et al. TASK-3 channel deletion in mice recapitulates low-renin essential hypertension. *Hypertension.* 2012;59(5):999-1005.
174. Grimm PR, Irsik DL, Settles DC, Holtzclaw JD, and Sansom SC. Hypertension of Kcnmb1-/- is linked to deficient K secretion and aldosteronism. *Proc Natl Acad Sci U S A.* 2009;106(28):11800-5.
175. Sausbier M, Arntz C, Bucurenciu I, Zhao H, Zhou XB, Sausbier U, et al. Elevated blood pressure linked to primary hyperaldosteronism and impaired vasodilation in BK channel-deficient mice. *Circulation.* 2005;112(1):60-8.
176. Bhandaru M, Kempe DS, Rotte A, Rexhepaj R, Kuhl D, and Lang F. Hyperaldosteronism, hypervolemia, and increased blood pressure in mice expressing defective APC. *Am J Physiol Regul Integr Comp Physiol.* 2009;297(3):R571-5.
177. Kakoki M, Pochynyuk OM, Hathaway CM, Tomita H, Hagaman JR, Kim HS, et al. Primary aldosteronism and impaired natriuresis in mice underexpressing TGFbeta1. *Proc Natl Acad Sci U S A.* 2013;110(14):5600-5.
178. Doi M, Takahashi Y, Komatsu R, Yamazaki F, Yamada H, Haraguchi S, et al. Salt-sensitive hypertension in circadian clock-deficient Cry-null mice involves dysregulated adrenal Hsd3b6. *Nat Med.* 2010;16(1):67-74.
179. Spyroglou A, Wagner S, Gomez-Sanchez C, Rathkolb B, Wolf E, Manolopoulou J, et al. Utilization of a mutagenesis screen to generate mouse models of hyperaldosteronism. *Endocrinology.* 2011;152(1):326-31.
180. Makhanova N, Hagaman J, Kim HS, and Smithies O. Salt-sensitive blood pressure in mice with increased expression of aldosterone synthase. *Hypertension.* 2008;51(1):134-40.
181. Gu H, Ma Z, Wang J, Zhu T, Du N, Shatara A, et al. Salt-dependent Blood Pressure in Human Aldosterone Synthase-Transgenic Mice. *Sci Rep.* 2017;7(1):492.
182. Scortegagna M, Berthon A, Settas N, Giannakou A, Garcia G, Li JL, et al. The E3 ubiquitin ligase Siah1 regulates adrenal gland organization and aldosterone secretion. *JCI Insight.* 2017;2(23).
183. Pignatti E, Leng S, Carlone DL, and Breault DT. Regulation of zonation and homeostasis in the adrenal cortex. *Mol Cell Endocrinol.* 2017;441:146-55.
184. Fern RJ, Hahm MS, Lu HK, Liu LP, Gorelick FS, and Barrett PQ. Ca2+/calmodulin-dependent protein kinase II activation and regulation of adrenal glomerulosa Ca2+ signaling. *Am J Physiol.* 1995;269(6 Pt 2):F751-60.
185. Ganguly A, and Davis JS. Role of calcium and other mediators in aldosterone secretion from the adrenal glomerulosa cells. *Pharmacol Rev.* 1994;46(4):417-47.
186. Hunyady L, Baukal AJ, Bor M, Ely JA, and Catt KJ. Regulation of 1,2-diacylglycerol production by angiotensin-II in bovine adrenal glomerulosa cells. *Endocrinology.* 1990;126(2):1001-8.
187. Hannemann A, and Wallaschofski H. Prevalence of primary aldosteronism in patient's cohorts and in population-based studies--a review of the current literature. *Horm Metab Res.* 2012;44(3):157-62.

188. Gekle M, and Grossmann C. Actions of aldosterone in the cardiovascular system: the good, the bad, and the ugly? *Pflugers Arch.* 2009;458(2):231-46.
189. Urban DJ, and Roth BL. DREADDs (designer receptors exclusively activated by designer drugs): chemogenetic tools with therapeutic utility. *Annu Rev Pharmacol Toxicol.* 2015;55:399-417.
190. Teissier A, Chemiakine A, Inbar B, Bagchi S, Ray RS, Palmiter RD, et al. Activity of Raphe Serotonergic Neurons Controls Emotional Behaviors. *Cell Rep.* 2015;13(9):1965-76.
191. Jain S, Ruiz de Azua I, Lu H, White MF, Guettier JM, and Wess J. Chronic activation of a designer G(q)-coupled receptor improves beta cell function. *J Clin Invest.* 2013;123(4):1750-62.
192. Alexander GM, Rogan SC, Abbas AI, Armbruster BN, Pei Y, Allen JA, et al. Remote control of neuronal activity in transgenic mice expressing evolved G protein-coupled receptors. *Neuron.* 2009;63(1):27-39.
193. Armbruster BN, Li X, Pausch MH, Herlitze S, and Roth BL. Evolving the lock to fit the key to create a family of G protein-coupled receptors potently activated by an inert ligand. *Proc Natl Acad Sci U S A.* 2007;104(12):5163-8.
194. Romero DG, Yanes LL, de Rodriguez AF, Plonczynski MW, Welsh BL, Reckelhoff JF, et al. Disabled-2 is expressed in adrenal zona glomerulosa and is involved in aldosterone secretion. *Endocrinology.* 2007;148(6):2644-52.
195. Peng KY, Chang HM, Lin YF, Chan CK, Chang CH, Chueh SJ, et al. miRNA-203 Modulates Aldosterone Levels and Cell Proliferation by Targeting Wnt5a in Aldosterone-Producing Adenomas. *J Clin Endocrinol Metab.* 2018;103(10):3737-47.
196. Tadjine M, Lampron A, Ouadi L, and Bourdeau I. Frequent mutations of beta-catenin gene in sporadic secreting adrenocortical adenomas. *Clin Endocrinol (Oxf).* 2008;68(2):264-70.
197. Tissier F, Cavard C, Groussin L, Perlemoine K, Fumey G, Hagnere AM, et al. Mutations of beta-catenin in adrenocortical tumors: activation of the Wnt signaling pathway is a frequent event in both benign and malignant adrenocortical tumors. *Cancer Res.* 2005;65(17):7622-7.
198. Davies LA, Hu C, Guagliardo NA, Sen N, Chen X, Talley EM, et al. TASK channel deletion in mice causes primary hyperaldosteronism. *Proc Natl Acad Sci U S A.* 2008;105(6):2203-8.
199. El Wakil A, Bandulik S, Guy N, Bendahhou S, Zennaro MC, Niehrs C, et al. Dkk3 is a component of the genetic circuitry regulating aldosterone biosynthesis in the adrenal cortex. *Human Molecular Genetics.* 2012;21(22):4922-9.
200. El Wakil A, Mari B, Barhanin J, and Lalli E. Genomic analysis of sexual dimorphism of gene expression in the mouse adrenal gland. *Horm Metab Res.* 2013;45(12):870-3.
201. Spyroglou A, Bozoglu T, Rawal R, De Leonardis F, Sterner C, Boulkroun S, et al. Diastrophic dysplasia sulfate transporter (SLC26A2) is expressed in the adrenal cortex and regulates aldosterone secretion. *Hypertension.* 2014;63(5):1102-9.
202. Guasti L, Paul A, Laufer E, and King P. Localization of Sonic hedgehog secreting and receiving cells in the developing and adult rat adrenal cortex. *Mol Cell Endocrinol.* 2011;336(1-2):117-22.

203. Whitesall SE, Hoff JB, Vollmer AP, and D'Alecy LG. Comparison of simultaneous measurement of mouse systolic arterial blood pressure by radiotelemetry and tail-cuff methods. *Am J Physiol Heart Circ Physiol.* 2004;286(6):H2408-15.
204. Miller WL, and Auchus RJ. The Molecular Biology, Biochemistry, and Physiology of Human Steroidogenesis and Its Disorders. *Endocrine Reviews.* 2011;32(1):81-151.
205. Baldán Á, Bojanic DD, and Edwards PA. The ABCs of sterol transport. *Journal of Lipid Research.* 2009;50(Supplement):S80-S5.
206. Bochem AE, Holleboom AG, Romijn JA, Hoekstra M, Dallinga-Thie GM, Motazacker MM, et al. High density lipoprotein as a source of cholesterol for adrenal steroidogenesis: a study in individuals with low plasma HDL-C. *Journal of Lipid Research.* 2013;54(6):1698-704.
207. Gwynne JT, and Strauss JF. The Role of Lipoproteins in Steroidogenesis and Cholesterol Metabolism in Steroidogenic Glands. *Endocrine Reviews.* 1982;3(3):299-329.
208. Hoekstra M, Ye D, Hildebrand RB, Zhao Y, Lammers B, Stitzinger M, et al. Scavenger receptor class B type I-mediated uptake of serum cholesterol is essential for optimal adrenal glucocorticoid production. *J Lipid Res.* 2009;50(6):1039-46.
209. Higashijima M, Kato K-I, Nawata H, and Ibayashi H. Studies on Lipoprotein and Adrenal Steroidogenesis: II. Utilization of Low Density Lipoprotein-and High Density Lipoprotein-Cholesterol for Steroid Production in Functioning Human Adrenocortical Adenoma Cells in Culture. *Endocrinologia Japonica.* 1987;34(5):647-57.
210. Higashijima M, Nawata H, Kato K-I, and Ibayashi H. Studies on Lipoprotein and Adrenal Steroidogenesis: I. Roles of Low Density Lipoprotein-and High Density Lipoprotein-Cholesterol in Steroid Production in Cultured Human Adrenocortical Cells. *Endocrinologia Japonica.* 1987;34(5):635-45.
211. Carr BR, and Simpson ER. Lipoprotein Utilization and Cholesterol Synthesis by the Human Fetal Adrenal Gland. *Endocrine Reviews.* 1981;2(3):306-26.
212. Stone NJ, Robinson J, Lichtenstein AH, Merz CN, Blum CB, Eckel RH, et al. 2013 ACC/AHA Guideline on the Treatment of Blood Cholesterol to Reduce Atherosclerotic Cardiovascular Risk in Adults: A Report of the American College of Cardiology/American Heart Association Task Force on Practice Guidelines. *Circulation.* 2013.
213. Lewis GF, and Rader DJ. New insights into the regulation of HDL metabolism and reverse cholesterol transport. *Circ Res.* 2005;96(12):1221-32.
214. Schaefer EJ. Effects of cholesteryl ester transfer protein inhibitors on human lipoprotein metabolism: why have they failed in lowering coronary heart disease risk? *Curr Opin Lipidol.* 2013;24(3):259-64.
215. Forrest MJ, Bloomfield D, Briscoe RJ, Brown PN, Cumiskey AM, Ehrhart J, et al. Torcetrapib-induced blood pressure elevation is independent of CETP inhibition and is accompanied by increased circulating levels of aldosterone. *Br J Pharmacol.* 2008;154(7):1465-73.

216. Remaley AT, Amar M, and Sviridov D. HDL-replacement therapy: mechanism of action, types of agents and potential clinical indications. *Expert Rev Cardiovasc Ther.* 2008;6(9):1203-15.
217. Yancey PG, Bortnick AE, Kellner-Weibel G, de la Llera-Moya M, Phillips MC, and Rothblat GH. Importance of Different Pathways of Cellular Cholesterol Efflux. *Arteriosclerosis, Thrombosis, and Vascular Biology.* 2003;23(5):712-9.
218. Nissen SE, Tsunoda T, Tuzcu E, and et al. Effect of recombinant apoa-i milano on coronary atherosclerosis in patients with acute coronary syndromes: A randomized controlled trial. *JAMA.* 2003;290(17):2292-300.
219. Tardif JC, Gregoire J, L'Allier PL, Ibrahim R, Lesperance J, Heinonen TM, et al. Effects of reconstituted high-density lipoprotein infusions on coronary atherosclerosis: a randomized controlled trial. *JAMA.* 2007;297(15):1675-82.
220. Khan M.L.N, Drake S.L, Crockatt J.G, and J.L.H D. Single-dose intravenous infusion of ETC-642, a 22-Mer ApoA-I analogue and phospholipids complex, elevates HDL-C in atherosclerosis patients. *Circulation* 2003(108):563-4.
221. Tardif JC, Ballantyne CM, Barter P, Dasseux JL, Fayad ZA, Guertin MC, et al. Effects of the high-density lipoprotein mimetic agent CER-001 on coronary atherosclerosis in patients with acute coronary syndromes: a randomized trial. *Eur Heart J.* 2014.
222. Tricoci P, D'Andrea DM, Gurbel PA, Yao Z, Cuchel M, Winston B, et al. Infusion of Reconstituted High-Density Lipoprotein, CSL112, in Patients With Atherosclerosis: Safety and Pharmacokinetic Results From a Phase 2a Randomized Clinical Trial. *J Am Heart Assoc.* 2015;4(8):e002171.
223. CSL B. A phase 2b study of CSL112 in subjects with acute myocardial infarction. In: http://ClinicalTrials.gov. Available from: https://clinicaltrials.gov/ct2/show/NCT02108262?term=CSL-112&rank=1. NLM Identifier: NCT02108262. Bethesda, MD: National Library of Medicine. 2000. Accessed May 20, 2016.
224. Wang T, Rowland JG, Parmar J, Nesterova M, Seki T, and Rainey WE. Comparison of aldosterone production among human adrenocortical cell lines. *Horm Metab Res.* 2012;44(3):245-50.
225. Parmar J, Key RE, and Rainey WE. Development of an adrenocorticotropin-responsive human adrenocortical carcinoma cell line. *J Clin Endocrinol Metab.* 2008;93(11):4542-6.
226. Di Bartolo BA, Vanags LZ, Tan JT, Bao S, Rye KA, Barter PJ, et al. The apolipoprotein A-I mimetic peptide, ETC-642, reduces chronic vascular inflammation in the rabbit. *Lipids Health Dis.* 2011;10:224.
227. Carr BR, Parker CR, Milewich L, Porter JC, Macdonald PC, and Simpson ER. The Role of Low Density, High Density, and Very Low Density Lipoproteins in Steroidogenesis by the Human Fetal Adrenal Gland. *Endocrinology.* 1980;106(6):1854-60.
228. Schimmer BP, Cordova M, Cheng H, Tsao A, Goryachev AB, Schimmer AD, et al. Global profiles of gene expression induced by adrenocorticotropin in Y1 mouse adrenal cells. *Endocrinology.* 2006;147(5):2357-67.

229. Acton S, Rigotti A, Landschulz KT, Xu S, Hobbs HH, and Krieger M. Identification of Scavenger Receptor SR-BI as a High Density Lipoprotein Receptor. *Science.* 1996;271(5248):518-20.
230. Fong LG, Bonney E, Kosek JC, and Cooper AD. Immunohistochemical localization of low density lipoprotein receptors in adrenal gland, liver, and intestine. *The Journal of Clinical Investigation.* 1989;84(3):847-56.
231. Faust JR, Goldstein JL, and Brown MS. Receptor-mediated uptake of low density lipoprotein and utilization of its cholesterol for steroid synthesis in cultured mouse adrenal cells. *Journal of Biological Chemistry.* 1977;252(14):4861-71.
232. Rainey WE, Rodgers RJ, and Mason JI. The role of bovine lipoproteins in the regulation of steroidogenesis and HMG-CoA reductase in bovine adrenocortical cells. *Steroids.* 1992;57(4):167-73.
233. Gwynne JT, Mahaffee D, Brewer HB, Jr., and Ney RL. Adrenal cholesterol uptake from plasma lipoproteins: regulation by corticotropin. *Proc Natl Acad Sci U S A.* 1976;73(12):4329-33.
234. Andersen JM, and Dietschy JM. Relative importance of high and low density lipoproteins in the regulation of cholesterol synthesis in the adrenal gland, ovary, and testis of the rat. *J Biol Chem.* 1978;253(24):9024-32.
235. Illingworth DR, and Orwoll ES. Low-density lipoproteins and adrenal cortisol production: studies in abetalipoproteinaemia and hypobetalipoproteinaemia. *Biochem Soc Trans.* 1981;9(1):50.
236. Illingworth DR, Orwoll ES, and Connor WE. Impaired cortisol secretion in abetalipoproteinemia. *J Clin Endocrinol Metab.* 1980;50(5):977-9.
237. Rainey WE, Shay JW, and Mason JI. ACTH induction of 3-hydroxy-3-methylglutaryl coenzyme A reductase, cholesterol biosynthesis, and steroidogenesis in primary cultures of bovine adrenocortical cells. *J Biol Chem.* 1986;261(16):7322-6.
238. Balasubramaniam S, Goldstein JL, and Brown MS. Regulation of cholesterol synthesis in rat adrenal gland through coordinate control of 3-hydroxy-3-methylglutaryl coenzyme A synthase and reductase activities. *Proc Natl Acad Sci U S A.* 1977;74(4):1421-5.
239. Balasubramaniam S, Goldstein JL, Faust JR, Brunschede GY, and Brown MS. Lipoprotein-mediated regulation of 3-hydroxy-3-methylglutaryl coenzyme A reductase activity and cholesteryl ester metabolism in the adrenal gland of the rat. *J Biol Chem.* 1977;252(5):1771-9.
240. Remaley AT, Thomas F, Stonik JA, Demosky SJ, Bark SE, Neufeld EB, et al. Synthetic amphipathic helical peptides promote lipid efflux from cells by an ABCA1-dependent and an ABCA1-independent pathway. *Journal of Lipid Research.* 2003;44(4):828-36.
241. Xie Q, Zhao SP, and Li F. D-4F, an apolipoprotein A-I mimetic peptide, promotes cholesterol efflux from macrophages via ATP-binding cassette transporter A1. *Tohoku J Exp Med.* 2010;220(3):223-8.
242. Liu XH, Xiao J, Mo ZC, Yin K, Jiang J, Cui LB, et al. Contribution of D4-F to ABCA1 expression and cholesterol efflux in THP-1 macrophage-derived foam cells. *J Cardiovasc Pharmacol.* 2010;56(3):309-19.

243. Li D, Gordon S, Schwendeman A, and Remaley AT. In: Anantharamaiah GM, and Goldberg D eds. *Apolipoprotein Mimetics in the Management of Human Disease*. Springer International Publishing Switzerland; 2015:29-42.
244. Vardy E, Robinson JE, Li C, Olsen RHJ, DiBerto JF, Giguere PM, et al. A New DREADD Facilitates the Multiplexed Chemogenetic Interrogation of Behavior. *Neuron.* 2015;86(4):936-46.
245. Agulhon C, Boyt KM, Xie AX, Friocourt F, Roth BL, and McCarthy KD. Modulation of the autonomic nervous system and behaviour by acute glial cell Gq protein-coupled receptor activation in vivo. *J Physiol.* 2013;591(22):5599-609.
246. Li JH, Jain S, McMillin SM, Cui Y, Gautam D, Sakamoto W, et al. A novel experimental strategy to assess the metabolic effects of selective activation of a G(q)-coupled receptor in hepatocytes in vivo. *Endocrinology.* 2013;154(10):3539-51.
247. Yagi H, Tan W, Dillenburg-Pilla P, Armando S, Amornphimoltham P, Simaan M, et al. A synthetic biology approach reveals a CXCR4-G13-Rho signaling axis driving transendothelial migration of metastatic breast cancer cells. *Sci Signal.* 2011;4(191):ra60.
248. Vaque JP, Dorsam RT, Feng X, Iglesias-Bartolome R, Forsthoefel DJ, Chen Q, et al. A genome-wide RNAi screen reveals a Trio-regulated Rho GTPase circuitry transducing mitogenic signals initiated by G protein-coupled receptors. *Mol Cell.* 2013;49(1):94-108.
249. Dell'Anno MT, Caiazzo M, Leo D, Dvoretskova E, Medrihan L, Colasante G, et al. Remote control of induced dopaminergic neurons in parkinsonian rats. *J Clin Invest.* 2014;124(7):3215-29.
250. Guettier JM, Gautam D, Scarselli M, Ruiz de Azua I, Li JH, Rosemond E, et al. A chemical-genetic approach to study G protein regulation of beta cell function in vivo. *Proc Natl Acad Sci U S A.* 2009;106(45):19197-202.
251. Cortinovis M, Perico N, Cattaneo D, and Remuzzi G. Aldosterone and progression of kidney disease. *Ther Adv Cardiovasc Dis.* 2009;3(2):133-43.
252. Martin-Fernandez B, Rubio-Navarro A, Cortegano I, Ballesteros S, Alia M, Cannata-Ortiz P, et al. Aldosterone Induces Renal Fibrosis and Inflammatory M1-Macrophage Subtype via Mineralocorticoid Receptor in Rats. *PLoS One.* 2016;11(1):e0145946.
253. Remuzzi G, Cattaneo D, and Perico N. The aggravating mechanisms of aldosterone on kidney fibrosis. *J Am Soc Nephrol.* 2008;19(8):1459-62.
254. Remuzzi G, Perico N, Macia M, and Ruggenenti P. The role of renin-angiotensin-aldosterone system in the progression of chronic kidney disease. *Kidney Int Suppl.* 2005(99):S57-65.
255. Tesch GH, and Young MJ. Mineralocorticoid Receptor Signaling as a Therapeutic Target for Renal and Cardiac Fibrosis. *Front Pharmacol.* 2017;8:313.
256. Zhu H, and Roth BL. Silencing synapses with DREADDs. *Neuron.* 2014;82(4):723-5.
257. Akhmedov D, Mendoza-Rodriguez MG, Rajendran K, Rossi M, Wess J, and Berdeaux R. Gs-DREADD Knock-In Mice for Tissue-Specific, Temporal Stimulation of Cyclic AMP Signaling. *Mol Cell Biol.* 2017;37(9).

258. Wettschureck N, Rutten H, Zywietz A, Gehring D, Wilkie TM, Chen J, et al. Absence of pressure overload induced myocardial hypertrophy after conditional inactivation of Galphaq/Galpha11 in cardiomyocytes. *Nat Med.* 2001;7(11):1236-40.
259. Mukai T, Kusaka M, Kawabe K, Goto K, Nawata H, Fujieda K, et al. Sexually dimorphic expression of Dax-1 in the adrenal cortex. *Genes Cells.* 2002;7(7):717-29.
260. De Gendt K, Swinnen JV, Saunders PT, Schoonjans L, Dewerchin M, Devos A, et al. A Sertoli cell-selective knockout of the androgen receptor causes spermatogenic arrest in meiosis. *Proc Natl Acad Sci U S A.* 2004;101(5):1327-32.